universität wien

DISSERTATION / DOCTORAL THESIS

Titel der Dissertation /Title of the Doctoral Thesis

„The indium-mediated allylation as key step for the synthesis of complex elongated disaccharidic carbohydrate structures“

verfasst von / submitted by

Christian Denner, BSc MSc

angestrebter akademischer Grad / in partial fulfilment of the requirements for the degree of

Doktor der Naturwissenschaften (Dr. rer. nat.)

Wien, 2020 / Vienna 2020

Studienkennzahl lt. Studienblatt / degree programme code as it appears on the student record sheet:	A 796 605 419
Studienrichtung lt. Studienblatt / degree programme as it appears on the student record sheet:	Chemie
Betreut von / Supervisor:	Univ.-Prof. Dr. Christian Friedrich Wilhelm Becker
Betreut von / Supervisor:	Univ.-Prof. Dipl.-Ing. Dr.techn. Tanja Wrodnigg

“That which can be asserted without evidence,

can be dismissed without evidence.”

—Christopher Hitchens

Danksagung

An dieser Stelle möchte ich mich bei all jenen bedanken, die mich in dieser aufregenden und teilweise doch sehr anstrengenden Zeit unterstützt und ermutigt haben.

Allen voran gilt mein ganz besonderer Dank Prof. Walther Schmid für die interessante Themenstellung, das stets offene Ohr für Probleme und Fragen aller Art und auch die eine oder andere sehr interessante abendliche Nachbesprechung, die ich nie vergessen werde. In diesem Sinne möchte ich mich auch bei Hanspeter Kählig und Harry Martin bedanken für viele Gespräche über organische Chemie, NMR und das Leben generell, die sich teilweise bis spät in die Nacht gezogen haben.

Besonderer Dank gilt auch Prof. Tanja Wrodnigg und Prof. Christian Becker, die in einer sehr schwierigen Zeit nicht gezögert haben meine Betreuung zu übernehmen und mir auch immer mit Rat und Tat zur Seite standen. Darüber hinaus möchte ich mich bei Tanja bedanken für die fachliche Betreuung und die vielen netten Tage und Abende in Wien und Graz, die dabei geholfen haben Publikationen und Arbeit voranzutreiben und alles einfacher und angenehmer gemacht haben.

Weiters möchte ich mich bei den Mitgliedern der AG Schmid für das ausgezeichnete Arbeitsklima und die vielen netten Unterhaltungen über Chemie und alle anderen relevanten Themen bedanken. Hervorheben möchte ich dabei meinen Labor- und Bürokollegen Manuel Gintner, sowie unsere Technikerin Gerlinde Benesch, die immer bei kleinen und großen Problemen, egal ob chemischer, technischer oder privater Natur, zur Verfügung standen.

Natürlich darf man auch alle Freunde und Kollegen nicht vergessen, die eine sehr spannende aber auch schwierige Zeit nicht nur erträglich, sondern auch schön und unvergesslich gemacht haben. Deswegen möchte ich mich hier auch bei Kathrin Hölz, Patric Berger, Alanca Schmid, Ricarda Mauthner, Lukas Scheibelberger, Karla Pelivan, Can Araman und Martin Berger bedanken.

Es gibt natürlich auch viele Menschen außerhalb der Universität denen hier Dank gebührt. Allen voran meinen Eltern und Christa Graf, die mich zu jeder Zeit emotional, finanziell und mit wertvollen Ratschlägen unterstützt haben.

Ebenfalls bedanken möchte ich mich bei meinen Freunden, die mich seit Jahren begleiten: Andreas Zausinger, Christian Herzig, Michael Knauseder, Annika Reidinger, Kristina Schodl, Josef Willinger und Anna-Luise Braune.

Ohne die Unterstützung und auch oft notwendige Ablenkung durch die hier genannten Personen wäre es wohl nicht so weit gekommen. Vielen Dank!

Abstract

The indium-mediated allylation (IMA) reaction represents a valuable tool for the elongation of the carbon skeleton of unprotected carbohydrates. Such elongated sugars are present in many metabolic pathways and are often found in cell-walls of different organisms. Therefore, the synthesis of such compounds is an important research goal in Glycoscience, to improve our understanding of these interactions and further explore the possibility of medical interventions such as drugs or vaccines. The aim of this PhD thesis was to introduce a concise synthetic method for the elongation of disaccharides such as melibiose, maltose, cellobiose as well as lactose employing an IMA - ozonolysis protocol. The IMA was optimized for disaccharides and the expected *syn* configuration of the new stereocenter was confirmed, for the main product, with the help of X-Ray crystallography. The resulting highly polar compounds were per-*O*-acetylated for the purification and separation of the resulting epimeric mixture. The pure allylated disaccharides were then deprotected using a Zemplén deacetylation and the resulting reaction mixture was directly diluted with dichloromethane and subsequently used for the ozonolysis step. The obtained product mixture of α/β-pyranoid as well as α/β-furanoid isomers was then per-*O*-acetylated and the main product purified for structural elucidation using nuclear magnetic resonance spectroscopy with the help of spin simulations (Daisy, TopSpin software, Bruker BioSpin). Interestingly, during the optimization process of the elongation of lactose a novel 12 membered bridged disaccharide has been identified. In this thesis the IMA reaction has been demonstrated to be a powerful synthetic tool for the efficient and diastereoselective elongation of disaccharides without affecting the existing glycosidic linkage, allowing for further options for the possible modifications of complex glycosides.

Zusammenfassung

Die Indium vermittelte Allylierung (IMA) von Aldehyden ist ein wertvolles Werkzeug für die Kettenverlängerung des Kohlenstoff-Grundgerüsts von ungeschützten Kohlenhydraten. Diese verlängerten Zucker spielen eine wichtige Rolle im Stoffwechsel von vielen Lebewesen und sind häufig Bestandteile von Zellwänden unterschiedlichster Organismen. Deshalb ist die Synthese solcher Verbindungen ein wichtiges Ziel in der Kohlenhydratchemie, um unser Verständnis ihrer Interaktionen zu verbessern und in Zukunft weitere Möglichkeiten zu finden solche Verbindungen für medizinische Behandlungen und als Impfstoffe einzusetzen. In dieser Arbeit wurde eine zuverlässige synthetische Methode für die Kettenverlängerung von Disacchariden wie Melibiose, Maltose, Cellobiose und Lactose über ein 'Indium Allylierung – Ozonolyse' Protokoll entwickelt. Die IMA wurde für ihre Anwendung an Zweifachzuckern optimiert und die erwartete *syn* Konfiguration des neu gebildeten Stereozentrums konnte mittels Kristallstrukturanalyse nachgewiesen werden. Die entstehenden sehr polaren Verbindungen wurden anschließend für die darauf folgende Reinigung und Trennung des entstehenden Epimerengemisches vollständig acetyliert. Die reinen allylierten Disaccharide wurden anschließend durch Zemplén Deacetylierung entschützt, die Reaktionslösung direkt mit Dichlormethan verdünnt und daraufhin für die Ozonolyse eingesetzt. Die entstehende Produktmischung enthält α/β-pyranoide als auch α/β-furanoide Isomere und wurde erneut vollständig acetyliert um die Hauptprodukte für die anschließende Strukturaufklärung durch Kernspinresonanzspektroskopie mit der Hilfe von Spinsimulationen (Daisy, TopSpin Software, Bruker BioSpin) zu reinigen. Während der Optimierung der Verlängerung von Lactose konnte außerdem ein interessantes neuartiges 12 gliedriges überbrücktes Disaccharid gefunden und vollständig identifiziert werden. In dieser Dissertation konnte gezeigt werden, dass die Indium vermittelte Allylierung eine sehr gute Synthesestrategie für die effiziente und diastereoselektive Verlängerung von Disacchariden ist, die glykosidische Bindungen unberührt lässt und weiter Optionen für denkbare Modifikationen komplexer Kohlenhydrate ermöglicht.

Contents

1 Introduction

Carbohydrates are one of the most essential molecules in life, as products of photosynthesis they are the most abundant substance class accounting for two thirds of all biomass. They consist of mono-, di-, oligo- and polysaccharides and their simple skeletal structure but high chemical and chiral diversity make them essential in many different areas such as energy metabolism, structural tissue of plants and insects as well as cell-cell interactions. Hence, they play key roles in life circles of living systems.

1.1 Carbohydrate metabolism

Energy metabolism is the transformation of nutrients for the generation or storage of energy. These metabolic reactions can be divided in anabolic and catabolic pathways.[1] Anabolic pathways construct molecules from smaller units and are usually synonymous with biosynthesis. Some of the mayor anabolic carbohydrate pathways are photosynthesis, glycogenesis and gluconeogenesis. Photosynthesis is the process used by plants, algae along with other organisms to convert carbon dioxide from the atmosphere with water and sunlight in oxygen and carbohydrates, in their chloroplasts. There are variations between the different organisms, but the main concept remains universal. The process starts with light-dependent reactions where sunlight is absorbed by proteins, containing chlorophyll or related pigments, which initiates the loss of an electron and starts an electron transport chain.[2] Chlorophyll later regains its electron when H_2O is split through photolysis and produces O_2 as a waste product. The resulting electron transport chain leads to the reduction of $NADP^+$ to NADPH. Additionally, the resulting proton gradient on the chloroplast membrane is used to synthesize ATP from ADP (Figure 1).[3]

$$2\ H_2O + 2\ NADP^+ + 10\ H^+_{stroma} \longrightarrow O_2 + 2\ NADPH + 12\ H^+_{lumen}$$
$$3\ ADP^{3-} + 3\ P_i^{2-} + 3\ H^+ + 12\ H^+_{lumen} \longrightarrow 3\ ATP^{4-} + 3\ H_2O + 12\ H^+_{stroma}$$

$$2\ NADP^+ + 3\ ADP^{3-} + 3\ P_i^{2-} + H^+ \longrightarrow O_2 + 2\ NADPH + 3\ ATP^{4-} + H_2O$$

Figure 1: Overall equation for the light-dependent reactions of photosynthesis.[3]

Simultaneously and at night the light-independent reactions take place. This pathway is also called Calvin cycle after the biochemist Melvin Calvin who discovered it. The enzyme RUBisCO captures CO_2 and releases three-carbon sugars under the consumption of ATP and NADPH which were generated in the light-dependent reactions (Figure 2).[4] These intermediate sugars are later combined to form the final carbohydrate products which are further used as building materials, precursors or for cellular respiration.

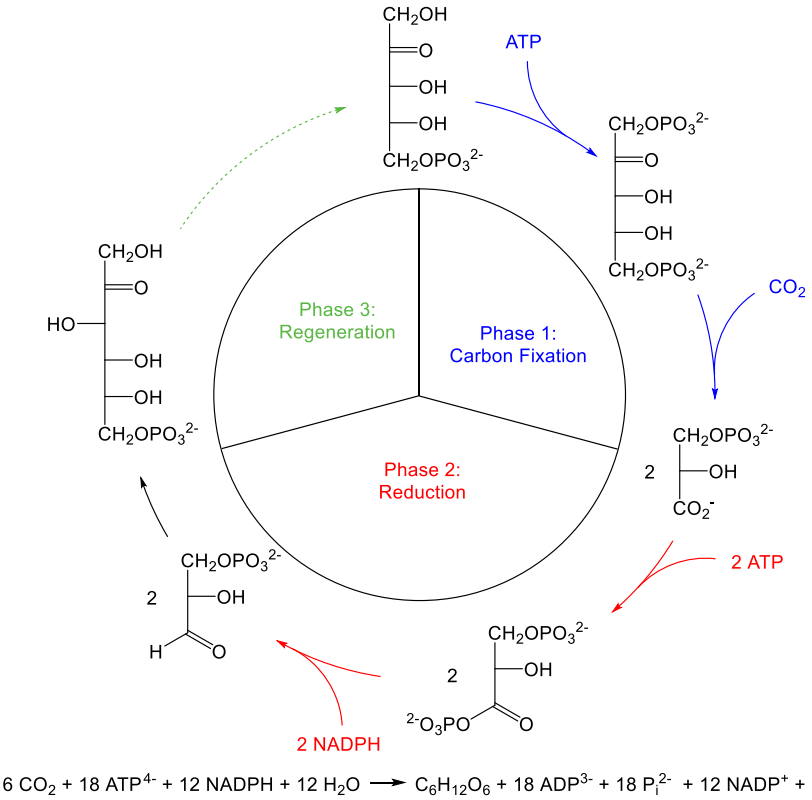

Figure 2: Light-independent reactions or Calvin cycle of photosynthesis.

Gluconeogenesis is the process which results in the generation of glucose from non-carbohydrate substrates. The organism mainly relies on this pathway in times of low caloric intake.[1] Precursors are mainly lactate, pyruvate, amino acids as well as glycerin, other substrates are transformed to pyruvate beforehand. Fatty acids in contrast cannot be converted to glucose and are metabolized in a different pathway with the help of lipases. Gluconeogenesis mainly takes place in the liver and kidney. The equilibrium of this pathway is on the side of pyruvate with an ΔG-value of -84 kJ mol^{-1}.[3] Therefore, some of the reactions have to be modified from the glycolysis pathway to achieve this conversion (Figure 3).

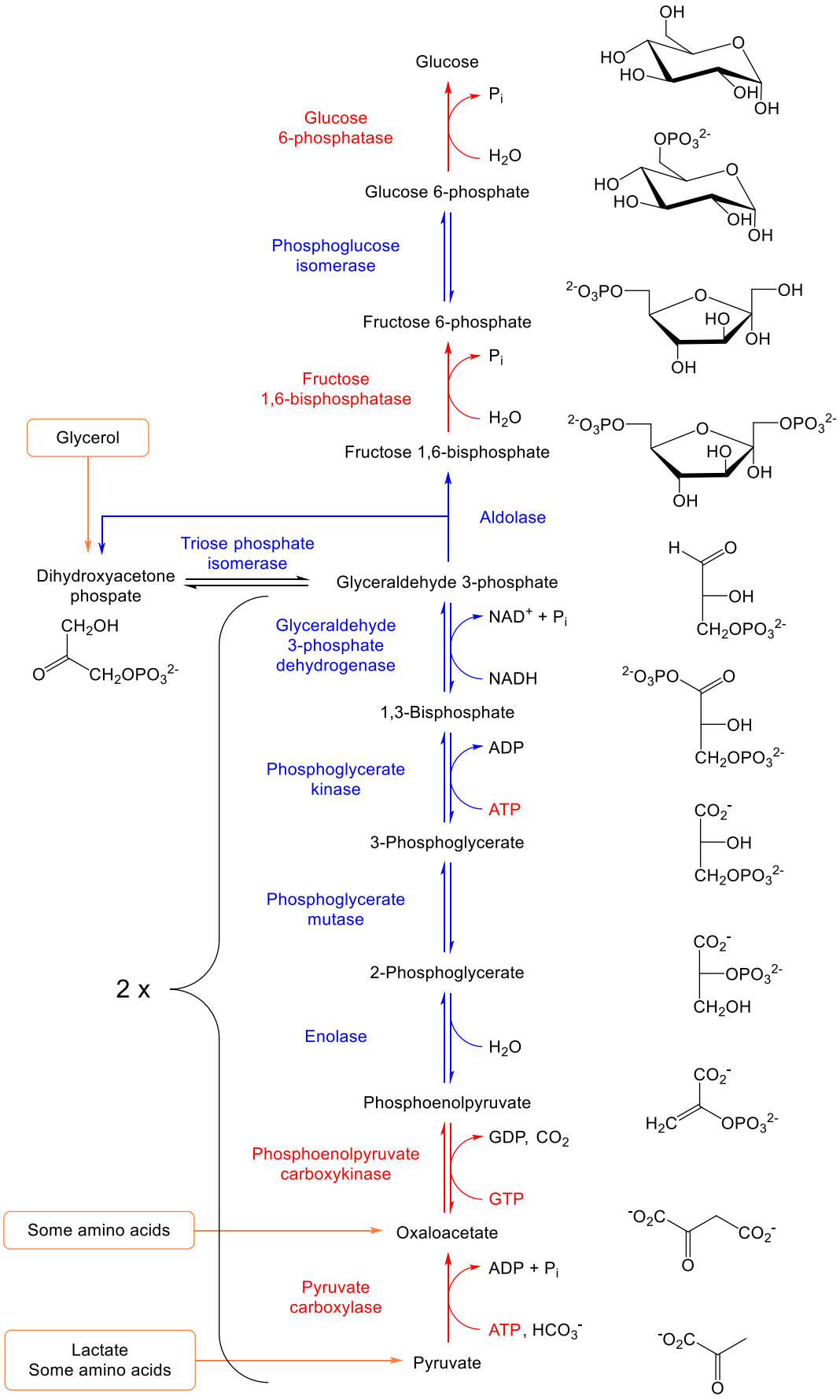

Figure 3: Pathway of the gluconeogenesis, distinct reactions not present in the glycolysis shown in red.[3]

Glycogenesis is used for the storage of energy in the form of glycogen in phases of high glucose levels. With glycogenin as the core, glucose is added with the help of UTP to generate long sugar chains with an 1,4-α-glycosidic linkage and periodically 1,6-α-glycosidic linkages as branches (Figure 4).[1] The average chain length is around 10 glucose units and between 2,000 - 60,000 residues per molecule of glycogen (Figure 4).[3]

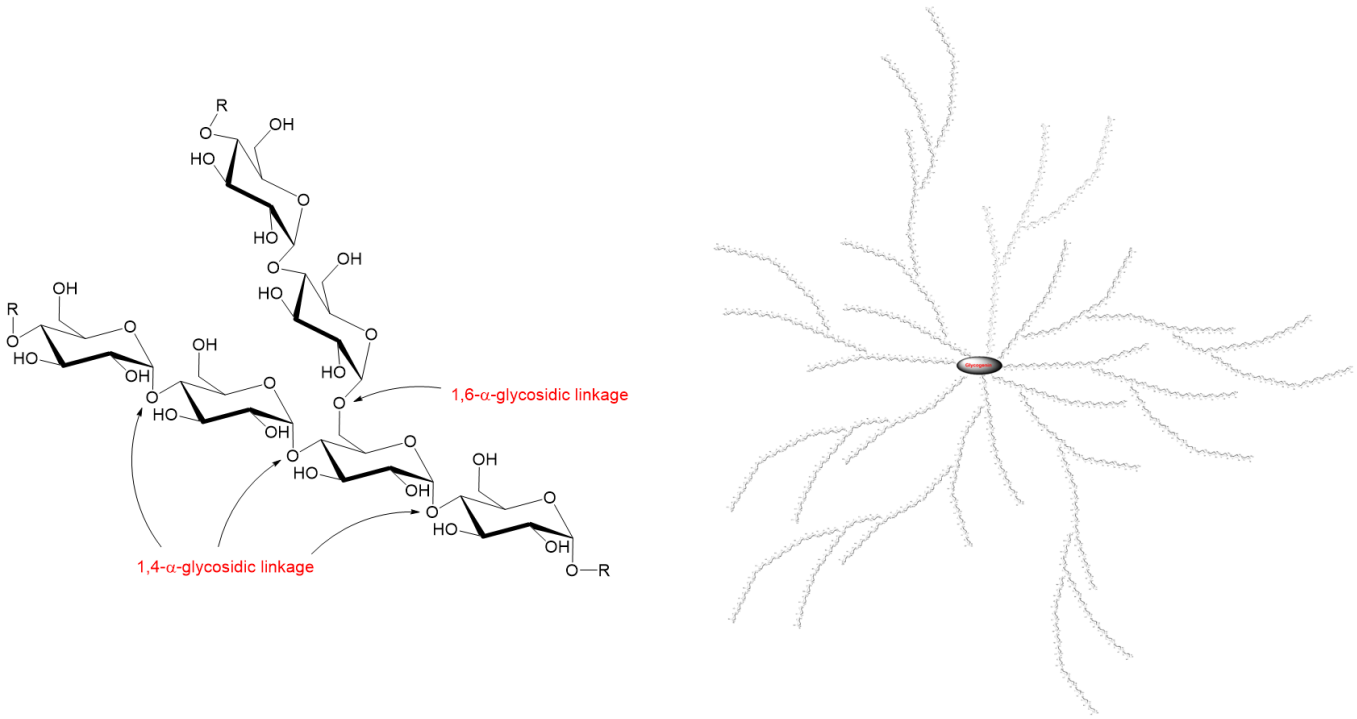

Figure 4: Glycogen with glycogenin as the center and the glucose linkages in glycogen.

The corresponding process in plants, which is responsible for the synthesis of starch is similar, but instead of UDP-glucose, ADP-glucose is used as activated precursor.[3] Additionally, starch has no central peptide and even amylopectin has a lower ratio of 1,6-α-glycosidic linkages. Furthermore, plants also use sucrose as energy storage which is synthesized in the cytoplasm.[3] There triosephosphate is converted to fructose-6-phosphate that reacts with UDP-glucose to sucrose-6-phosphate which is hydrolyzed to sucrose (Scheme 1).

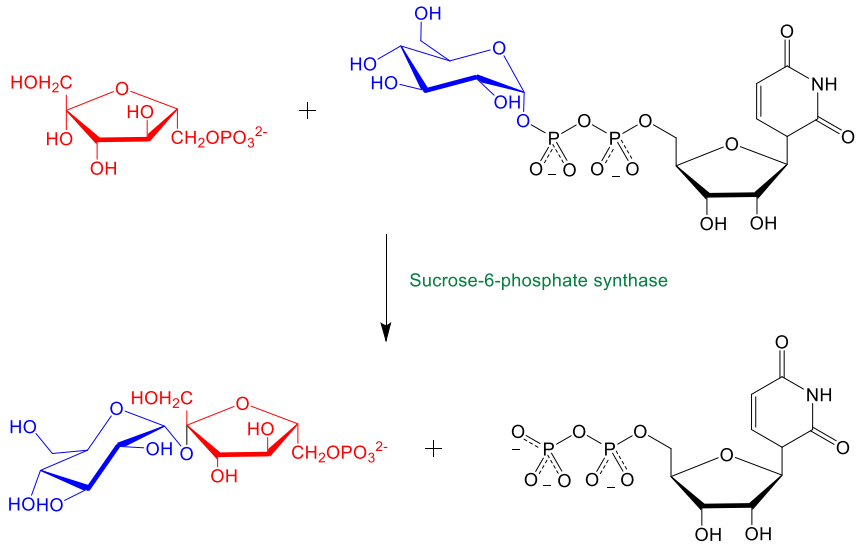

Scheme 1: Biosynthesis of Sucrose by sucrose-6-phospate synthase.

Catabolic pathways include glycogenolysis which is the reverse reaction of glycogenesis. In case of high energy demand glucose-1-phosphate is cleaved from glycogen with the help of glycogen phosphorylase (Scheme 2).[3] Afterwards it is converted to glucose-6-phosphate by the phosphoglucomutase which then is mainly used in glycolysis.

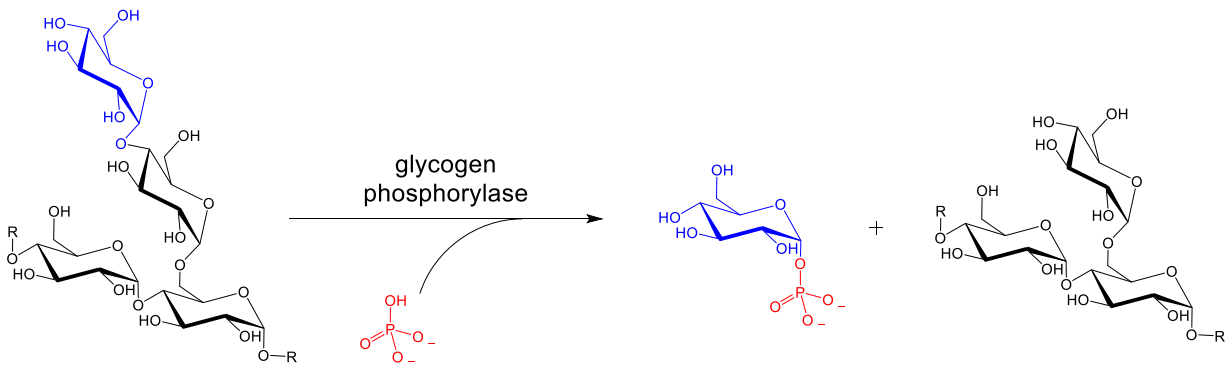

Scheme 2: Glycogenolysis of glycogen with the help of glycogen phosphorylase.

Glycolysis is one of the main processes of cellular respiration. It is the first step and involves the anaerobic degradation of glucose to pyruvate which then gets further metabolized with the help of oxygen in the Krebs cycle.[5] The three irreversible reactions with the highest reduction of free enthalpy are different from the gluconeogenesis. These reactions are catalyzed by hexokinase, phosphofructokinase and pyruvate-kinase and are responsible for a ΔG-value of -72 kJ mol^{-1} (Figure 5).[3]

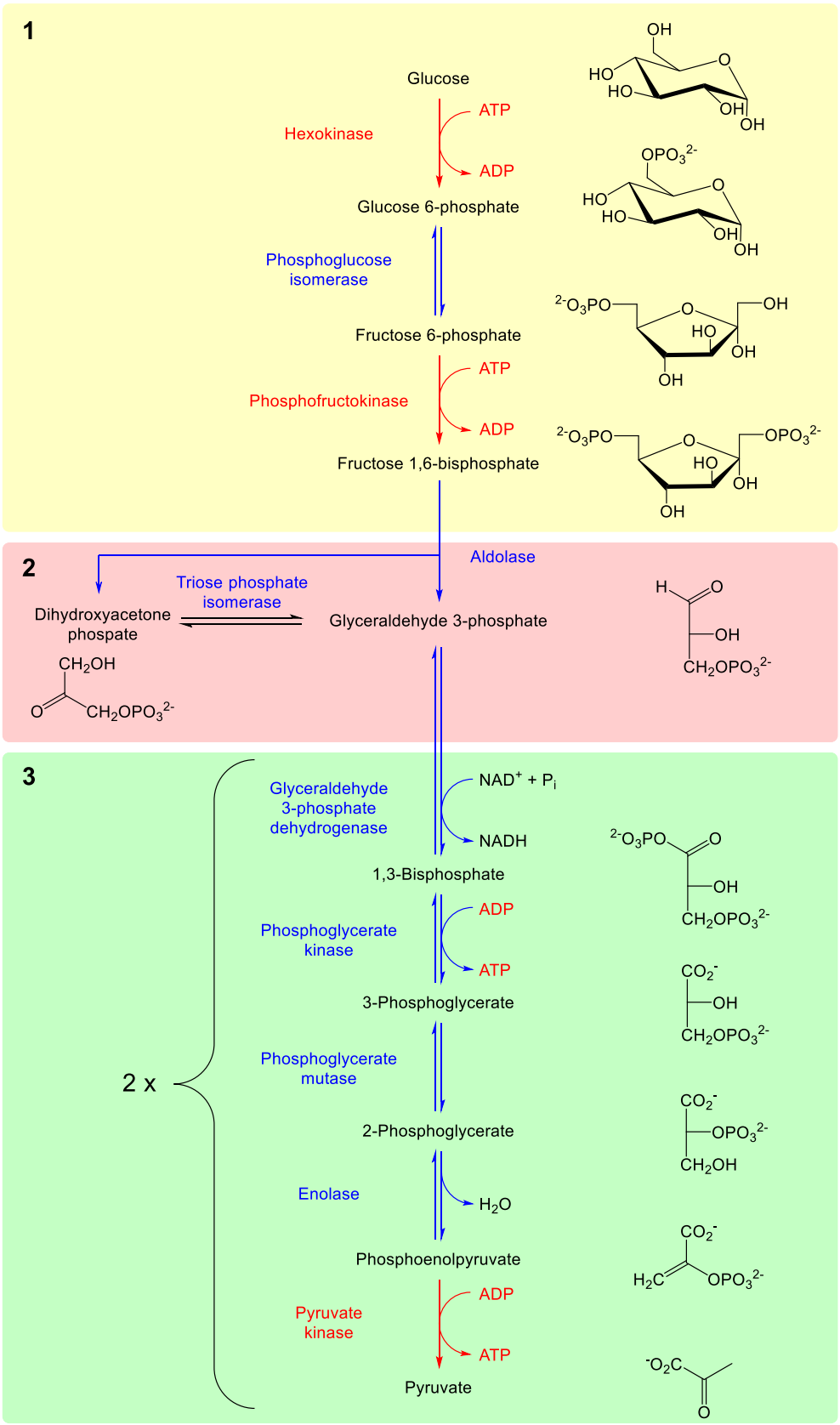

Figure 5: The three stages of glycolysis. 1) Glucose is destabilized 2) Fructose is cleaved resulting in the generation of two interconvertible three-carbon sugars 3) ATP is generated.[3]

There are also some pathways which cannot be strictly categorized as anabolic or catabolic. The pentose phosphate pathway for instance metabolizes glucose to ribulose-5-phosphate but then further converts it into different sugars as precursors for nucleotides and aromatic amino acids (Figure 6).[3]

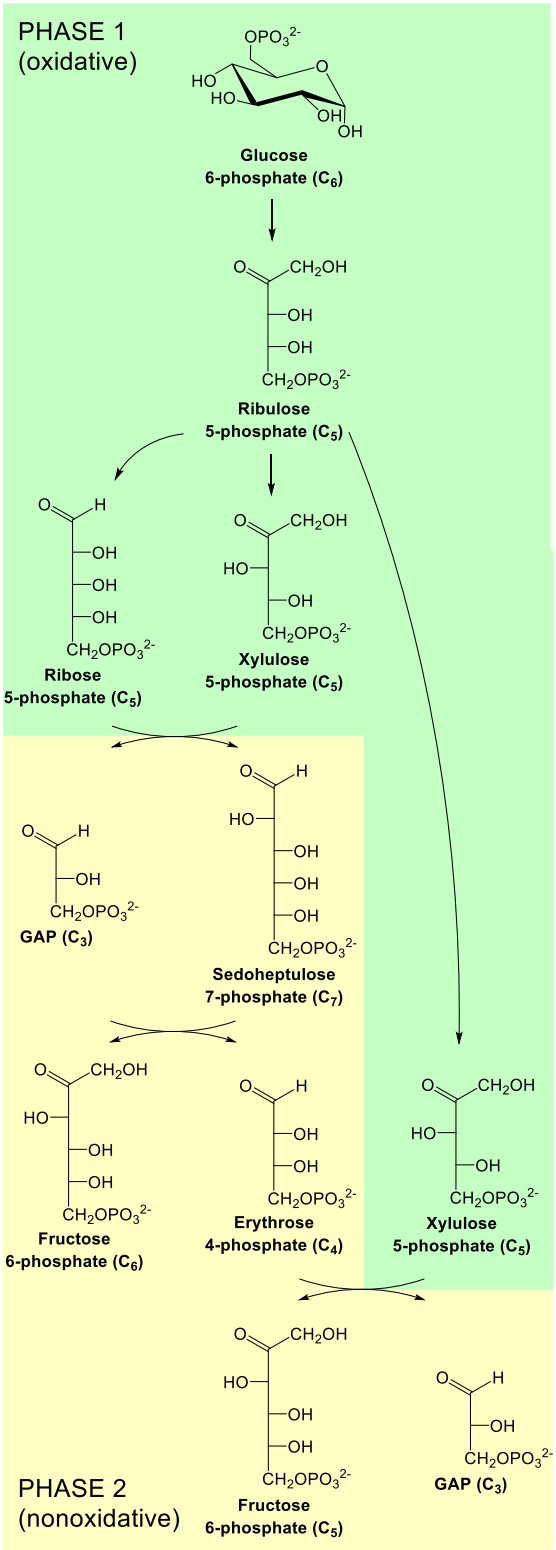

Figure 6: Pentose phosphate pathway. Phase 1 oxidative phase. Phase 2 interconversion of phosphorylated sugars.[3]

1.2 Structural carbohydrates

When organisms get more complex additional mechanical stability is necessary for protection and further cell diversification. This demand is mostly accommodated by polymer compounds. Animals and humans use collagen and hydroxyapatite for their skeleton, but many other organisms such as plants and insects get their structural integrity from carbohydrates. Cellulose is the most abundant organic molecule on earth with approximately 10^{15} kg synthesized every year by photosynthesis.[6] It is the main structural element of plants protecting not only cells but the whole organism. It consists of glucose with unbranched 1,4-β-glycosidic linkages up to 15000 units.[6,7] The resulting straight chains can be parallel to each other and form microfibrils through intermolecular hydrogen bonds that are important for the high tensile strength of cellulose (Figure 7).[3]

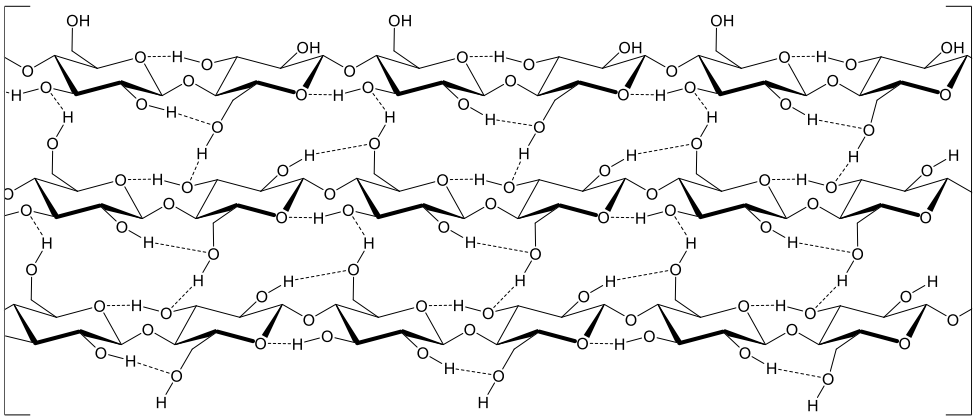

Figure 7: Structure and hydrogen bonds in Cellulose microfibrils.

Additionally, there are different forms of hemicellulose such as xylan as well as arabinoxylan. They consist of 1,4-β linked xylose in case of arabinoxylan mixed with 2,3-linked arabinose residues.[7] Together with pectin a heteropolysaccharide generally consisting of galacturonic acid these compounds are the main components of cell walls and wood and together with lignin responsible for the structural integrity (Figure 8).[7,8]

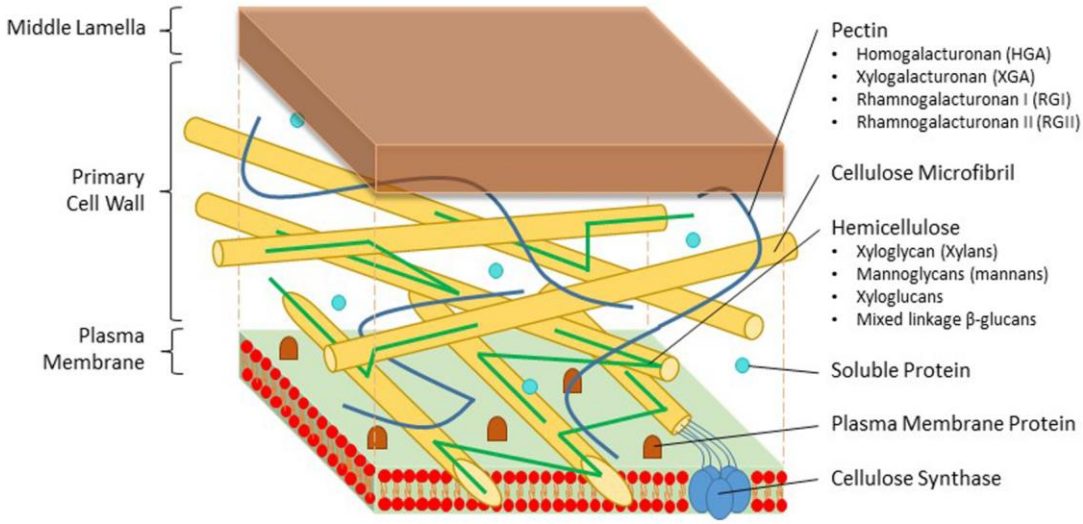

Figure 8: Primary cell wall consisting of cellulose microfibrils, different forms of hemicellulose as well as pectin.[8]

Chitin is a long chain biopolymer synthesized from *N*-acetylglucosamine. It is abundant in the cell wall of fungi and algae, the main component of the exoskeleton of invertebrates such as crustaceans, insects as well as molluscs and can also be found in fish scales.[9–11] It has the same 1,4-β-glycosidic linkage as cellulose (Figure 9).[10] Nonetheless, chitin has a more diverse secondary and tertiary structure and many different additives, such as proteins and minerals, in different species.

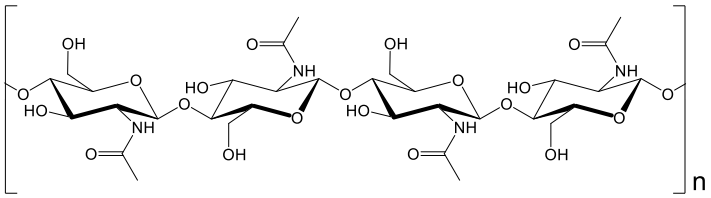

Figure 9: Structure of the biopolymer Chitin.

1.3 Carbohydrates in cell-cell interactions

Cellular processes such as differentiation, growth, motility as well as morphology are controlled to a certain degree by extracellular signals received at the cell surface. Some of these signals come from hormones or neurotransmitters but others can exert their effects only through direct cell-cell contact.[12,13] Specific cell-surface receptors can recognize molecular signals on a different cell via specific binding and translate that

into a cellular response.[14] These responses can range from pathogens that bind to their target tissues, interaction among cells in the immune system and even differentiation during embryonic development.[14] Carbohydrates are one important class of molecules responsible for biological recognition events, cell adhesion as well as cell communication.[10,15] These cell surface carbohydrates are concentrated on the glycocalyx, a complex pericellular environment created mainly from glycoproteins and glycolipids specific for each organism (Figure 10).[16,17] Its composition can vary greatly depending on the development status of the cell or due to pathological modifications such as cancer.[10,17]

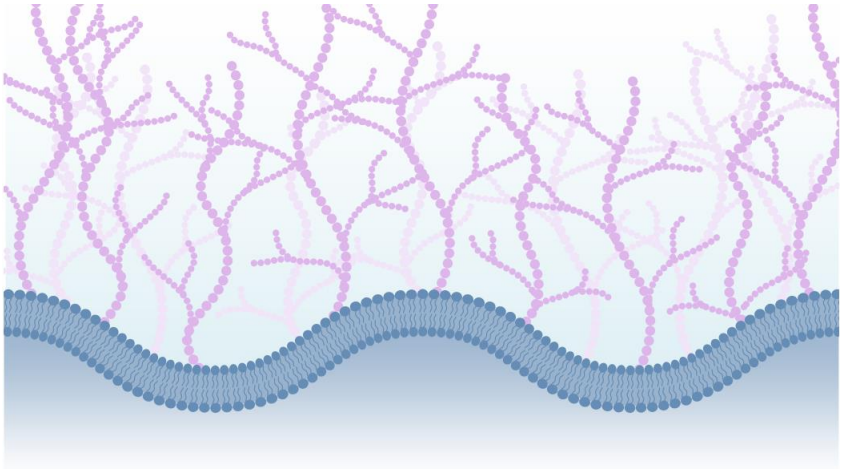

Figure 10: Glycocalyx on the surface of an endothelial cell.[16]

The glycocalyx serves as a site for docking of other molecules, pathogens or cells. In case of cell-cell interactions glycoconjugates on the cell surface may bind to the complementary lectin, a carbohydrate binding protein, on other cells thereby initiating a specific reaction.[14] The best universally known example of such carbohydrate induced cell-cell interactions is the AB0 blood group system. Where the difference of one sugar unit on an oligosaccharide determines the possibility of safe blood transfusion. There are three different antigens that result in four different phenotypes of the red blood cells.[10] If there is no further modifications to A- or B-type structures the resulting phenotype is called 0 or H and the antigen has an α-1,2-fucosylated galactose as the terminal carbohydrate. In blood type A the galactose is further glycosylated with an α-1,3-GalNAc in case of B-type blood a terminal α-1,3-Gal is

present, AB blood has both antigens present on the cell surface of their erythrocytes. These antigens in combination with the respective antibodies anti-A and anti-B are the basis for safe blood transfusions.

Phenotype of red blood cells	Minimal determinant saccharide (blood group antigen)	Antibodies found in plasma
A	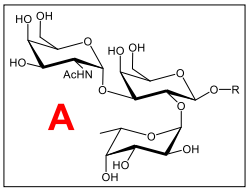	anti-B
B	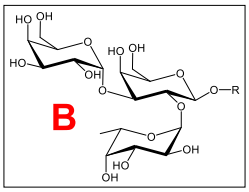	anti-A
AB	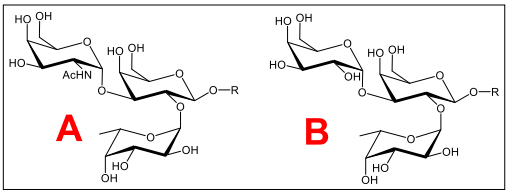	no antibodies
0	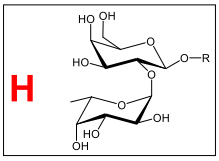	anti-A and anti-B

Figure 11: AB0 blood group system.

The glycoconjugates of most organisms are mostly composed of five- and six-carbon sugars, but there are some very important exceptions.[18] Sialic acids are α-keto acids with a nine-carbon backbone. They are a subset of nonulosonic acids that have a remarkable number of modifications causing a diverse class of more than 50 structurally distinct molecules (Figure 12).[18] Their terminal position on glycocalyx glycoconjugates, various sialyl linkages as well as diverse underlying glycans gives them an important role in biological, pathological and immunological processes.[19] Additionally, KDO (2-keto-3-deoxy-D-mannooctulosonic acid), an eight-carbon α-keto acid, can be found on the outer membrane of Gram-negative bacteria and in plants.[18]

In bacteria it is present in the form of lipopolysaccharides on the cell wall and normally induces a strong immune response in animals and humans.

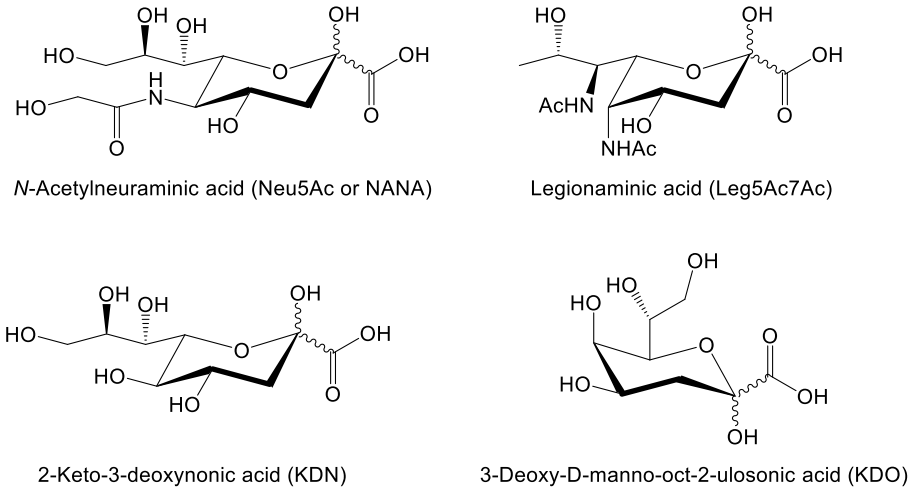

Figure 12: Human sialic acid Neu5Ac, bacterial sialic acid Leg5Ac7Ac, the deaminated neuraminic acid KDN and KDO.

1.4 Carbohydrate elongation

Elongated carbohydrates are present in metabolic pathways and the cell-walls of many organisms. Therefore, they are interesting targets in the form of metabolic tracers and especially important in the interactions of the human body with malignant cells as well as pathogens such as bacteria and viruses. Consequently, the synthesis of such compounds is an important research goal in Glycoscience, to improve our understanding of these interactions and further explore the possibility of medical interventions such as drugs or vaccines.

1.4.1 Formose reaction

The first example for the total synthesis and the elongation of carbohydrates is the formose reaction, which was first published by Butlerow in 1861.[20] In this reaction oligomerization of formaldehyde in the presence of $Ca(OH)_2$ generates a mixture of racemic aldoses and ketoses (Scheme 3).[21,22]

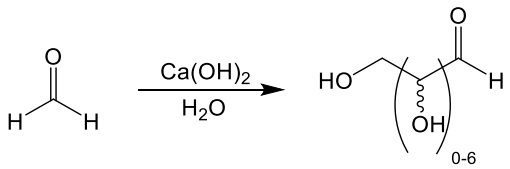

Scheme 3: Formose reaction generates a mixture of racemic carbohydrates.

In general under basic conditions a formaldehyde solution only undergoes the Cannizzaro reaction, a disproportionation which produces methanol and acetic acid.[23] However, for the initiation of the formose reaction glycolaldehyde is needed, the mechanism, which possibly involves a very slow light induced free radical process, is still under debate.[24,25] Nonetheless, after the first molecule of glycolaldehyde is introduced the reaction proceeds autocatalytic. The first mechanism was proposed by Breslow in 1959, although there is still a discussion on the exact conversions, the intermediates proposed by Breslow are confirmed to be present in the reaction mixture of the formose reaction (Scheme 4).[24–26]

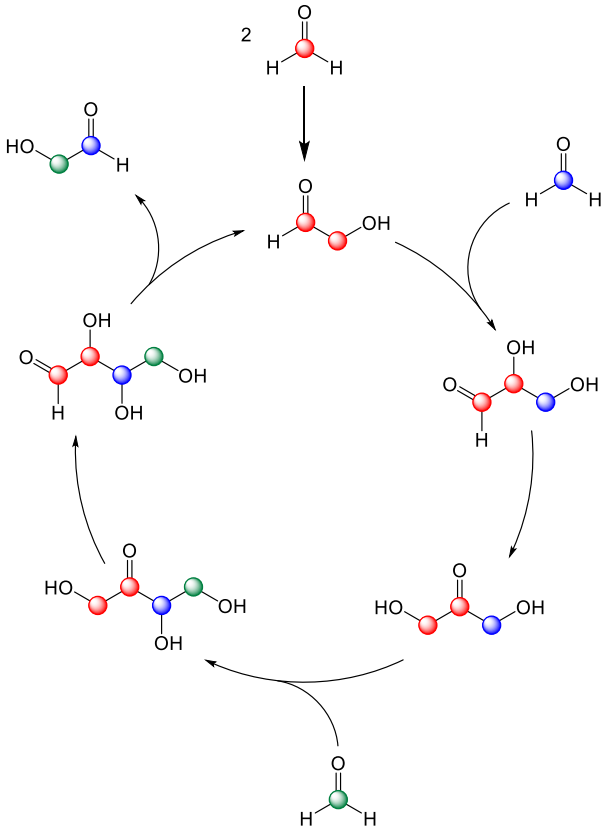

Scheme 4: Autocatalytic cycle as proposed by Breslow.

The diverse set of products and also the lack of stereo control renders the reaction mostly undesirable for modern synthesis, but it is still researched as a scenario of chemical evolution which could have produced the first carbohydrates on earth.[27–29]

1.4.2 Kiliani–Fischer synthesis

The Kiliani-Fischer Synthesis is a method which extends a carbohydrate chain by a single carbon. It is amongst the first discovered methods for the elongation of carbohydrates and is named after Heinrich Kiliani and Emil Fischer.[30] The original version is performed through the addition of aqueous hydrogen cyanide to a sugar solution, which leads to nucleophilic addition of the cyanide at the carbonyl group (Scheme 5). The resulting cyanohydrin is heated in water to facilitates hydrolyzation to the carboxylic acid group which subsequently undergoes lactonization. Finally, the resulting epimeric lactones are separated and reduced with sodium amalgam (Scheme 5).[30,31]

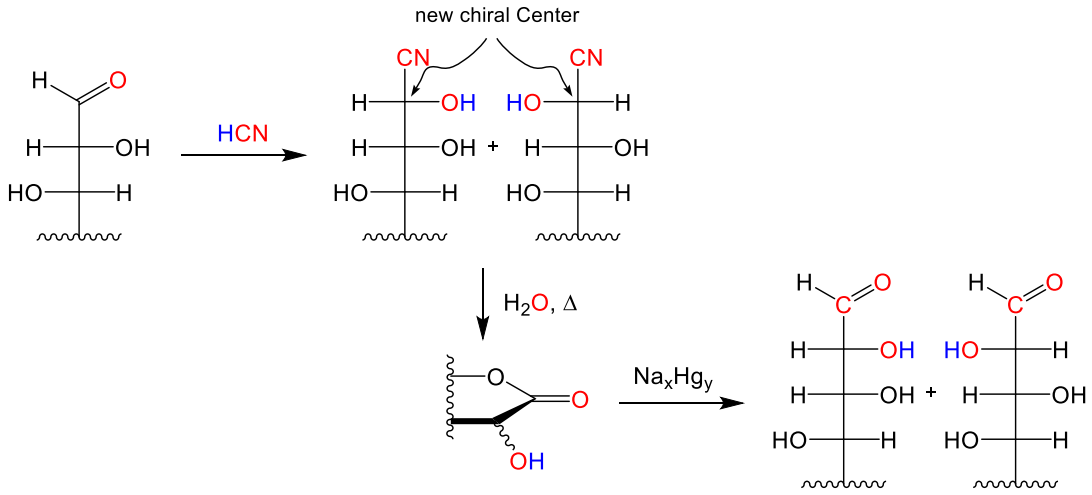

Scheme 5: Original version of the Kiliani-Fischer synthesis.

Yields of this sequence tend to be around 30 % or lower in most cases, improved versions use sodium cyanide and reduce the formed cyanohydrin to the imine through hydrogen, with catalytic amounts of palladium on barium sulfate or Lindlar palladium in an aqueous solution. The sugars are formed by hydrolyzation over only two steps and overall higher yields (Scheme 6).[32]

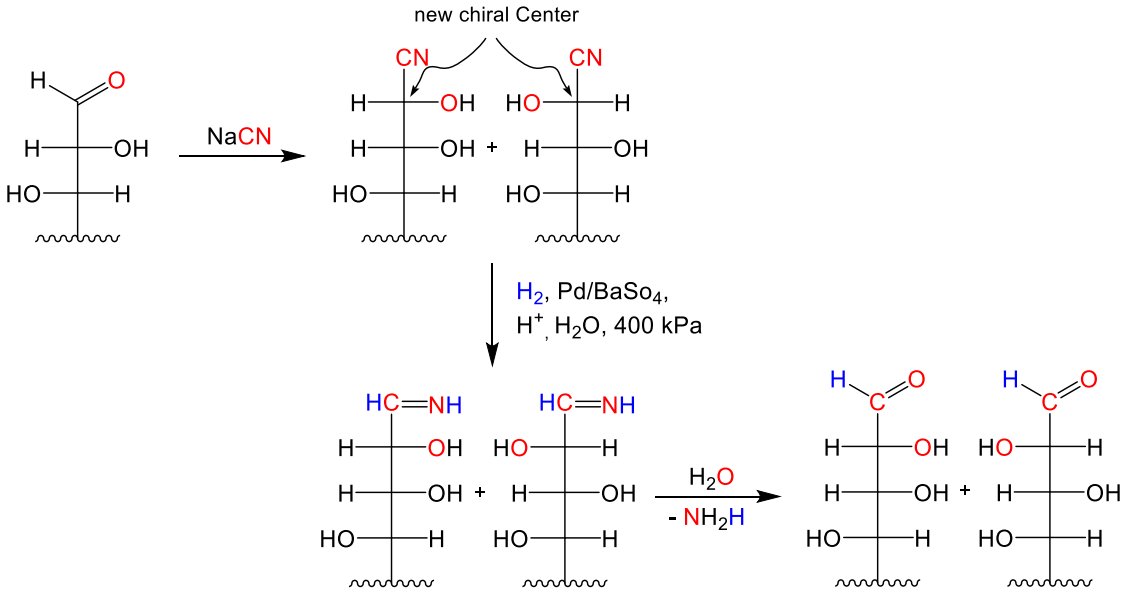

Scheme 6: Improved version of the Kiliani-Fischer synthesis.

1.4.3 Aldol reaction

The Aldol reaction was independently discovered by Alexander Borodin and Charles-Adolphe Wurtz around 1870. Victor von Richter wrote about Borodines findings in "Berichte der deutschen chemischen Gesellschaft" in 1869 where he mentioned the reaction of Valerianaldehyd and Oenanthaldehyd which lead to a condensation reaction.[33] 1872 Wurtz made a more detailed investigation with his work on the reaction of acetaldehyde in a hydrogen chloride solution (Scheme 7). He could identify the Aldol- and also the condensation product.[34]

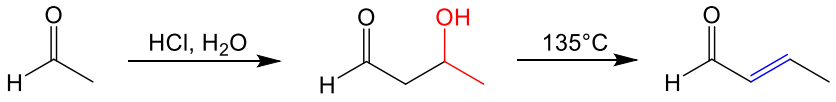

Scheme 7: Aldol reaction as described by Wurtz in 1872.

The aldol reaction describes the conversion of two carbonyl compounds, where one functions as a nucleophile and the other as an electrophile, to form a β-hydroxy carbonyl compound or, after further conversion, an α,β-unsaturated carbonyl compound (Scheme 8). It can be acid or base catalyzed and, depending on the starting materials, conditions as well as catalysts, there is a wide variety of different products which can be synthesized in a chemo and stereoselective way. Depending on the

conditions there are two different mechanisms for the aldol reaction, the enol or the enolate mechanism (Scheme 8). If the reaction is acid catalyzed an enol is formed in the equilibrium, subsequently the carbonyl oxygen gets protonated and can react with the nucleophilic enol to form the aldol product after deprotonation. In case the resulting hydroxy functionality undergoes protonation the α,β-unsaturated carbonyl compound can be formed through elimination. In the base catalyzed mechanism, an enolate is formed which attacks the carbonyl group of the other molecule, after formation of the β-hydroxy carbonyl compound an E1cB elimination reaction can lead to the α,β-unsaturated carbonyl compound (Scheme 8).

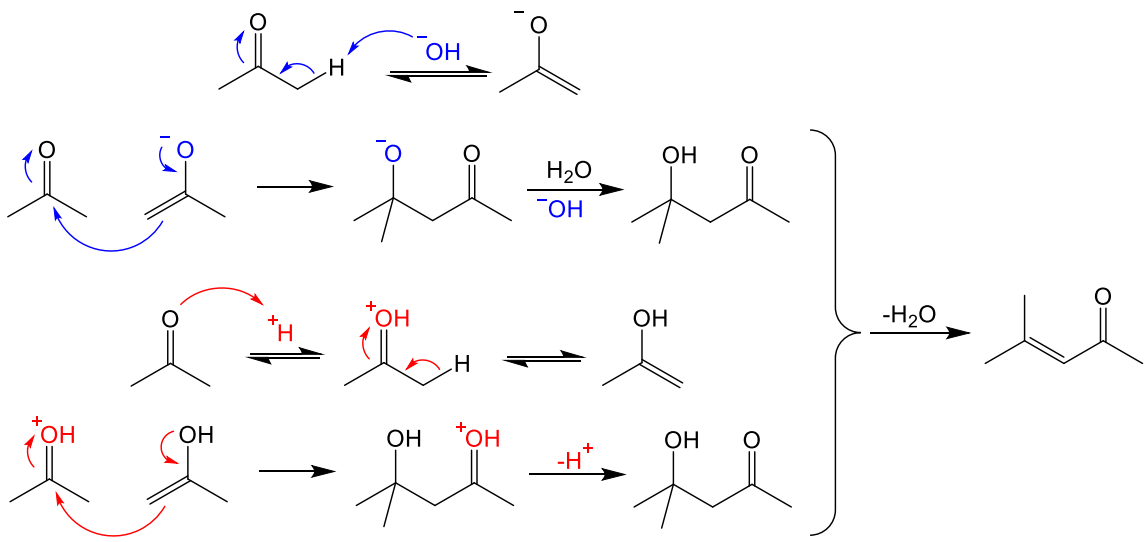

Scheme 8: Base and acid-catalyzed Aldol reaction and following condensation.

In many cases stoichiometric amounts of base such as lithium diisopropylamide (LDA) are used making the enolate formation irreversible thereby enhancing reaction rates. Due to the many different possible products a deep understanding and controlled conditions are of paramount importance performing preparative aldol reaction in the aldol reaction (Scheme 9).

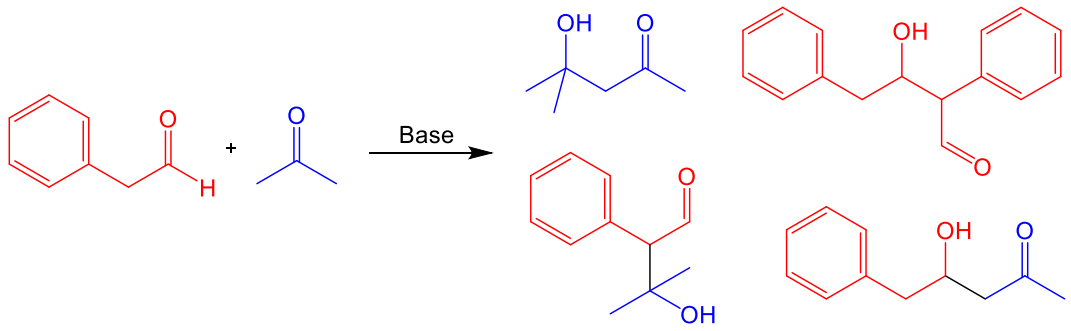

Scheme 9: Possible self and cross-coupling products of the aldol reaction.

The Zimmerman-Traxler model gives insight into the six-membered chair like transition state of some aldol reactions. *E*-Enolates favor *anti*-products whereas *Z*-enolates give rise to mainly *syn*-product (Scheme 10). Therefore, the enol formation is a crucial part and has been studied extensively, in most cases it is possible to generate the desired enol with the appropriate base and reaction conditions.[35] These enolate formations also determine the nucleophilic reactant in crossed-aldol reactions which prevents self-condensation products especially in kinetic controlled aldol reactions.

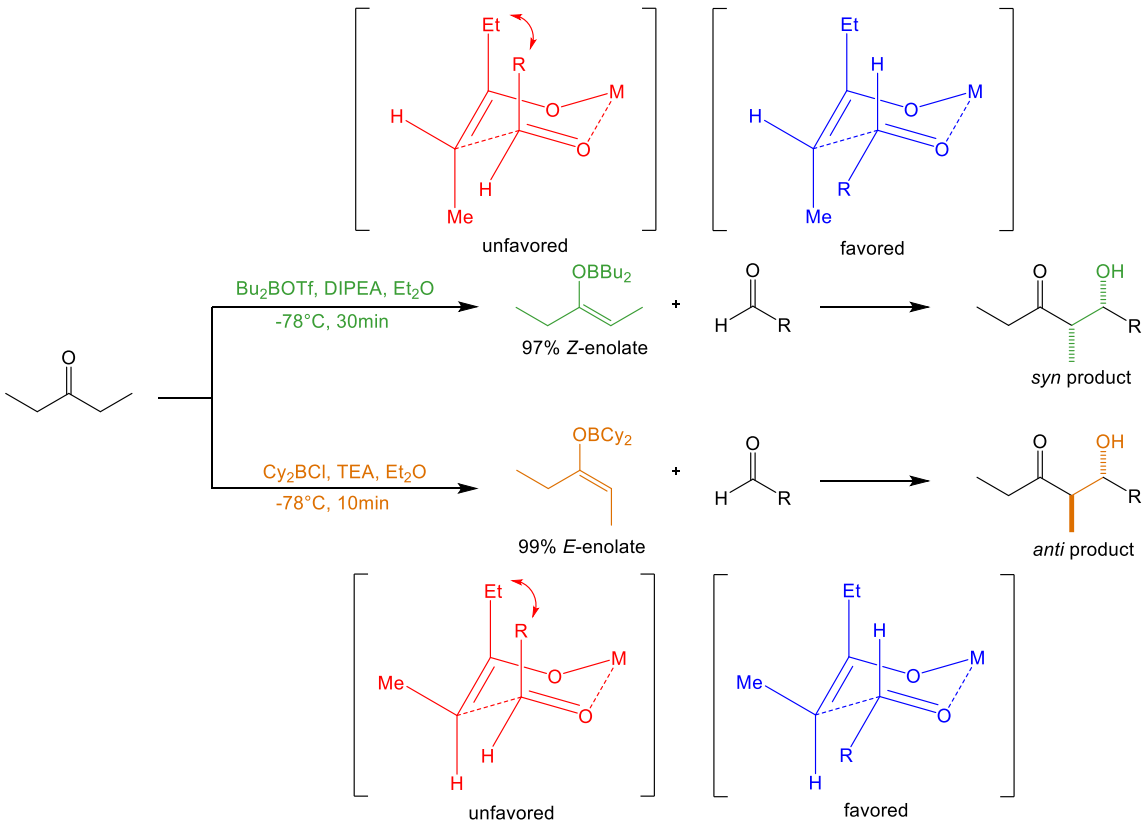

Scheme 10: Zimmerman-Traxler model of the product formation from E *and* Z*-enolates.*

Other ways to reduce the problem of self-condensation is the use of only one substrate with acidic protons were the enolate formation is only possible in one reactant. Stereochemistry is one of the most important parts of synthetic carbohydrate chemistry and additionally to the already mentioned *syn*/*anti* control, which depends on the used enolates, it gets more complex with the use of chiral starting materials. In case of an α-stereocenter on the enolate an 1,3-*syn* configuration is favored between the newly formed stereocenter and the existing sterically subordinate substituent (Scheme 11).[36] α-Stereocenters on the attacked aldehyde leads to an 1,2-*syn* conformation with *E*-enolates over a Felkin diastereoface selection or an 1,2-*anti* conformation with *Z*-enolates through a less selective *anti*-Felkin transition state (Scheme 11).[37,38]

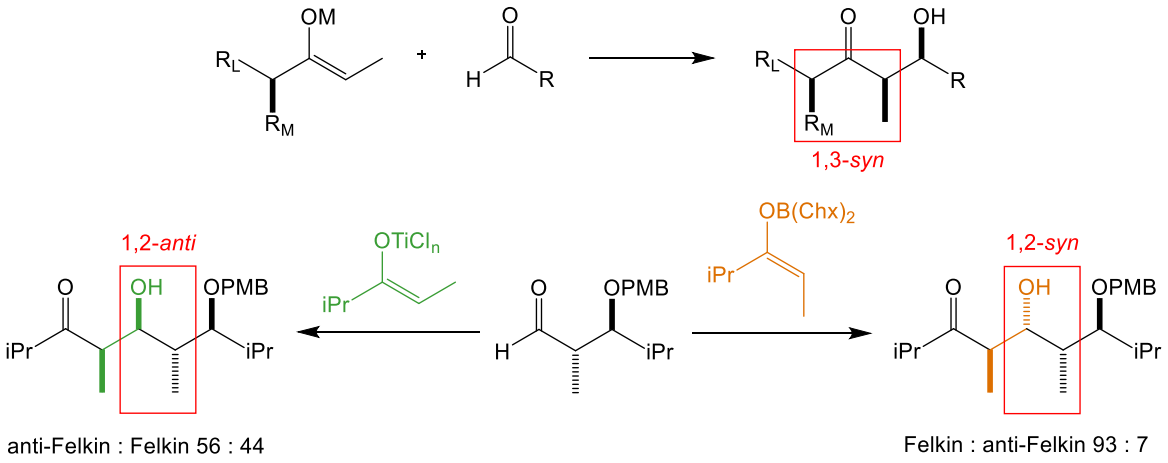

Scheme 11: Diastereoselectivity with chiral aldehydes or enoles.

Although these protocols allow the synthesis of targeted molecules, the diastereomeric ratios and yields often do not meet the demand of modern organic synthesis. Over the years many more sophisticated approaches have replaced the traditional aldol reactions. For instance, the Evans aldol reaction can achieve controlled absolute stereochemistry through the application of attached chiral auxiliaries in the enol component.[39] This pair of oxazolidinone (Scheme 12) was developed by Evans and his co-workers and can be synthesized in high enantiopurity.[40]

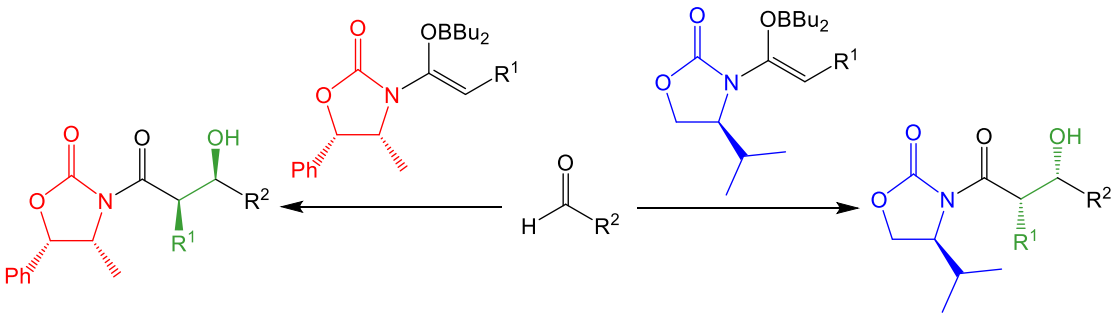

Scheme 12: Evans aldol reaction with oxazolidinone as a chiral auxiliary.

Moreover, catalytic asymmetric aldol reactions have been studied extensively for many years.[39,41] Hajos and co-workers as well as Wiechert and co-workers used proline in an asymmetric aldol cyclization in the 1970s.[42,43] Since then many different variations of proline (Scheme 13) and other catalysts have found its use in organic synthesis and have improved reactivity, selectivity as well as substrate scope of aldol reactions and have enabled the synthesis of complex molecular targets.[39,41]

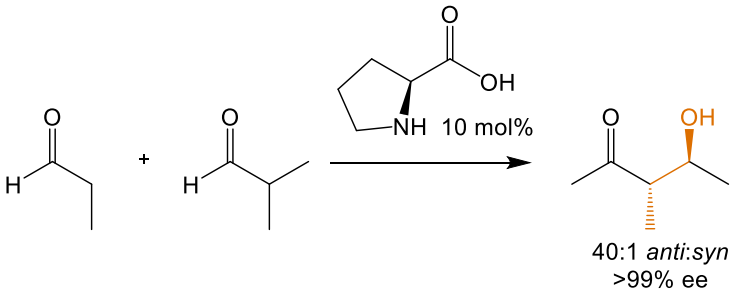

Scheme 13: Proline catalyzed aldol reaction with high diastereoselectivity.

1.4.4 Barbier reaction

The Barbier reaction (BR) is named after Philippe Barbier who first reported it in 1899.[44] It is the predecessor to a number of important reactions in organic synthesis such as the Grignard reaction or the indium-mediated allylation (IMA).[45] Contrary to the Grignard reaction in the BR organometallic reagents are generated in the presence of the carbonyl compound to produce an immediate conversion. The mechanism of the Barbier reaction as well as the Grignard reaction is substrate dependent, it can either proceed via nucleophilic addition or single electron transfer (Scheme 14).[46,47]

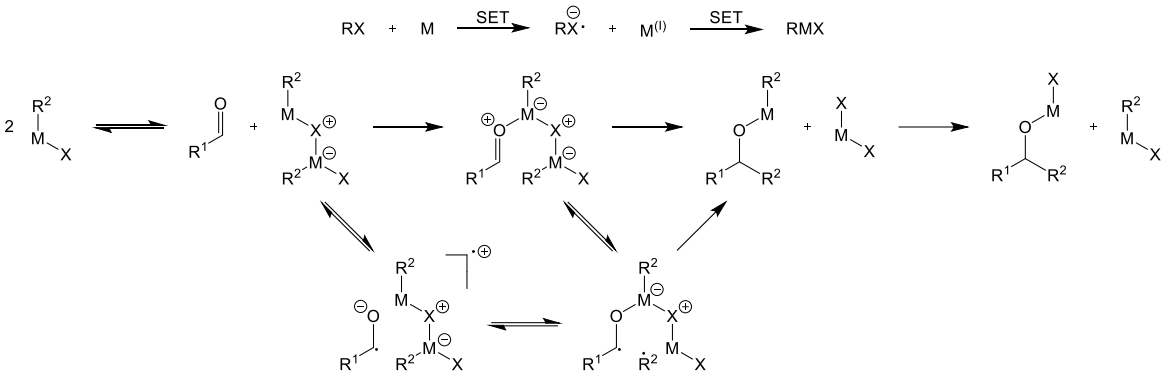

Scheme 14: Mechanism of the Grignard reaction through nucleophilic addition or single electron transfer.

Different Metals can be used in the Barbier reaction for instance magnesium, calcium, zinc, tin, und indium.[48] Tin and indium proofed to be especially potent in carbohydrate chemistry.[49,50] Over the years indium showed its superiority over tin and therefore gave rise to the indium-mediated allylation.[51]

1.4.5 Indium-mediated allylation

Indium was discovered in 1863 by the German chemists Ferdinand Reich and Hieronymous Theodor Richter when they distilled raw zinc chloride.[52] It is the softest metal despite the alkali metals and silvery-white in appearance (Figure 13).

Figure 13: Pure indium Ingot (source: pngwave.com)

It is a post-transition metal with the atomic number of 49 and an atomic weight of 114.82 g/mol.[53] It's creation through slow neutron-capture and the extremely long

half-life makes ^{115}In the most abundant isotope over the stable ^{113}In.[54] Besides its importance in chemistry it is used in semiconductors, displays, solar panels and as an inorganic pigment in combination with yttrium, manganese and other metals (Figure 14).[55–58]

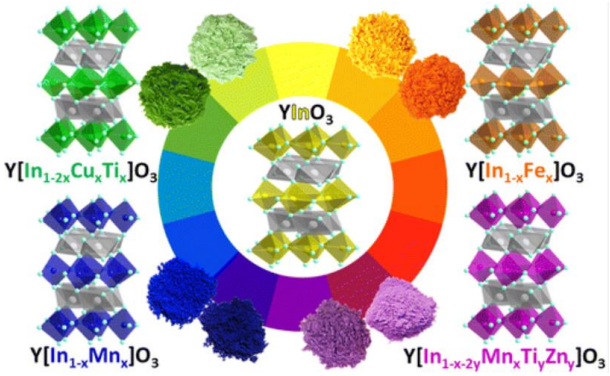

Figure 14: "YInMn Blue" the first inorganic blue pigment discovered since 1802 and other related indium pigments.[58]

Hofmann described the first organoindium compound, cyclopentadienylindium(I), in 1957.[59] The first report of an indium-mediated carbon-carbon bond formation was published by Chao and Rieke in 1975 (Scheme 15).[60]

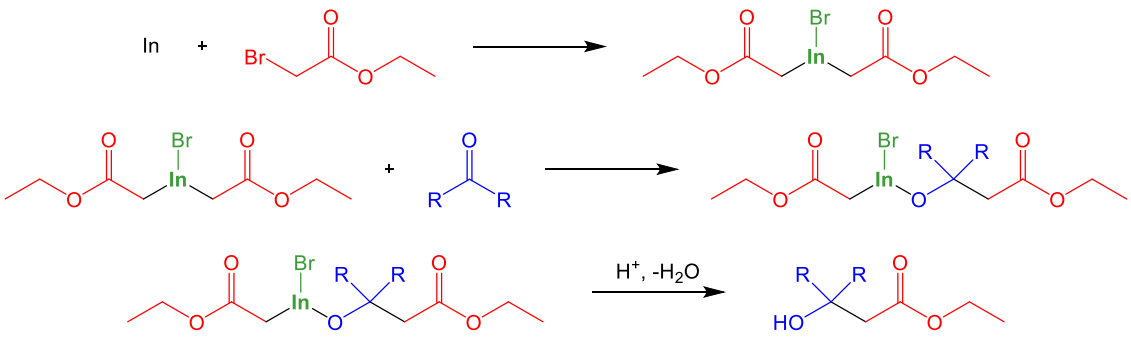

Scheme 15: First indium-mediated carbon-carbon bond formation as performed by Chao and Rieke.

In the late 1980s Araki and co-workers contributed significantly to the further exploration of this chemistry in anhydrous solvents and were the first to use allylic indium reagents.[61] Thereafter, Li and Chan could show that the indium-mediated allylation can be performed in water, showing even better results than in organic solvents.[62] Consequently, many others such as Paquette, Whitesides and Schmid

(Scheme 16) have contributed to various aspects of the indium-mediated allylation reaction in organic and especially carbohydrate chemistry.[49,63,64]

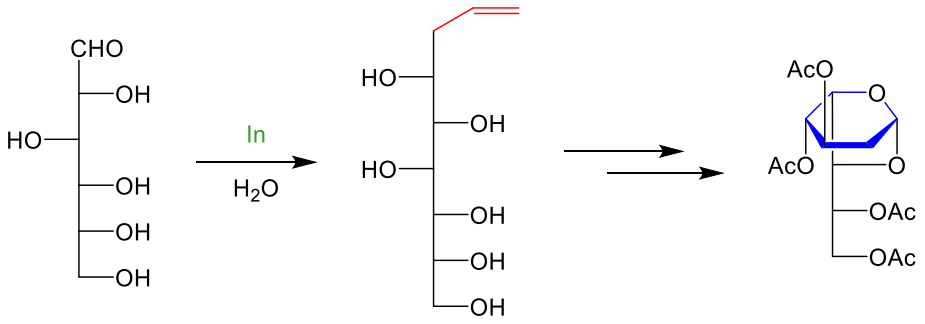

Scheme 16: Indium-mediated allylation of unprotected carbohydrates by Whitesides and Schmid.[49]

1.4.5.1 Allylindium reagents

The mechanism of the indium-mediated allylation and also the exact organoindium intermediate is still not fully understood.[65] The allylindium intermediate can be generated by the direct insertion of indium(0) into allyl halides. The formed reactive species is strongly solvent dependent, with organic solvents, such as DMF and THF, an allylindium sesquihalide is formed whereas reaction in water leads to allylindium(I) (Scheme 17).[66]

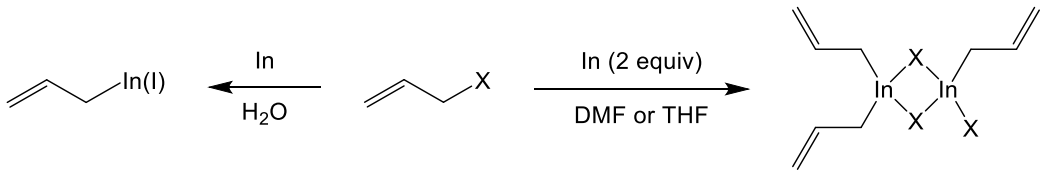

Scheme 17: Organoindium intermediate formation in water and organic solvents.

Most commonly allyl bromide and allyl iodide are used as substrates, whereas allyl chloride is relatively unreactive towards indium insertion under the same conditions. Indium can be used as a powder or in granular form, although there is evidence that in some cases 'finer' or even nano particles can improve reactivity, this trend seems not to be universal (Scheme 18).[60]

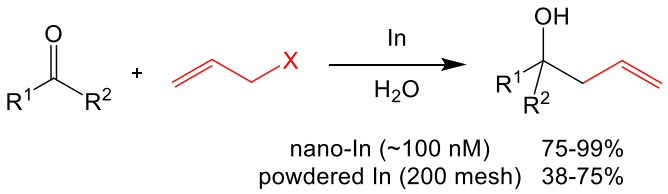

Scheme 18: Influence of indium particle size on the indium-mediated allylation.

Other sources of indium such as indium halides have been used successfully, but because of their higher costs their use has not been widely adopted (Scheme 19).[66]

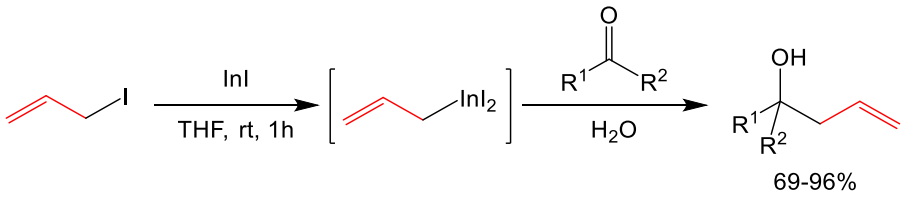

Scheme 19: Indium halides for the formation of organoindium intermediates.

1.4.5.2 Regioselectivity

In-depth studies show that indium insertion generally proceeded exclusively at the α-position.[61] Nonetheless, the reaction with the carbonyl compound takes place at the more substituted carbon regardless of the position in the starting material (Scheme 20). However, with relatively large γ-substituents such as trimetylsilyl or *tert*-butyl, α-selectivity can be observed. At this point it has to be noted that the important factor is the steric size not the degree of substitution (Scheme 20).[67]

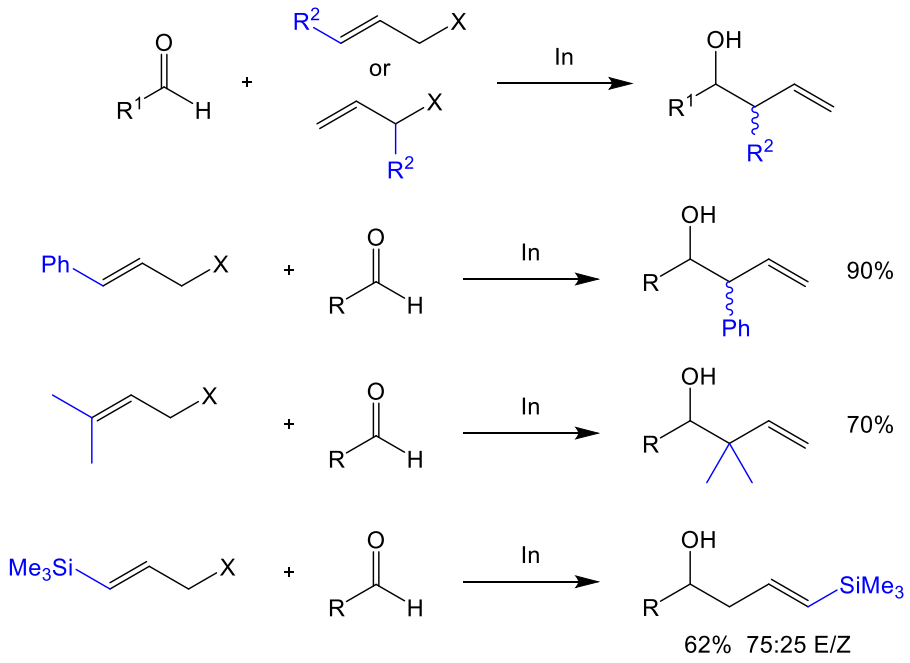

Scheme 20: The γ- and α-selectivity of the indium-mediated allylation.

The regioselectivity of the reaction is not affected by conjugation and can produce deconjugated products, additionally, *E* or *Z*-double bonds give the same product (Scheme 22).[68]

1.4.5.3 Diastereoselectivity

Depending on the substrates there are up to two new stereocenters generated in the indium-mediated allylation. The first one is the newly formed hydroxy group and the second is a possible substituent present in the allylation reagent (Scheme 21).

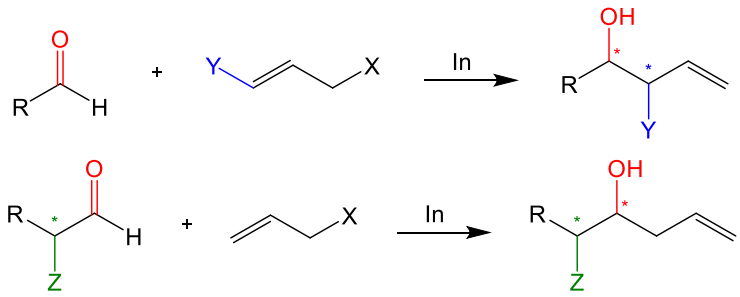

Scheme 21: The two possibilities of new stereocenters generated by the indium-mediated allylation and the possible interaction with existing stereocenters.

If there is a substituent on the allyl compound the diastereoselectivity depends on the aldehyde and the allylic halide, but not on the double bond geometry (Scheme 22). Bulkier substituents on the allyl compound and the aldehyde significantly increase *anti* selectivity up to the point where α-selectivity takes place (Scheme 20 & Scheme 22).[66]

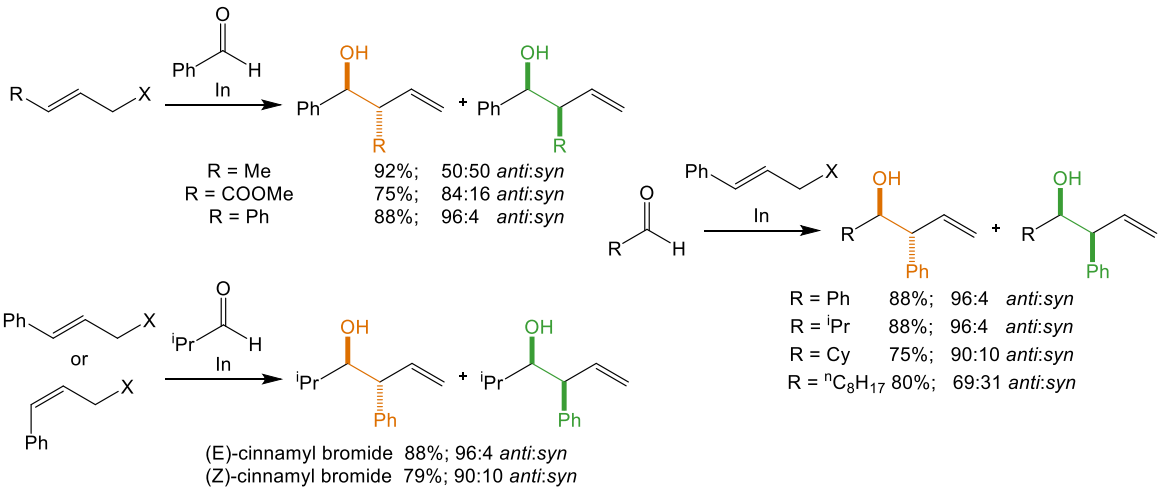

Scheme 22: Influence of the α-substituents on the diastereoselectivity of the indium-mediated allylation.

The diastereoselectivity of the newly formed hydroxy group can be either *anti* or *syn* and is strongly dependent on the α-substituent on the carbonyl. If the substituent is a strong α-chelating group, such as hydroxyl, the product has developed *syn* configuration.[68] This can be explained by a Cram-chelation model involving the chelation of allylindium with α-chelating group on the aldehyde.[66] However, a weak or non-chelating group leads to *anti* configuration and proceeds over a Felkin-Ahn transition state (Scheme 23).[68]

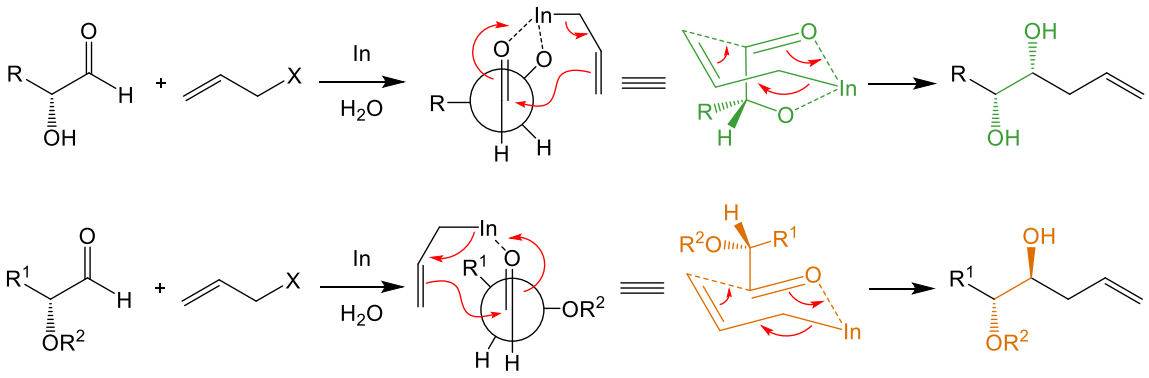

Scheme 23: Transition states of chelating and non-chelating substituents on the α-position.

1.4.5.4 Indium-mediated allylations of carbohydrates

Many of the mentioned properties make the indium-mediated allylation especially useful in carbohydrate chemistry. The use of protic solvents makes it possible to work with unprotected carbohydrates. Additionally, the diastereoselectivity can be easily controlled with the corresponding protection of the α-substituent of the carbohydrate (Scheme 23).[69] Therefore, carbohydrate chemists were the first who explored this reaction type. One prominent contribution has been made by Li and Chan who could synthesis KDO in only 3 steps from D-mannose in 1992 (Scheme 24).[63]

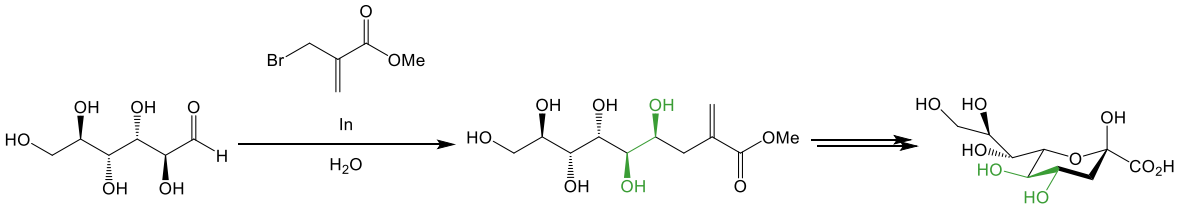

Scheme 24: Synthesis of KDO as performed by Li and Chan.

Only one year later Schmid, Kim and Whitesides explored the possibilities of the indium-mediated allylation with an extensive look at many different solvent systems, allylation reagents and carbohydrate based substrates and compared it to their earlier work with tin.[49,50] Over the following years until now the indium-mediated allylation proofed its versatility in carbohydrate chemistry and has been used to solve many different as well as difficult synthetic problems.[69–72]

1.5 Structural elucidation of carbohydrates

1.5.1 Historical structural elucidation

1.5.1.1 Conformation

Many different discoveries contributed to the first structural elucidation of carbohydrates. The molecular formula, the reduction of Tollen's reagent and the formation of a pentaacetate established that glucose is a pentahydroxy aldehyde with six carbon atoms. Furthermore, its straight-chain structure could be determined through different derivatizations such as the reduction to n-heptanoic acid (Figure 15).

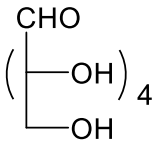

Figure 15: Known structure for glucose.

Nonetheless, there were still some properties of carbohydrates, like the mutarotation that occurs in aqueous solutions, which could not be explained. Extensive research of this anomaly, which was discovered by Dubrunfaut, led to the conclusion that it could be attributed to the existence of two interconvertible stereoisomer that were designated as α- and β-form.[73] Tollens proposed a five-membered cyclic oxide structure to account for this phenomenon (Figure 16).[74]

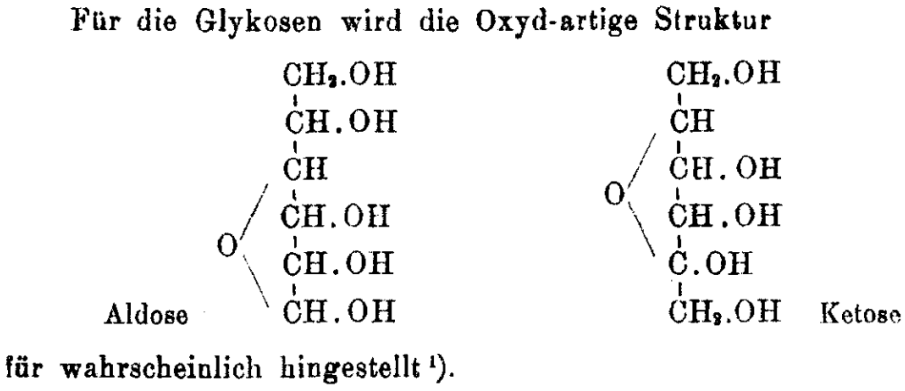

Figure 16: Tollens proposed structure for glucose.[74]

However, at that time there was no experimental evidence and it took 12 years until Tanret could isolate the two forms of glucose.[75] Haworth and others were then able to confirm the six-membered cyclic hemiacetyl structure (Figure 17).[76]

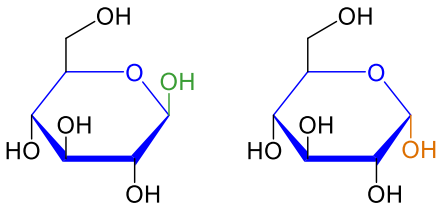

Figure 17: Haworth projection of D-Glucose.

1.5.1.2 Stereochemistry

The discovery of phenylhydrazine by Emil Fischer was an important milestone in carbohydrate chemistry.[77] It allowed him and others to separate crystallize and categorize carbohydrates with the help of their osazones (Scheme 25).

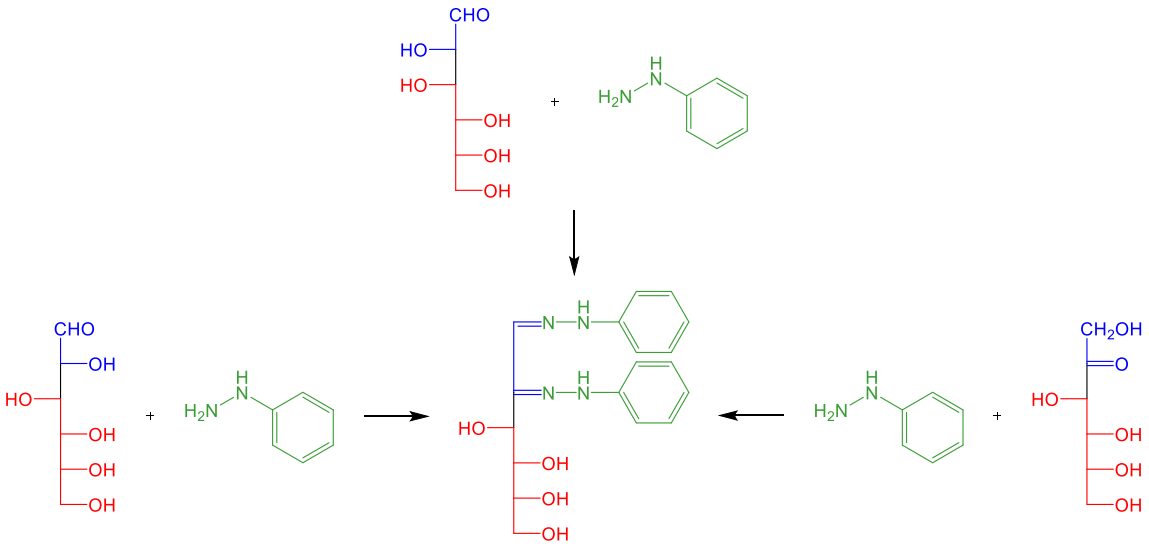

Scheme 25: Reactions of mannose, glucose and fructose to their osazone.

Heinrich Kiliani could differentiate glucose and fructose as aldohexose and ketohexose, respectively. They were found to give the same phenylosazone as mannose. Therefore, Fischer could determine that they have the same configuration at carbon 3, 4 and 5 (Scheme 25).[78] This in combination with the Kiliani-Fischer synthesis and the Wohl degradation (Scheme 26), which was invented in Fischer's laboratory, were powerful tools which led to the discovery of the carbohydrate "family tree" (Figure 18).[78]

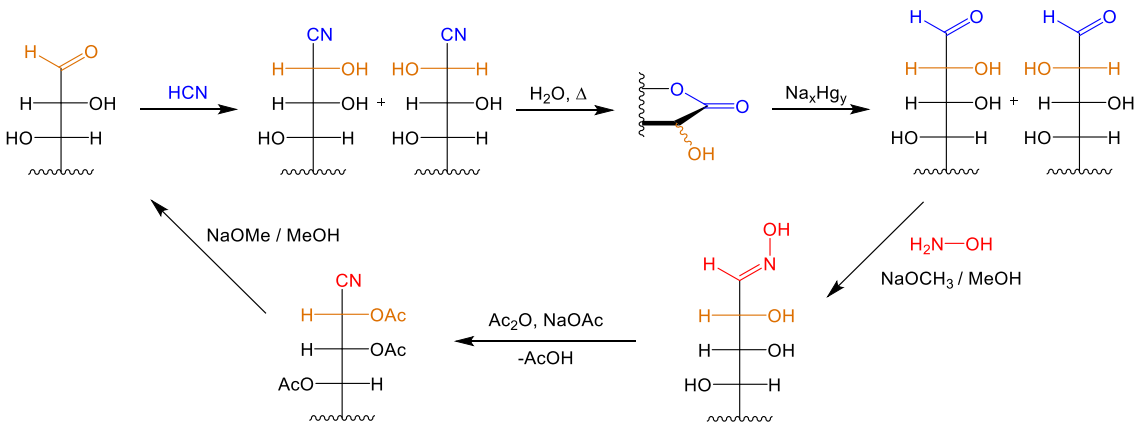

Scheme 26: Kiliani-Fischer synthesis and the Wohl degradation of carbohydrates.

Additionally, the conversion of carbohydrates to alditols or into dicarboxylic acids and comparison of the optical activity of the products gave further insights into their stereochemistry and their chiral relation. Observations from the first synthesis of glucose also proved crucial in structural elucidation of aldoses.[78] These tools and their thorough use on different carbohydrates and the extensive comparison of the physical as well as chemical properties of the resulting compounds made it possible to elucidate the stereochemistry in the carbohydrate tree by Fischer (Figure 18). Although, he could only determine the relative stereochemistry, he was aware that the decision for an absolute configuration was arbitrary.[78] The fact that he has chosen the correct configuration can be considered lucky and has not been realized until after his death.

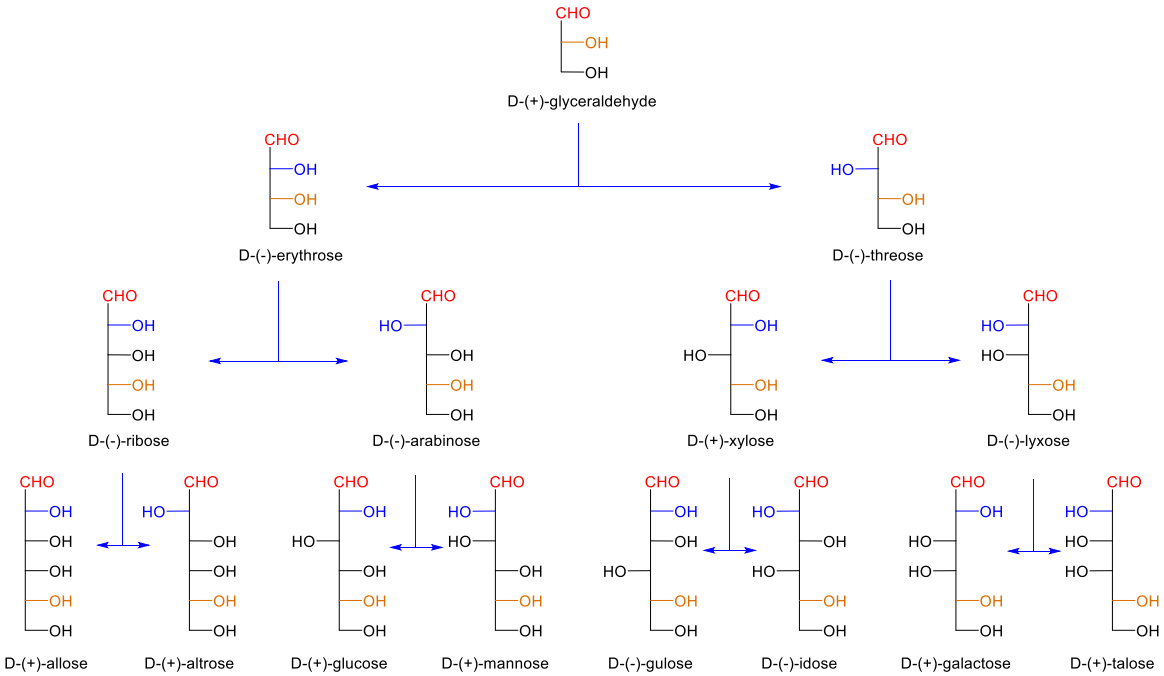

Figure 18: Family tree of D-aldoses.

These historic findings lead to the development of modern systematic carbohydrate chemistry. Nowadays, scientist have more sophisticated tools for the structural elucidation of carbohydrates such as nuclear magnetic resonance (NMR), mass spectrum and X-ray crystallography.

1.5.2 Mass spectrometry

Mass spectrometric methods are analytical techniques for the measurement of the mass-to-charge ratio of ions. It can be used for the identification of pure synthetic compounds as well as for the identification of complex mixtures coupled with separation techniques such as high-performance liquid chromatography and capillary electrophoresis.[79] Although fragmentation experiments are possible, in synthetic carbohydrate chemistry it is mostly used for the identification of the molecular formula. However it is still a very important tool in glycobiology, for the structural analysis of poly- and oligosaccharides.[10] There it can be used for the characterization of pure individual glycopolymers that are too complex for conventional NMR analysis or the screening of cell- and tissue-extracts. The use of databases as well as fingerprinting of samples in the recent years have led to a significant increase in research and output in this field.[80]

1.5.3 X-Ray

X-Ray crystallography can determine the atomic and molecular structure of a crystal. Although the typical configurational heterogeneity of carbohydrates in solution tends to inhibit crystallization, if crystals can be obtained it is one of the most powerful experimental methods for the structural elucidation of carbohydrates.[81] It is also possible to investigate the exact angles around the glycosidic linkage and hydrogen bonds between the different monosaccharide units in the crystal of an oligosaccharide. Additionally, there are an increasing number of crystal structures for glycoproteins and protein-carbohydrate complexes.[81] Despite the fact that this information is not necessary an exact representation of the configuration in solution, it gives further insight into the interactions of carbohydrates with proteins.

1.5.4 Nuclear magnetic resonance (NMR)

NMR allows the analysis of the molecular structure by observing and measuring the selective absorption of high-frequency radio waves by certain atomic nuclei when placed in a powerful magnetic field. Only isotopes with a nonzero nuclear spin are applicable in NMR spectroscopy. The most frequently measured isotopes are ^{1}H and ^{13}C, but many other elements have NMR active isotopes as well. In case such heteronuclei are part of the carbohydrate structure, NMR experiments involving isotopes like ^{15}N, ^{19}F or ^{31}P can provide additional valuable information. Generally, NMR is the most useful analytical tool for the structural elucidation of organic compounds. The chemical shift assignment is the first essential step for the structural analysis. As the observed resonance frequency is influenced by the electron density around the spin of interest, it allows insight into the chemical environment, substitution as well as three-dimensional structure. The chemical shift range for carbohydrates is very narrow, in case of aldoses two well-defined regions can be addressed, namely the anomeric region at 4.5-6.0 ppm and the “bulk” region from 3.0-4.5 ppm.[82,83] Figure 19 gives an example showing simulated subspectra for the two anomeres of glucose. Having only one neighbor hydrogen the anomeric proton appears as a doublet sharing a spin-coupling with H-2 at a chemical shift of around 5.2

ppm for the α-pyranose configuration or at 4.7 ppm for the β-pyranose in the unprotected form.

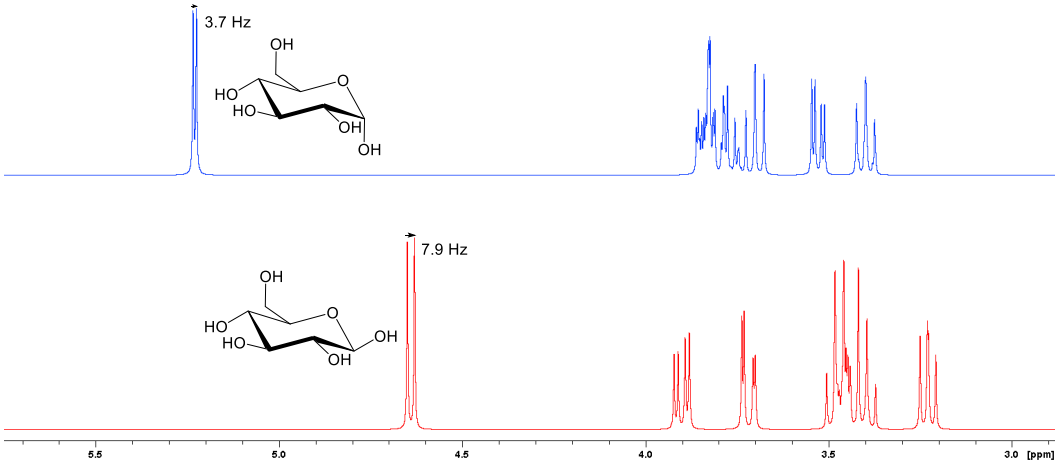

Figure 19: ^{1}H-NMR spectrum of α- and β-D-glucopyranose.

Spin-coupling constants are the second important NMR information, as such a fine splitting of individual signals induced by neighboring spins will establish a close connectivity in the binding network. This is particularly useful in carbohydrate NMR, because the coupling constant additionally gives insight into the dihedral angle of vicinal protons necessary to evaluate ring conformations especially for pyranoses.[83]

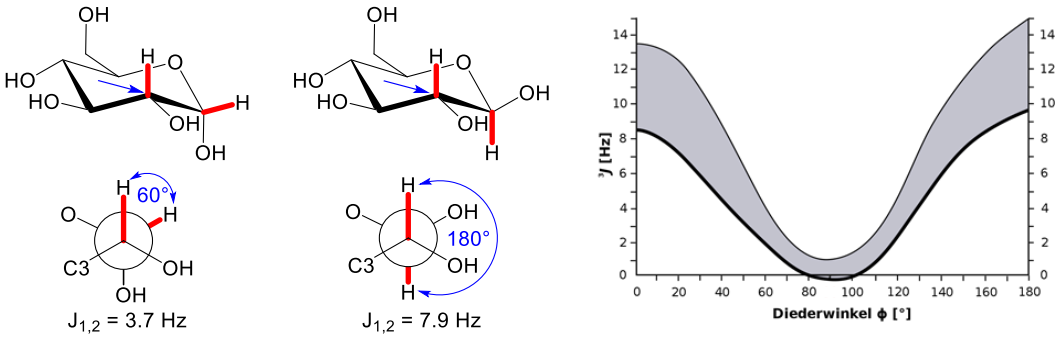

Figure 20: Karplus relationship and coupling constants of α- and β-D-glucopyranose.

Additionally, 2D NMR experiments can give further information on bond or spatial relationships by resolving the very narrow and thus overcrowded chemical shift region of carbohydrates on a second frequency axis. Homonuclear through-bond experiments

like COSY or TOCSY show correlations over two or three bonds or elucidate whole spin systems, respectively. Heteronuclear experiments like HSQC and HMBC show ^{1}H-^{13}C cross-peaks either over one bond or establish long-range correlations over usually up to three bonds. Furthermore, through-space correlation methods such as NOESY can show spatial relationships independently from the number of bonds between the dipolar coupled spins.

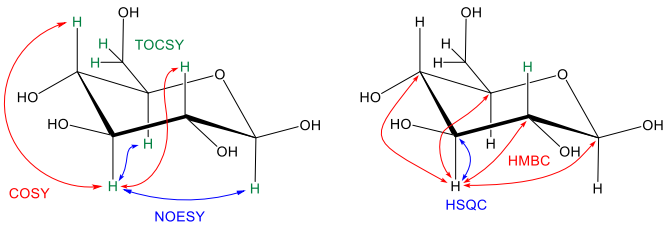

Figure 21: Cross-peaks from H-3 in different 2D NMR experiments; on the left homonuclear and on the right heteronuclear experiments.

Although these experiments may solve most of the problems in the structural elucidation of organic compounds the relative crowded "bulk" region of carbohydrates can lead to second order effects in the fine splitting of spin-coupled protons.[84] In first order spectra chemical shift (δ) and coupling (*J*) values are directly measurable from line positions. However, this is only true if the chemical shift difference (Δν) between spin-coupled protons are large compared to the coupling constants, if Δν/*J* (in Hz) is smaller than 5, second order effects appear. The so called "roof effect" is a striking example of such phenomena leading to changes in the intensity of individual lines within a multiplet. If the ratio Δν/*J* moves closer to 1 second order effects become very pronounced, additional lines and severe distortions in intensity show up. As a consequence, chemical shifts and coupling constants can no longer be measured directly in the spectrum, but rather need to be calculated with a spin simulation based on the solution of the time-independent Schroedinger equation.

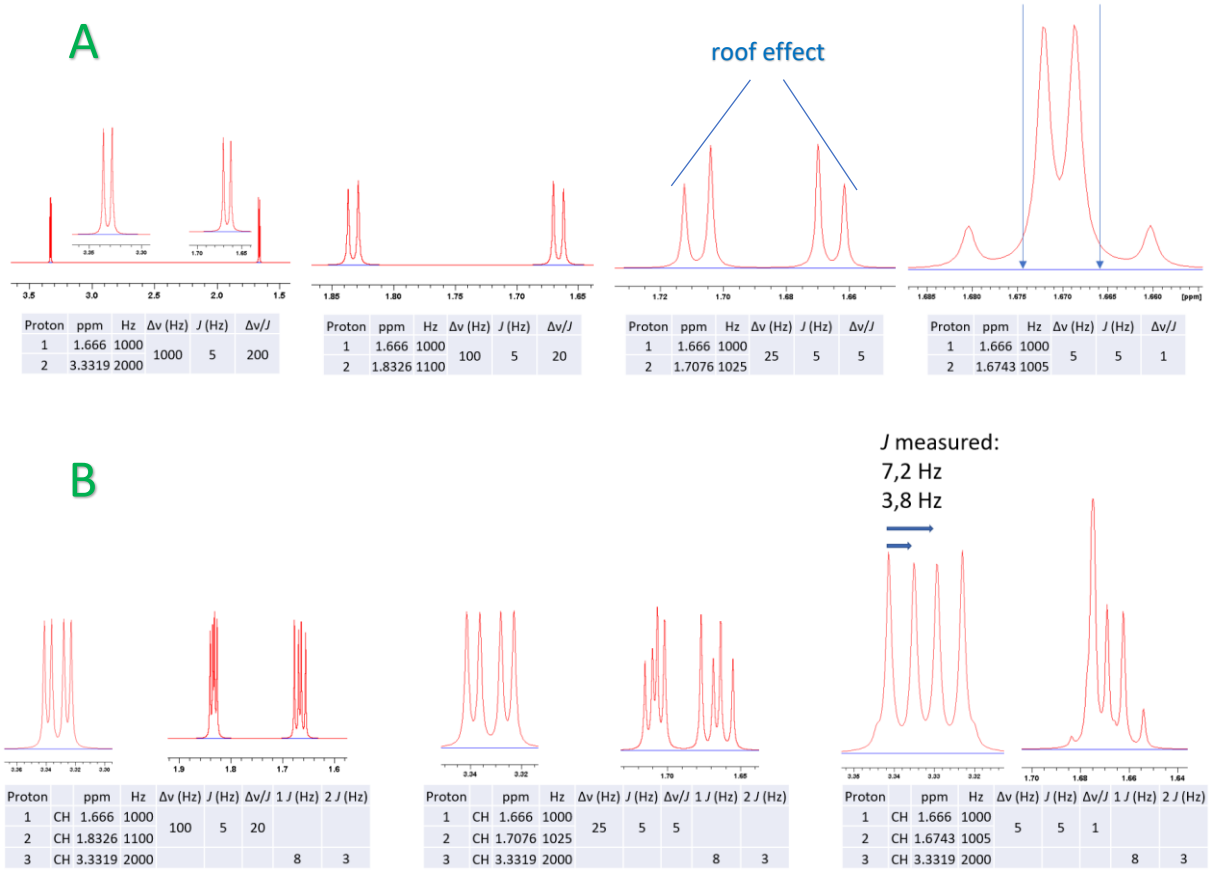

Proton	ppm	Hz	Δν (Hz)	J (Hz)	Δν/J
1	1.666	1000	1000	5	200
2	3.3319	2000			

Proton	ppm	Hz	Δν (Hz)	J (Hz)	Δν/J
1	1.666	1000	100	5	20
2	1.8326	1100			

Proton	ppm	Hz	Δν (Hz)	J (Hz)	Δν/J
1	1.666	1000	25	5	5
2	1.7076	1025			

Proton	ppm	Hz	Δν (Hz)	J (Hz)	Δν/J
1	1.666	1000	5	5	1
2	1.6743	1005			

Proton		ppm	Hz	Δν (Hz)	J (Hz)	Δν/J	1 J (Hz)	2 J (Hz)
1	CH	1.666	1000	100	5	20		
2	CH	1.8326	1100					
3	CH	3.3319	2000				8	3

Proton		ppm	Hz	Δν (Hz)	J (Hz)	Δν/J	1 J (Hz)	2 J (Hz)
1	CH	1.666	1000	25	5	5		
2	CH	1.7076	1025					
3	CH	3.3319	2000				8	3

Proton		ppm	Hz	Δν (Hz)	J (Hz)	Δν/J	1 J (Hz)	2 J (Hz)
1	CH	1.666	1000	5	5	1		
2	CH	1.6743	1005					
3	CH	3.3319	2000				8	3

Figure 22: A) Represents an AB-system with constant coupling and decreasing shift difference and "roof effect" and the real shift for the last system. B) Shows an ABX-system and the effects of an AB-system on coupled protons.

Nonetheless, NMR is the most universal and potent analytical tool for the analysis of synthetic carbohydrate compounds. Further improvements in instrument performance and computational assistance in the form of simulations and predictions will only further enhance this trend.[85]

1.6 Abbreviations

ADP	Adenosine diphosphate
ATP	Adenosine triphosphate
BR	Barbier reaction
COSY	Correlation spectroscopy
DIPEA	*N*,*N*-Diisopropylethylamine
DMF	Dimethylformamide
HMBC	Heteronuclear multiple-bond correlation spectroscopy
HSQC	Heteronuclear single-quantum correlation spectroscopy
IMA	Indium-mediated allylations
KDN	2-Keto-3-deoxy-D-*glycero*-D-*galacto*-nononic acid
KDO	3-Deoxy-D-*manno*-oct-2-ulosonic acid
LDA	Lithium diisopropylamide
MS	Mass spectrometry
NADP	Nicotinamide adenine dinucleotide phosphate
NADPH	Nicotinamide adenine dinucleotide phosphate hydrogen
NMR	Nuclear magnetic resonance
NOESY	Nuclear Overhauser effect spectroscopy
RUBisCO	Ribulose-1,5-bisphosphate carboxylase oxygenase
SET	Single-electron transfer
TEA	Triethylamine
THF	Tetrahydrofuran
TOCSY	Total correlation spectroscopy
UDP	Uridine diphosphate
UTP	Uridine triphosphate

1.7 References

(1) Sanders, L. M. *Carbohydrate: Digestion, Absorption and Metabolism*, 1st ed.; Elsevier Ltd., **2015**.

(2) Nelson, N.; Yocum, C. F. Structure and Function of Photosystems I and II. *Annu. Rev. Plant Biol.* **2006**, *57*, 521–565.

(3) Stryer, L.; Tymoczko, J.; Berg, J. *Stryer Biochemie*, 6th ed.; Spektrum Akademischer Verlag, **2007**.

(4) Spreitzer, R. J.; Salvucci, M. E. Rubisco: Structure, Regulatory Interactions, and Possibilities for a Better Enzyme. *Annu. Rev. Plant Biol.* **2002**, *53*, 449–475.

(5) Fernie, A. R.; Carrari, F.; Sweetlove, L. J. Respiratory Metabolism: Glycolysis, the TCA Cycle and Mitochondrial Electron Transport. *Curr. Opin. Plant Biol.* **2004**, *7*, 254–261.

(6) Klemm, D.; Heublein, B.; Fink, H. P.; Bohn, A. Cellulose: Fascinating Biopolymer and Sustainable Raw Material. *Angew. Chemie - Int. Ed.* **2005**, *44*, 3358–3393.

(7) Cosgrove, D. J. Growth of the Plant Cell Wall. *Nat. Rev. Mol. Cell Biol.* **2005**, *6*, 850–861.

(8) Loix, C.; Huybrechts, M.; Vangronsveld, J.; Gielen, M.; Keunen, E.; Cuypers, A. Reciprocal Interactions between Cadmium-Induced Cell Wall Responses and Oxidative Stress in Plants. *Front. Plant Sci.* **2017**, *8*, 1–19.

(9) Tang, W. J.; Fernandez, J. G.; Sohn, J. J.; Amemiya, C. T. Chitin Is Endogenously Produced in Vertebrates. *Curr. Biol.* **2015**, *25*, 897–900.

(10) Lindhorst, T. K. *Essentials of Carbohydrate Chemistry and Biochemistry*; Wiley-VCH: Weinheim, **2007**.

(11) Zaku, S. G.; Aguzue, S. A. E. O. C.; Thomas, S. A. Extraction and Characterization of Chitin ; a Functional Biopolymer Obtained from Scales of Common Carp Fish (*Cyprinus Carpio* l .): A Lesser Known Source. *African J. Food Sci.* **2011**, *5*, 478–483.

(12) Tilghman, S. L.; Nierth-Simpson, E. N.; Wallace, R.; Burow, M. E.; McLachlan, J. A.

Environmental Hormones: Multiple Pathways for Response May Lead to Multiple Disease Outcomes. *Steroids* **2010**, *75*, 520–523.

(13) Bucior, I.; Burger, M. M. Carbohydrate-Carbohydrate Interaction as a Major Force Initiating Cell-Cell Recognition. *Glycoconj. J.* **2004**, *21*, 111–123.

(14) Brandley, B. K.; Schnaar, R. L. Cell-Surface Carbohydrates in Cell Recognition and Response. *J. Leukoc. Biol.* **1986**, *40*, 97–111.

(15) Bucior, I.; Scheuring, S.; Engel, A.; Burger, M. M. Carbohydrate-Carbohydrate Interaction Provides Adhesion Force and Specificity for Cellular Recognition. *J. Cell Biol.* **2004**, *165*, 529–537.

(16) Strzyz, P. Bend It like Glycocalyx. *Nat. Rev. Mol. Cell Biol.* **2019**, *20*, 388.

(17) Shurer, C. R.; Kuo, J. C. H.; Roberts, L. D. M.; Gandhi, J. G.; Colville, M. J.; Enoki, T. A.; Pan, H.; Su, J.; Noble, J. M.; Hollander, M. J.; O'Donnell, J. P.; Yin, R.; Pedram, K.; Möckl, L.; Kourkoutis, L. F.; Moerner, W. E.; Bertozzi, C. R.; Feigenson, G. W.; Reesink, H. L.; Paszek, M. J. Physical Principles of Membrane Shape Regulation by the Glycocalyx. *Cell* **2019**, *177*, 1757–1770.

(18) Angata, T.; Varki, A. Chemical Diversity in the Sialic Acids and Related α-Keto Acids: An Evolutionary Perspective. *Chem. Rev.* **2002**, *102*, 439–469.

(19) Chen, X.; Varki, A. Advances in the Biology and Chemistry of Sialic Acids. *ACS Chem. Biol.* **2010**, *5*, 163–176.

(20) Butlerov, A. – Formation Synthétiqued'une. *Justus Liebigs Ann. Chem.* **1861**, *120*, 295–298.

(21) Delidovich, I. V.; Simonov, A. N.; Taran, O. P.; Parmon, V. N. Catalytic Formation of Monosaccharides: From the Formose Reaction towards Selective Synthesis. *ChemSusChem* **2014**, *7*, 1833–1846.

(22) Levy, D. E.; Fügedi, P. *The Organic Chemistry of Sugars*, 1st ed.; Taylor & Francis Group, **2005**.

(23) Cannizzaro, S. Ueber Den Der Benzoësäure Entsprechenden Alkohol. *Justus Liebigs Ann. Chem.* **1853**, *88*, 129–130.

(24) Breslow, R. On the Mechanism of the Formose Reaction. *Tetrahedron Lett.* **1959**, *1*, 22–26.

(25) Appayee, C.; Breslow, R. Deuterium Studies Reveal a New Mechanism for the Formose Reaction Involving Hydride Shifts. *J. Am. Chem. Soc.* **2014**, *136*, 3720–3723.

(26) Ricardo, A.; Frye, F.; Carrigan, M. A.; Tipton, J. D.; Powell, D. H.; Benner, S. A. 2-Hydroxymethylboronate as a Reagent to Detect Carbohydrates: Application to the Analysis of the Formose Reaction. *J. Org. Chem.* **2006**, *71*, 9503–9505.

(27) Jalbout, A. F.; Abrell, L.; Adamowicz, L.; Polt, R.; Apponi, A. J.; Ziurys, L. M. Sugar Synthesis from a Gas-Phase Formose Reaction. *Astrobiology* **2007**, *7*, 433–442.

(28) Kopetzki, D.; Antonietti, M. Hydrothermal Formose Reaction. *New J. Chem.* **2011**, *35*, 1787–1794.

(29) Thripati, S.; Ramabhadran, R. O. Metal-Ion- and Hydrogen-Bond-Mediated Interstellar Prebiotic Chemistry: The First Step in the Formose Reaction. *J. Phys. Chem. A* **2017**, *121*, 8659–8674.

(30) Kiliani, H.; Hco, C.; Choh, O. H. 767 163. Heinrich Kiliani: Ueber Die Einwirkung. *Berichte der Dtsch. Chem. Gesellschaft* **1886**, *19*, 767–772.

(31) Monrad, R. N.; Madsen, R. Modern Methods for Shortening and Extending the Carbon Chain in Carbohydrates at the Anomeric Center. *Tetrahedron* **2011**, *67*, 8825–8850.

(32) Kuhn, R.; Grassner, H. MECHANISMUS DER KATALYTISCHEN HYDRIERUNG VON HYDROXYNITRILEN. A-D-Fructoheptose Aus D-Fructosecyanhydrin. *Justus Liebigs Ann. Chem.* **1958**, *612*, 55–64.

(33) von Richter, V. V. von Richter, Aus St. Petersburg Am 17. October 1869. *Berichte der Dtsch. Chem. Gesellschaft* **1869**, *2*, 552–553.

(34) Wurtz, A. Ueber Einen Aldehyd-Alkohol. *J. für Prakt. Chemie* **1872**, *5*, 457–464.

(35) Brown, H. C.; Dhar, R. K.; Bakshi, R. K.; Pandiarajan, P. K.; Singaram, B. Major Effect of the Leaving Group in Dialkylboron Chlorides and Triflates in Controlling

the Stereospecific Conversion of Ketones into Either (E)- or (Z)-Enol Borinates. *J. Am. Chem. Soc.* **1989**, *111*, 3441–3442.

(36) Evans, D. A.; Rieger, D. L.; Bilodeau, M. T.; Urpi, F. Stereoselective Aldol Reactions of Chlorotitanium Enolates. An Efficient Method for the Assemblage of Polypropionate-Related Synthons. *J. Am. Chem. Soc.* **1991**, *113*, 1047–1049.

(37) Evans, D. A.; Dart, M. J.; Duffy, J. L.; Rieger, D. L. Double Stereodifferentiating Aldol Reactions. The Documentation of "Partially Matched" Aldol Bond Constructions in the Assemblage of Polypropionate Systems. *J. Am. Chem. Soc.* **1995**, *117*, 9073–9074.

(38) Roush, W. R. Concerning the Diastereofacial Selectivity of the Aldol Reactions of α-Methyl Chiral Aldehydes and Lithium and Boron Propionate Enolates. *J. Org. Chem.* **1991**, *56*, 4151–4157.

(39) Palomo, C.; Oiarbide, M.; García, J. M. Current Progress in the Asymmetric Aldol Addition Reaction. *Chem. Soc. Rev.* **2004**, *33*, 65–75.

(40) Evans, D. A.; Bartroli, J.; Shih, T. L. Enantioselective Aldol Condensations. 2. Erythro-Selective Chiral Aldol Condensations via Boron Enolates. *J. Am. Chem. Soc.* **1981**, *103*, 2127–2129.

(41) Trost, B. M.; Brindle, C. S. The Direct Catalytic Asymmetric Aldol Reaction. *Chem. Soc. Rev.* **2010**, *39*, 1600–1632.

(42) Hajos, Z. G.; Parrish, D. R. Asymmetric Synthesis of Bicyclic Intermediates of Natural Product Chemistry. *J. Org. Chem.* **1974**, *39*, 1615–1621.

(43) Eder, B. U.; Sauer, G.; Wiechert, R. New Type of Asymmetric Cyclization to Optically Active Steroid CD Partial Structures. *Angew. Chemie - Int. Ed.* **1971**, *10*, 496–497.

(44) Barbier, P. Synthèse Du Diéthylhepténol. *C. R. Hebd. Seances Acad. Sci.* **1899**, *128*, 110–111.

(45) Grignard, V. Sur Quelques Nouvelles Combinaisons Organométalliques Du Magnèsium et Leur Application à Des Synthèses d'alcools et d'hydrocarbures. *C.*

R. Hebd. Seances Acad. Sci. **1900**, *130*, 1322–1324.

(46) Maruyama, K.; Katagiri, T. Mechanism of the Grignard Reaction. *J. Phys. Org. Chem.* **1989**, *2*, 205–213.

(47) Brückner, R. *Reaktionsmechanismen: Organische Reaktionen, Stereochemie, Moderne Synthesemethoden*, 3rd ed.; Springer Verlag, **2004**.

(48) Blomberg, C.; Hartog, F. A. The Barbier Reaction - A One-Step Alternative for Syntheses via Organomagnesium Compounds. *Synthesis (Stuttg).* **1977**, No. 1, 18–30.

(49) Kim, E.; Gordon, D. M.; Schmid, W.; Whitesides, G. M. Tin- and Indium-Mediated Allylation in Aqueous Media: Application to Unprotected Carbohydrates. *J. Org. Chem.* **1993**, *58*, 5500–5507.

(50) Schmid, W.; Whitesides, G. M. Carbon-Carbon Bond Formation in Aqueous Ethanol: Diastereoselective Transformation of Unprotected Carbohydrates to Higher Carbon Sugars Using Allyl Bromide and Tin Metal. *J. Am. Chem. Soc.* **1991**, *113*, 6674–6675.

(51) Paquette, L. A. Fundamental Mechanistic Characteristics and Synthetic Applications of Allylations Promoted by Indium Metal in Aqueous Media. In *Synthesis*; Georg Thieme Verlag Stuttgart, **2003**; Vol. 5, pp 765–774.

(52) Reich, F.; Richter, T. XXII. Ueber Das Indium. *J. für Prakt. Chemie* **1863**, *90*, 172–176.

(53) Alfantazi, A. M.; Moskalyk, R. R. Processing of Indium: A Review. *Miner. Eng.* **2003**, *16*, 687–694.

(54) Boothroyd, A. I. Heavy Elements in Stars. *Science* **2006**, *314*, 1690–1691.

(55) Surmann, P.; Zeyat, H. Voltammetric Analysis Using a Self-Renewable Non-Mercury Electrode. *Anal. Bioanal. Chem.* **2005**, *383*, 1009–1013.

(56) Powalla, M.; Dimmler, B. Scaling up Issues of CIGS Solar Cells. *Thin Solid Films* **2000**, *361*, 540–546.

(57) Smith, A. E.; Mizoguchi, H.; Delaney, K.; Spaldin, N. A.; Sleight, A. W.;

Subramanian, M. A. Mn3+ in Trigonal Bipyramidal Coordination: A New Blue Chromophore. *J. Am. Chem. Soc.* **2009**, *131*, 17084–17086.

(58) Li, J.; Lorger, S.; Stalick, J. K.; Sleight, A. W.; Subramanian, M. A. From Serendipity to Rational Design: Tuning the Blue Trigonal Bipyramidal Mn3+ Chromophore to Violet and Purple through Application of Chemical Pressure. *Inorg. Chem.* **2016**, *55*, 9798–9804.

(59) Fischer, E. O.; Hofmann, H. P. Metall-cyclopentadienyle Des Indiums. *Angew. Chemie* **1957**, *69*, 639–640.

(60) Chao, L.-C. chung; Rieke, R. D. Activated Metals. IX. A New Reformatsky Reagent Involving Activated Indium for the Preparation of β-Hydroxy Esters. *J. Org. Chem.* **1975**, *40*, 2253–2255.

(61) Araki, S.; Shimizu, T.; Johar, P. S.; Jin, S. J.; Butsugan, Y. Preparation and Some Reactions of Allylic Indium Reagents. *J. Org. Chem.* **1991**, *56*, 2538–2542.

(62) Li, C. J.; Chan, T. H. Organometalllc Reactions in Aqueous Media. *Tetrahedron Lett.* **1991**, *32*, 7017–7020.

(63) Chan, T. H.; Li, C. J. A Concise Chemical Synthesis of (+)-3-Deoxy-D-Glycero-D-Galacto-Nonulosonic Acid (KDN). *J. Chem. Soc. Chem. Commun.* **1992**, No. 10, 747–748.

(64) Paquette, L. A.; Mitzel, T. M. Chelation Control Associated with Organometallic Addition Reactions in Water. The High Stereoselectivity Offered by α- and β-Hydroxyl Substituents Obviates the Need for Protecting Groups. *Tetrahedron Lett.* **1995**, *36*, 6863–6866.

(65) Bowyer, W. J.; Singaram, B.; Sessler, A. M. Nature of the Intermediates Formed during Indium Mediated Allylation under Barbier Conditions . Spectroscopic and Experimental Data on Allylindium Species. *Tetrahedron* **2011**, *67*, 7449–7460.

(66) Shen, Z.; Wang, S.; Chok, Y.; Xu, Y.; Loh, T. Organoindium Reagents : The Preparation and Application in Organic Synthesis. *Chem. Rev.* **2013**, *113*, 271–401.

(67) Isaac, M.; Chan, T. Lndium Mediated Coupling of Aldehydes with Allyl Bromides in Aqueous Media. The Issue of Regio- and Diastereo-Selectivity. *Tetrahedron Lett.* **1995**, *36*, 8957–8960.

(68) Li, C. J.; Chan, T.-H. Organic Syntheses Using Indium-Mediated and Catalyzed Reactions in Aqueous Media. *Tetrahedron* **1999**, *55*, 11149–11176.

(69) Gintner, M.; Denner, C.; Schmölzer, C.; Fischer, M.; Frühauf, P.; Kählig, H.; Schmid, W. Synthesis of 3-Deoxy-2-Uloses via the Indium-Mediated Allylation Reaction. *Monatshefte fur Chemie* **2019**, *150*, 849–860.

(70) Prenner, R. H.; Schmid, W. Indium Mediated Allylation in Carbohydrate Chemistry : A Convenient Synthesis of 3-Deoxy-D-Arabino-2-Heptulosonic Acid (DAH) and 3-Deoxy-D-Arabino-2-Heptulose (Kamusol). *Monatshefte für Chemie* **1996**, *127*, 1045–1050.

(71) Balla, E.; Zamyatina, A.; Hofinger, A.; Kosma, P. Synthesis of a Deoxy Analogue of ADP L-Glycero-d-Manno-Heptose. *Carbohydr. Res.* **2007**, *342*, 2537–2545.

(72) Denner, C.; Gintner, M.; Kählig, H.; Schmid, W. Indium-Mediated C-Allylation of Melibiose. *Beilstein J. Org. Chem.* **2019**, *15*, 2458–2464.

(73) Dubrunfaut, A.-P. Note Sur Quelques Phénomènes Rotatoires et Sur Quelques Propriétés Des Sucres. *C. R. Hebd. Seances Acad. Sci.* **1846**, *23*, 38–44.

(74) Wallach, O. Bernhard Tollens. *Berichte der Dtsch. Chem. Gesellschaft* **1918**, *51*, 1539–1555.

(75) Tanret, C. J. Sur Les Modifications Moléculaires Du Glucose. *C. R. Hebd. Seances Acad. Sci.* **1895**, *120*, 1060–1062.

(76) Haworth, W. N. A New Method of Preparing Alkylated Sugars. *J. Chem. Soc.* **1915**, *107*, 8–16.

(77) Fischer, E. Über Aromatische Hydrazinverbindungen. *Berichte der Dtsch. Chem. Gesellschaft* **1875**, *8*, 589–594.

(78) Freudenberg, K. Emil Fischer and His Contribution to Carbohydrate Chemistry. *Adv. Carbohydr. Chem.* **1967**, *21*, 1–38.

(79) Rodrigues, J. A.; Taylor, A. M.; Sumpton, D. P.; Reynolds, J. C.; Pickford, R.; Thomas-Oates, J. Mass Spectrometry of Carbohydrates: Newer Aspects. *Adv. Carbohydr. Chem. Biochem.* **2007**, *61*, 59–141.

(80) Kailemia, M. J.; Ruhaak, L. R.; Lebrilla, C. B.; Amster, I. J. Oligosaccharide Analysis by Mass Spectrometry: A Review of Recent Developments. *Anal. Chem.* **2014**, *86*, 196–212.

(81) Roberts, G. C. K. X-Ray Diffraction and Crystallography of Oligosaccharides and Polysaccharides. In *Encyclopedia of Biophysics*; Springer-Verlag Berlin Heidelberg, **2013**; pp 2767–2777.

(82) Battistel, M. D.; Azurmendi, H. F.; Yu, B.; Freedberg, D. I. NMR of Glycans: Shedding New Light on Old Problems. *Prog. Nucl. Magn. Reson. Spectrosc.* **2014**, *79*, 48–68.

(83) Bagno, A.; Rastrelli, F.; Saielli, G. Prediction of the 1H and 13C NMR Spectra of α-D-Glucose in Water by DFT Methods and MD Simulations. *J. Org. Chem.* **2007**, *72*, 7373–7381.

(84) Stevenson, P. J. Second-Order NMR Spectra at High Field of Common Organic Functional Groups. *Org. Biomol. Chem.* **2011**, *9*, 2078–2084.

(85) Toukach, F. V.; Ananikov, V. P. Recent Advances in Computational Predictions of NMR Parameters for the Structure Elucidation of Carbohydrates: Methods and Limitations. *Chem. Soc. Rev.* **2013**, *42*, 8376–8415.

2 Results

The presented cumulative PhD thesis consists of two peer-reviewed publications, listed in chronological order:

1. **Indium-mediated C-allylation of melibiose**

   Christian Denner, Manuel Gintner, Hanspeter Kählig, Walther Schmid;

   Beilstein Journal of Organic Chemistry, **2019**, 15, 2458–2464.

2. **Indium-mediated allylation of disaccharides**

   Christian Denner, Manuel Gintner, Hanspeter Kählig, Tanja M. Wrodnigg, Walther Schmid;

   Carbohydrate Research, **2020**, 498, 108170.

2.1 Publication I

Indium-mediated C-allylation of melibiose

Christian Denner, Manuel Gintner, Hanspeter Kählig, Walther Schmid

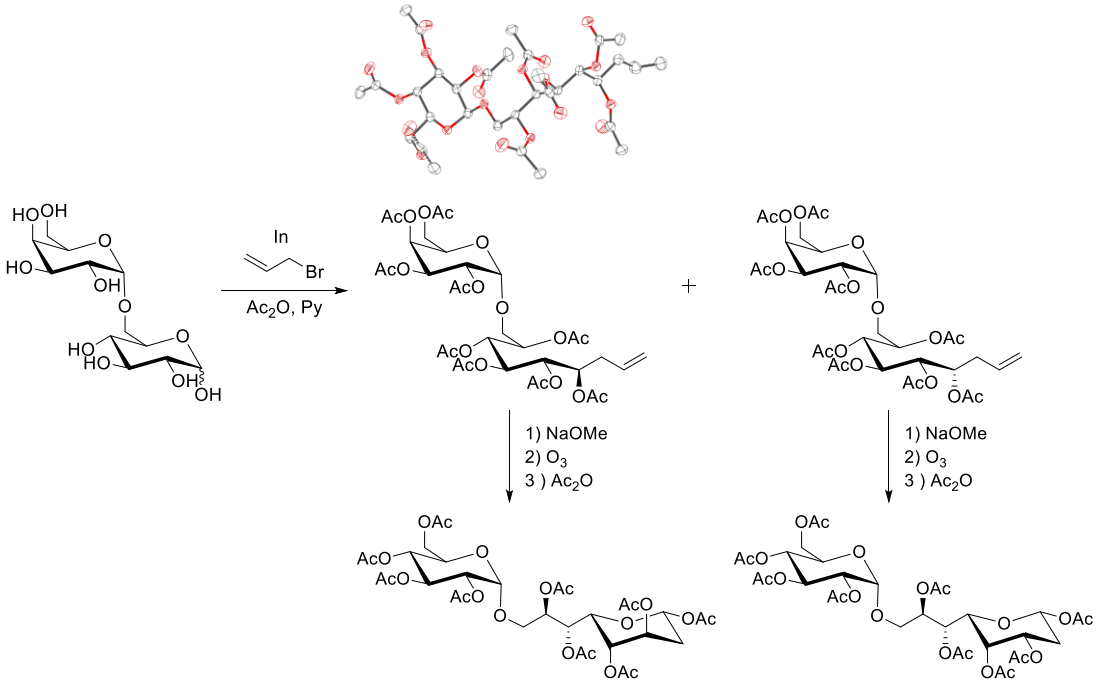

Beilstein Journal of Organic Chemistry, **2019**, 15, 2458–2464.

Within this work, as the first author I developed, conducted and optimized the reaction sequence as well as the purification procedures. Subsequently, I prepared the analytical samples and either tested them myself or gave them to the corresponding center for measurements (NMR and MS). Furthermore, I performed most of the structural elucidation of main and side products. I am the corresponding author of this publication.

BEILSTEIN JOURNAL OF ORGANIC CHEMISTRY

Indium-mediated C-allylation of melibiose

Christian Denner*, Manuel Gintner, Hanspeter Kählig and Walther Schmid§

Full Research Paper

Open Access

Address:
Institute of Organic Chemistry, University of Vienna, Währinger Straße 38, A-1090, Vienna, Austria

Email:
Christian Denner* - christian.denner@univie.ac.at

* Corresponding author
§ deceased, Dec 2017

Keywords:
carbohydrates; C–C bond formation; indium-mediated allylation; melibiose; ozonolysis

Beilstein J. Org. Chem. **2019,** *15,* 2458–2464.
doi:10.3762/bjoc.15.238

Received: 26 July 2019
Accepted: 25 September 2019
Published: 16 October 2019

Associate Editor: S. Flitsch

Abstract

The indium-mediated allylation reaction has been applied to melibiose, a disaccharidic substrate. This elongation methodology allows for a short, efficient and diastereoselective approach towards complex glycosylated carbohydrate structures. The stereochemical outcome of the key intermediates, allylated disaccharides, has been determined by X-ray analysis. Ozonolysis of the introduced double bond yielded the unprotected elongated disaccharides in the equilibrium of the pyranoid as well as furanoid isomers in both anomeric forms, respectively. Per-*O*-acetylation has been performed to facilitate separation of the isomeric mixture for structural identification. The main product revealed to adopt a β-pyranoid form of the elongated unit at the reducing end of the disaccharide.

Introduction

The tin and indium-mediated allylation (IMA) proved to be useful synthetic tools for the chain elongation of unprotected carbohydrates at the anomeric position to obtain higher complex sugar structures. Prior to the establishment of these methods, synthetic approaches towards these compounds had to be performed on protected carbohydrates, increasing the number of synthetic steps intrinsically [1]. In 1991, Schmid and Whitesides reported for the first time a tin-mediated allylation of unprotected carbohydrates followed by ozonolysis allowing for easy accessibility of the corresponding elongated sugars [2]. In the same year, Chan and Li introduced indium for the allylation of aldehydes and furthermore demonstrated the applicability of this post-transition metal for the elongation of carbohydrates [3-5]. Additional contributions were reported in the literature by Paquette and co-workers concerning indium-mediated reactions in water and their stereochemistry [6,7]. Based on these findings this elongation method has been established as reliable and efficient approach in carbohydrate chemistry, shown by many examples reported in the literature [8-12]. Thus far, this method has been applied to monosaccharides [13,14]. In this context, the development of diastereoselective and efficient synthetic routes to elongated disaccharides employing glycosylated substrates has been the focus of our interest. The demand for such elaborate compounds is undoubted and contin-

uously increasing, constituting an important research aim in glycosciences. Herein, we describe the optimization of reaction conditions and structural elucidation of compounds derived from the indium-mediated C-allylation reaction employing melibiose (**1**) as disaccharidic substrate.

Results and Discussion

We employed melibiose (**1**) as model substrate for the indium-mediated allylation reaction. In this disaccharide the glycosidic linkage is present at position O-6 of the glucose moiety allowing most spatial freedom for the elongation reaction at the anomeric position of the reducing end of the disaccharide (Scheme 1). First, we investigated different reaction parameters such as the metal species, the solvent system, the activation by sonication as well as the temperature concerning their effects on the conversion rate as well as the diastereoselectivity (Table 1).

Concerning the metal species, it is known that indium provides several advantages compared to other allylation-mediating metals such as tin, as it allows the reaction to proceed under very mild conditions without the need for acid catalysis or other promotors [15]. This was also observed in our studies reflected in the significantly higher conversion rates employing indium versus tin (Table 1, entries 1 and 3).

With respect to the solvent system, different ratios of an ethanol/water mixture were investigated showing that these have only minor effects on the conversion. However, the best results were obtained with a ratio of 4:1 (v/v) ethanol/water (Table 1, entries 2–4).

Although activation via sonication proved to be beneficial in our previous studies in the C-allylation of monosaccharides [16], in this case this form of energy input itself turned out to be insufficient. The best results were obtained by heating the reaction mixture with a conventional oil bath under vigorous stirring. This can be rationalized by the lower spacial availability at the reducing end of disaccharides compared to simple monosaccharides. Temperatures up to 65 °C led to elevated reaction rates (Table 1, entries 3, 5 and 6). However, higher temperatures caused concentration phenomena, which derived from the reflux of ethanol leading to precipitation of the starting material, which resulted in a significant decrease of the reaction rate. Additionally, intense stirring of the reaction mixture thereby preventing indium powder cluster formation (Table 1, entry 7) turned out to be of advantage for the progress of the reaction.

After the allylation subsequent per-*O*-acetylation gave a mixture of respective epimeric products at position C-4, **2-*syn*** and

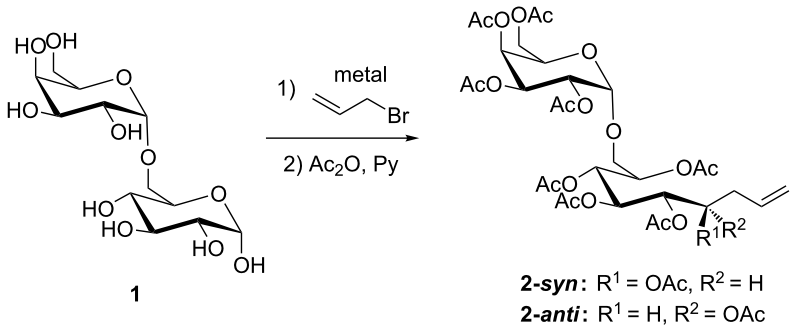

Scheme 1: Indium-mediated allylation of melibiose (**1**).

Table 1: Optimization of the reaction conditions of the indium-mediated allylation of melibiose.

Entry	Metal	Solvent[a]	Method	Time (h)	Conversion (%)[b]
1	Sn	4:1	sonication	24	19
2	In	1:1	sonication	24	44
3	In	4:1	sonication	24	56
4	In	9:1	sonication	24	45
5	In	4:1	sonication	46	78
6	In	4:1	65 °C	7	88
7[c]	In	4:1	65 °C	4	98

[a]General conditions: 200 mg (0.577 mmol) of melibiose (**1**), 4 equiv of indium and 6 equiv of allyl bromide in 20 mL of the solvent mixture ethanol/water. [b]Determined by NMR spectroscopy. [c]Vigorous stirring.

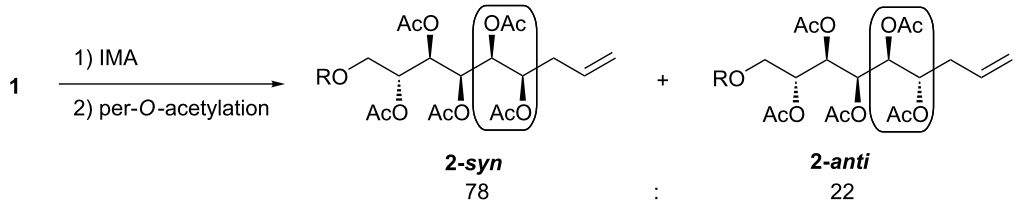

Scheme 2: Diastereomeric ratio of allylation; R = per-*O*-Ac-α-Gal.

2-*anti*, respectively, as well as the α,β-mixture of unreacted melibiose (**1**). Separation of the reaction mixture could be achieved by silica gel column chromatography. The diastereomeric ratio of 78:22 (**2-*syn*/2-*anti***) remained unchanged throughout the different conditions of optimization procedures (Scheme 2).

The overall yield of the isolated epimers was 92%. According to Binder et al. [17] and our own experience [18], we expected the *syn*-product (**2-*syn***) to be the main diastereomer. However, the determination of the configuration is not possible by NMR analysis. Consequently, the main product was crystallized and the configuration was determined by X-ray analysis proving the expected *syn*-configuration (compound **2-*syn***) [CCDC 1922520] (Figure 1).

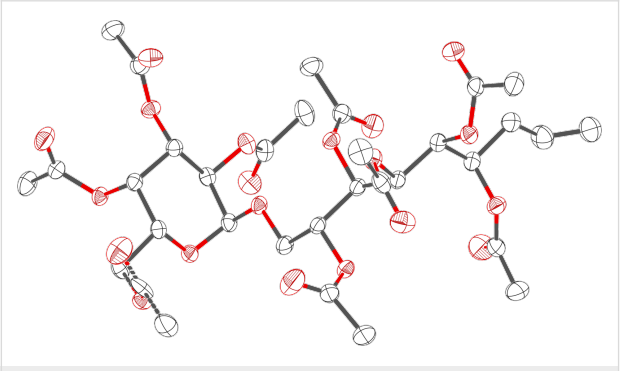

Figure 1: X-ray analysis of the main C-allylation product **2-*syn*** [CCDC 1922520].

Epimer **2-*syn*** was applied to Zemplén conditions prior to the ozonolysis. Conventional work-up, neutralization with acidic ion exchange resin followed by filtration and removal of the solvent under reduced pressure, led to precipitation of compound **3-*syn***, thereby causing problems during the ozonolysis. Thus, dichloromethane was added to the reaction mixture immediately after completed Zemplén-deprotection (as indicated by TLC) without further work up. This reaction mixture was cooled to −78 °C, purged with ozone for two minutes followed by reductive work-up employing triphenylphosphine which gave the corresponding glycosylated elongated aldoses **4-*syn*** in full conversion as determined by TLC. Epimer **2-*anti*** was reacted accordingly, after Zemplén-deprotection and ozonolysis compound **4-*anti*** was obtained. Purification at this stage utilizing conventional column chromatography was not feasible due to the high polarity of the obtained compound mixture, which contained pyranoid as well as furanoid isomers in their α,β-forms. Thus, per-*O*-acetylation was conducted leading to a mixture of all four species, indicated by NMR analysis (Scheme 3).

In the case of **2-*syn*** the β-pyranose species **5-*syn*-β** was obtained as the main product, besides α-pyranose (**5-*syn*-α**) as well as both anomers of the furanoid form (Scheme 4). The overall yield obtained over three steps was 72% (4 species), from this mixture the main product **5-*syn*-β** was isolated in 58% yield and could be fully characterized by NMR (Supporting Information File 1).

In the case of **2-*anti*** the same reaction sequence gave an overall yield of 65%, which is a slightly lower conversion compared to **2-*syn***. However, the main species, **5-*anti*-β** was obtained in 60% from this mixture (Figure 2).

Conclusion

For the first time, an indium-mediated allylation reaction was employed with a disaccharide, melibiose (Gal*p*α1-6Glc, **1**), as substrate, achieving good diastereoselectivity and excellent yields. Best conversion (98%) was obtained by employing indium as the metal species, a solvent mixture of ethanol/water 4:1 (v/v), at a temperature of 65 °C under vigorous stirring. The resulting epimeric forms were isolated and the stereochemical outcome was determined via X-ray structure analysis of the per-*O*-acetylated species, **2-*syn*/2-*anti*** 78:22. Subsequent ozonolysis applied on deprotected elongated compounds **3** generated the respective glycosylated aldoses in an anomeric mixture of both, pyranoid and furanoid forms. Per-*O*-acetylation of this mixture facilitated purification by silica gel chromatography. The main product turned out to adopt the β-pyranoid form, **5-*syn*-β** and **5-*anti*-β**, respectively, determined by thorough NMR analysis, in an overall yield of 40% and 42% over three steps calculated from epimers **2-*syn*** and **2-*anti*,** respectively.

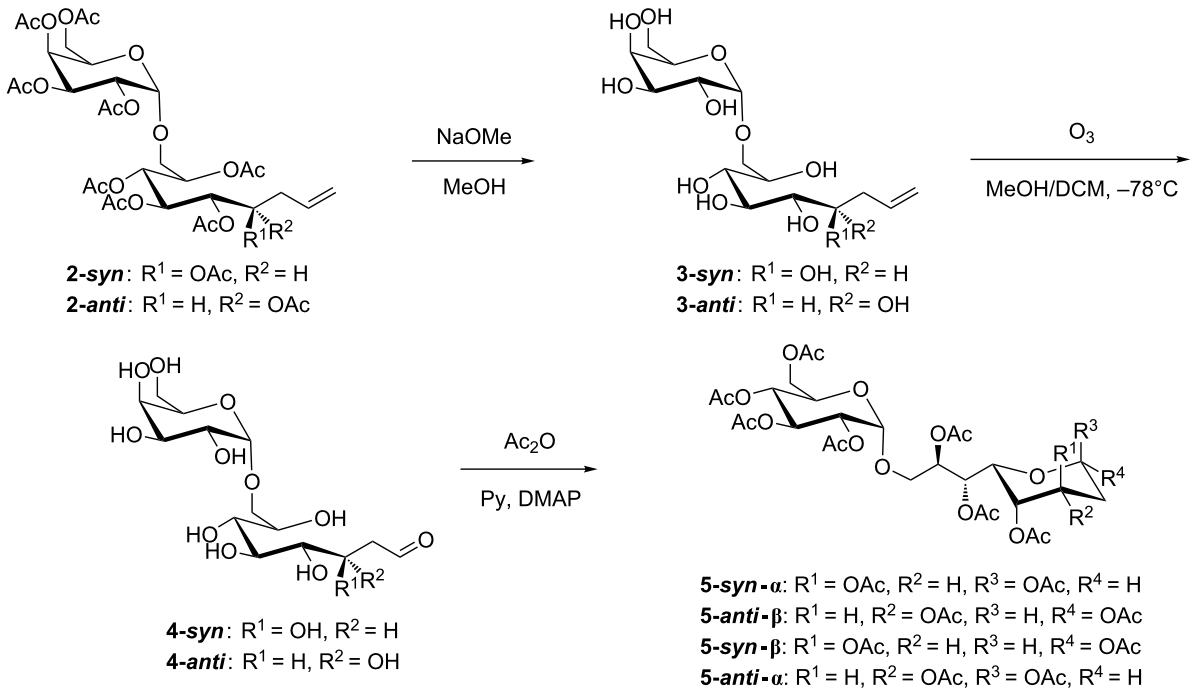

Scheme 3: Reaction scheme of the ozonolysis sequence.

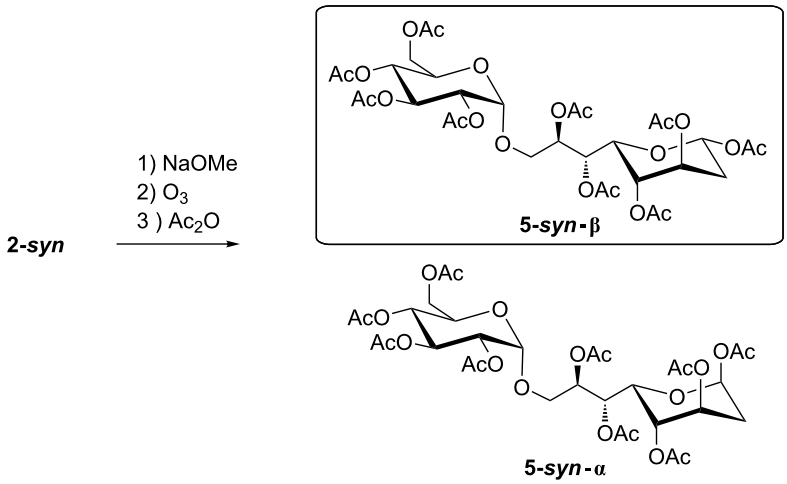

Scheme 4: Ozonolysis sequence for the *syn*-product.

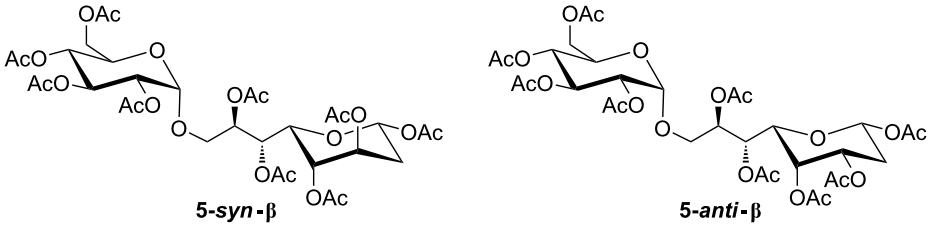

Figure 2: Structures of the main products **5-*syn*-β** and **5-*anti*-β**.

This work demonstrates the indium-mediated allylation reaction to be a powerful synthetic tool for the efficient and diastereoselective elongation of melibiose (**1**) without affecting the existing glycosidic linkage, allowing for additional options for further modifications of complex glycosides.

Experimental

2',3',4',6'-Tetra-*O*-acetyl-α-D-galactopyranosyl-(1'→1)-2,3,4,5,6-penta-*O*-acetyl-7,8,9-trideoxy-D-*glycero*-L-*gulo*-8,9-nonenitol (2-*syn*) and 2',3',4',6'-tetra-*O*-acetyl-α-D-galactopyranosyl-(1'→1)-2,3,4,5,6-penta-*O*-acetyl-7,8,9-trideoxy-L-*glycero*-L-*gulo*-8,9-nonenitol (2-*anti*): Indium (263 mg, 2.29 mmol, 4 equiv) and allyl bromide (420 mg, 3.47 mmol, 6 equiv) were added to 20 mL of an ethanol/water solution (4:1, v/v) and heated to 65 °C under vigorous stirring. Subsequently, melibiose (**1**, 208 mg, 0.577 mmol, 1 equiv) was added and the reaction mixture was stirred at 65 °C for 4 h, until no further conversion of the starting material has been observed, indicated by TLC analysis (1-butanol/acetone/water 5:4:1, v/v/v). The reaction mixture was filtered over celite and the filtrate concentrated under reduced pressure, leaving a colorless oil. The crude material was dissolved in pyridine (10 mL) and treated with acetic anhydride (10 mL). A catalytic amount of DMAP was added at 0 °C and the reaction mixture was stirred for 3 h while the solution was allowed to come to room temperature (rt), until a single spot was detected by TLC analysis (heptane/ethyl acetate 1:2, v/v). The reaction mixture was diluted with toluene and the solvents evaporated under reduced pressure. The residue was separated in water and ethyl acetate, the aqueous phase was washed with ethyl acetate (3 × 5 mL), the combined organic layers were washed consecutively with water and brine, and dried over $MgSO_4$. The solvent was evaporated under reduced pressure leading to a colorless highly viscous oil (405 mg, 0.531 mmol, 92%, **2-*syn*/2-*anti*** 78:22). Separation of the resulting epimeric mixture was achieved via silica gel column chromatography (heptane/ethyl acetate 1:1, v/v).

Analytical data for (**2-*syn***): R_f = 0.6 (heptane/ethyl acetate 1:2, v/v); $[\alpha]_D^{20}$ +83.3 (*c* 1.0, dichloromethane); mp 120–124 °C (methanol used for crystallization); ^{1}H NMR (600.25 MHz, $CDCl_3$, 25 °C) δ 5.653 (dddd, $^3J_{8,9a}$ = 17.0 Hz, $^3J_{8,9b}$ = 10.2 Hz, $^3J_{8,7b}$ = 7.3 Hz, $^3J_{8,7a}$ = 6.9 Hz, 1H, H-8), 5.449 (dd, $^3J_{4',3'}$ = 3.4 Hz, $^3J_{4',5'}$ = 1.2 Hz, 1H, H-4'), 5.416 (dd, $^3J_{3,2}$ = 7.5 Hz, $^3J_{3,4}$ = 3.3 Hz, 1H, H-3), 5.308 (dd, $^3J_{4,5}$ = 7.8 Hz, $^3J_{4,3}$ = 3.3 Hz, 1H, H-4), 5.304 (ddd, $^3J_{3',2'}$ = 11.0 Hz, $^3J_{3',4'}$ = 3.4 Hz, $^4J_{3',5'}$ = 0.3 Hz, 1H, H-3'), 5.193 (ddd, $^3J_{6,7b}$ = 8.4 Hz, $^3J_{6,7a}$ = 4.8 Hz, $^3J_{6,5}$ = 3.4 Hz, 1H, H-6), 5.116 (dd, $^3J_{2',3'}$ = 11.0 Hz, $^3J_{2',1'}$ = 3.7 Hz, 1H, H-2'), 5.106 (dd, $^3J_{5,4}$ = 7.8 Hz, $^3J_{5,6}$ = 3.4 Hz, 1H, H-5), 5.089 (d, $^3J_{1',2'}$ = 3.7 Hz, 1H, H-1'), 5.066 (dddd, $^3J_{9a,8}$ = 17.0 Hz, $^2J_{9a,9b}$ = 1.8 Hz, $^4J_{9a,7a}$ = 1.5 Hz, $^4J_{9a,7b}$ = 1.5 Hz, 1H, H-9a), 5.063 (dddd, $^3J_{9b,8}$ = 10.2 Hz, $^2J_{9b,9a}$ = 1.8 Hz, $^4J_{9b,7a}$ = 1.0 Hz, $^4J_{9b,7b}$ = 1.0 Hz, 1H, H-9b), 4.962 (ddd, $^3J_{2,3}$ = 7.5 Hz, $^3J_{2,1a}$ = 5.6 Hz, $^3J_{2,1b}$ = 3.8 Hz, 1H, H-2), 4.174 (dddd, $^3J_{5',6'b}$ = 7.2 Hz, $^3J_{5',6'a}$ = 6.1 Hz, $^3J_{5',4'}$ = 1.2 Hz, $^4J_{5',3'}$ = 0.3 Hz, 1H, H-5'), 4.079 (dd, $^2J_{6'a,\ 6'b}$ = 11.2 Hz, $^3J_{6'a,5'}$ = 7.2 Hz, 1H, H-6'a), 4.051 (dd, $^2J_{6'b,\ 6'a}$ = 11.2 Hz, $^3J_{6'b,5'}$ = 6.1 Hz, 1H, H-6'b), 3.679 (dd, $^2J_{1a,1b}$ = 11.5 Hz, $^3J_{1a,2}$ = 5.6 Hz, 1H, H-1a), 3.605 (dd, $^2J_{1b,1a}$ = 11.5 Hz, $^3J_{1b,2}$ = 3.8 Hz, 1H, H-1b), 2.265 (ddddd, $^2J_{7a,7b}$ = 15.4 Hz, $^3J_{7a,8}$ = 6.9 Hz, $^3J_{7a,6}$ = 4.8 Hz, $^4J_{7a,9a}$ = 1.5 Hz, $^4J_{7a,9b}$ = 1.0 Hz, 1H, H-7a), 2.258 (ddddd, $^2J_{7b,7a}$ = 15.4 Hz, $^3J_{7b,6}$ = 8.4 Hz, $^3J_{7b,8}$ = 7.3 Hz, $^4J_{7b,9a}$ = 1.5 Hz, $^4J_{7b,9b}$ = 1.0 Hz, 1H, H-7b), 2.125, 2.116, 2.093, 2.085, 2.085, 2.038, 2.034, 2.011, 1.955 (9s, 27H, 9 × OAc) ppm; ^{13}C NMR (150.93 MHz, $CDCl_3$, 25 °C) δ 170.57, 170.41, 170.15, 170.14, 169.81, 169.81, 169.78, 169.77, 169.49, (9 × O(*C*=O)CH_3), 132.18 (C-8), 118.81 (C-9), 95,83 (C-1'), 70.35 (C-5), 70.03 (C-6), 68.87 (C-3), 68.74 (C-2), 68.37 (C-4), 67.67 (C-2'), 67.94 (C-4'), 67.28 (C-3'), 66.60 (C-5'), 65.44 (C-1), 61.59 (C-6'), 35.34 (C-7), 20.69, 20.66, 20.63, 20.63, 20.62, 20.61, 20.61, 20.56, 20.50 (9 × O(C=O)*C*H_3) ppm; HRMS (ESI$^+$) *m/z*: [M + Na]$^+$ calcd for $C_{33}H_{46}O_{20}Na^+$, 785.2475; found, 785.2473. CCDC 1922520 contains the supplementary crystallographic data for compound **2-*syn***. These data can be obtained from The Cambridge Crystallographic Data Centre, http://www.ccdc.cam.ac.uk/data_request/cif.

Analytical data for (**2-*anti***): R_f = 0.7 (heptane/ethyl acetate 1:2, v/v); $[\alpha]_D^{20}$ +64.1 (*c* 1.0, dichloromethane); ^{1}H NMR (600.25 MHz, $CDCl_3$, 25 °C) δ 5.729 (dddd, $^3J_{8,9a}$ = 17.0 Hz, $^3J_{8,9b}$ = 10.2 Hz, $^3J_{8,7a}$ = 7.2 Hz, $^3J_{8,7b}$ = 6.6 Hz, 1H, H-8), 5.468 (dd, $^3J_{4',3'}$ = 3.5 Hz, $^3J_{4',5'}$ = 1.3 Hz, 1H, H-4'), 5.396 (dd, $^3J_{4,5}$ = 5.7 Hz, $^3J_{4,3}$ = 5.1 Hz, 1H, H-4), 5.369 (dd, $^3J_{3,2}$ = 6.3 Hz, $^3J_{3,4}$ = 5.1 Hz, 1H, H-3), 5.308 (dd, $^3J_{3',2'}$ = 10.0 Hz, $^3J_{3',4'}$ = 3.5 Hz, 1H, H-3'), 5.301 (dd, $^3J_{5,4}$ = 5.7 Hz, $^3J_{5,6}$ = 5.5 Hz, 1H, H-5), 5.143 (dddd, $^3J_{9a,8}$ = 17.0 Hz, $^2J_{9a,9b}$ = 1.8 Hz, $^4J_{9a,7a}$ = 1.4 Hz, $^4J_{9a,7b}$ = 1.4 Hz, 1H, H-9a), 5.110 (d, $^3J_{1',2'}$ = 3.7 Hz, 1H, H-1'), 5.097 (dd, $^3J_{2',3'}$ = 10.0 Hz, $^3J_{2',1'}$ = 3.7 Hz, 1H, H-2'), 5.088 (dddd, $^3J_{9b,8}$ = 10.2 Hz, $^2J_{9b,9a}$ = 1.8 Hz, $^4J_{9b,7a}$ = 1.1 Hz, $^4J_{9b,7b}$ = 1.1 Hz, 1H, H-9b), 4.988 (ddd, $^3J_{2,3}$ = 6.3 Hz, $^3J_{2,1a}$ = 6.1 Hz, $^3J_{2,1b}$ = 4.3 Hz, 1H, H-2), 4.936 (ddd, $^3J_{6,7b}$ = 6.8 Hz, $^3J_{6,7a}$ = 6.0 Hz, $^3J_{6,5}$ = 5.5 Hz, 1H, H-6), 4.202 (ddd, $^3J_{5',6'b}$ = 6.7 Hz, $^3J_{5',6'a}$ = 6.5 Hz, $^3J_{5',4'}$ = 1.3 Hz, 1H, H-5'), 4.091 (dd, $^2J_{6'a,\ 6'b}$ = 11.3 Hz, $^3J_{6'a,5'}$ = 6.5 Hz, 1H, H-6'a), 4.063 (dd, $^2J_{6'b,\ 6'a}$ = 11.3 Hz, $^3J_{6'b,5'}$ = 6.7 Hz, 1H, H-6'b), 3.716 (dd, $^2J_{1a,1b}$ = 11.3 Hz, $^3J_{1a,2}$ = 6.1 Hz, 1H, H-1a), 3.615 (dd, $^2J_{1b,1a}$ = 11.3 Hz, $^3J_{1b,2}$ = 4.3 Hz, 1H, H-1b), 2.360 (ddddd, $^2J_{7a,7b}$ = 15.0 Hz, $^3J_{7a,8}$ = 6.6 Hz, $^3J_{7a,6}$ = 6.0 Hz, $^4J_{7a,9a}$ = 1.4 Hz, $^4J_{7a,9b}$ = 1.1 Hz, 1H, H-7a), 2.355 (ddddd, $^2J_{7b,7a}$ = 15.0 Hz, $^3J_{7b,8}$ = 7.2 Hz, $^3J_{7b,6}$ = 6.8 Hz, $^4J_{7b,9a}$ = 1.4 Hz, $^4J_{7b,9b}$ = 1.1 Hz, 1H, H-7b), 2.133,

2.122, 2.111, 2.102, 2.038, 2.026, 2.015, 1.962, 1.962 (9s, 27H, OAc) ppm; ^{13}C NMR (150.93 MHz, $CDCl_3$, 25 °C) δ 170.57, 170.36, 170.12, 170.11, 170.01, 169.98, 169.82, 169.69, 169.56 (9 × O(*C*=O)CH_3), 132.67 (C-8), 118.54 (C-9), 96,09 (C-1'), 70.97 (C-5), 70.17 (C-6), 69.31 (C-3), 69.01 (C-2), 68.54 (C-4), 67.93 (C-2'), 67.93 (C-4'), 67.35 (C-3'), 66.64 (C-5'), 65.63 (C-1), 61.57 (C-6'), 34.09 (C-7), 20.75, 20.70, 20.70, 20.66, 20.65, 20.63, 20.59, 20.58, 20.53 (9 × O(C=O)*C*H_3) ppm; HRMS (ESI$^+$) *m*/*z*: [M + Na]$^+$ calcd for $C_{33}H_{46}O_{20}Na^+$, 785.2475; found, 785.2479.

2',3',4',6'-Tetra-*O*-acetyl-α-D-galactopyranosyl-(1'→8)-1,3,4,6,7-penta-*O*-acetyl-2-deoxy-α-D-*glycero*-D-*ido*-octopyranose (5-*syn*-β): Compound (**2-*syn***) (115 mg, 0.151 mmol) was dissolved in MeOH (15 mL) and treated with NaOMe (pH 9) until a pH around 9 was reached. The solution was stirred at rt for 2 h, until reaction monitoring via TLC analysis (1-butanol/acetone/H_2O 5:4:1, v/v/v) showed complete conversion of the starting material. The reaction mixture was diluted with dichloromethane (dichloromethane/MeOH, 1:1, v/v) and subsequently cooled to −78 °C. Ozone was bubbled through the reaction with a gas inlet tube until a clear blue color was observed (2 min). Subsequently, the O_3 generation was stopped allowing the gas flow to purge the reaction mixture for additional 15 min. PPh_3 (80 mg, 0.305 mmol, 2 equiv) was added and stirring continued over night at rt. The solvents were evaporated under reduced pressure and the residue was separated between dichloromethane and water. The aqueous phase was washed with dichloromethane (3 × 10 mL, to separate PPh_3). The water was removed under reduced pressure leaving a light yellow oil. The oil was diluted with pyridine (10 mL), and treated with acetic anhydride (10 mL) at 0 °C. A catalytic amount of DMAP was added and the reaction mixture was stirred for 3 h while the solution was allowed to come to room temperature until complete conversion could be observed on TLC analysis (heptane/ethyl acetate 1:2, v/v). The reaction mixture was diluted with toluene and the solvent removed under reduced pressure. The residue was separated between water and ethyl acetate and the aqueous phase was extracted with ethyl acetate (3 × 5 mL), the combined organic layers were washed subsequently with water, brine and dried over $MgSO_4$. The solvent was removed under reduced pressure leaving a colorless highly viscous liquid. Separation of the resulting mixture of ring size and anomeric configuration was achieved via silica gel column chromatography (heptane/ethyl acetate 1:1, v/v) to give compound **5-*syn*-β** (48 mg, 0.063 mmol, 42%) as colorless oil. R_f = 0.5 (heptane/ethyl acetate 1:2, v/v); $[\alpha]_D^{20}$ +88.2 (*c* 0.5, dichloromethane); ^{1}H NMR (600.25 MHz, $CDCl_3$, 25 °C) δ 5.791 (dd, $^3J_{1,2a}$ = 10.4 Hz, $^3J_{1,2b}$ = 2.2 Hz, 1H, H-1), 5.453 (dd, $^3J_{4',3'}$ = 3.4 Hz, $^3J_{4',5'}$ = 1.3 Hz, 1H, H-4'), 5.441 (dd, $^3J_{6,5}$ = 6.7 Hz, $^3J_{6,7}$ = 4.0 Hz, 1H, H-6), 5.280 (dd, $^3J_{3',2'}$ = 11.0 Hz, $^3J_{3',4'}$ = 3.4 Hz, 1H, H-3'), 5.129 (d, $^3J_{1',2'}$ = 3.7 Hz, 1H, H-1'), 5.103 (ddd, $^3J_{3,2a}$ = 3.4 Hz, $^3J_{3,4}$ = 3.1 Hz, $^3J_{3,2b}$ = 2.8 Hz, 1H, H-3), 5.095 (dd, $^3J_{2',3'}$ = 11.0 Hz, $^3J_{2',1'}$ = 3.7 Hz, 1H, H-2'), 5.000 (ddd, $^3J_{7,8a}$ = 7.3 Hz, $^3J_{7,6}$ = 4.0 Hz, $^3J_{7,8b}$ = 3.2 Hz, 1H, H-7), 4.790 (dd, $^3J_{4,3}$ = 3.1 Hz, $^3J_{4,5}$ = 1.5 Hz, 1H, H-4), 4.186 (ddd, $^3J_{5',6'b}$ = 7.1 Hz, $^3J_{5',6'a}$ = 6.4 Hz, $^3J_{5',4'}$ = 1.3 Hz, 1H, H-5'), 4.119 (dd, $^3J_{5,6}$ = 6.7 Hz, $^3J_{5,4}$ = 1.5 Hz, 1H, H-5), 4.084 (dd, $^2J_{6'a,6'b}$ = 12.0 Hz, $^3J_{6'a,5'}$ = 6.4 Hz, 1H, H-6'a), 4.083 (dd, $^2J_{6'b,6'a}$ = 12.0 Hz, $^3J_{6'b,5'}$ = 7.1 Hz, 1H, H-6'b), 3.813 (dd, $^2J_{8a,\ 8b}$ = 11.7 Hz, $^3J_{8a,7}$ = 7.3 Hz, 1H, H-8a), 3.695 (dd, $^2J_{8b,8a}$ = 11.7 Hz, $^3J_{8b,7}$ = 3.2 Hz, 1H, H-8b), 2.174, 2.134, 2.128, 2.103, 2.087, 2.086, 2.045, 2.043 (8s, 24H, OAc), 2.026 (ddd, $^2J_{2a,2b}$ = 14.3 Hz, $^3J_{2a,1}$ = 10.4 Hz, $^3J_{2a,3}$ = 3.4 Hz, 1H, H-2a), 1.978 (1s, 3H, OAc), 1.948 (ddd, $^2J_{2b,2a}$ = 14.3 Hz, $^3J_{2b,3}$ = 2.8 Hz, $^3J_{2b,1}$ = 2.2 Hz, 1H, H-2b) ppm; ^{13}C NMR (150.93 MHz, $CDCl_3$, 25 °C) δ 170.59, 170.34, 170.17, 169.93, 169.92, 169.82, 169.79, 169.08, 168.92 (O(*C*=O)CH_3), 96.33 (C-1'), 90.47 (C-1), 72.31 (C-5), 70.76 (C-7), 70.36 (C-6), 67.93 (C-2'), 67.79 (C-4'), 67.69 (C-3), 67.37 (C-3'), 66.45 (C-5'), 65.77 (C-4), 65.74 (C-8), 61.35 (C-6'), 29.95 (C-2), 20.97, 20.92, 20.80, 20.74, 20.72, 20.70, 20.66, 20.66, 20.62 (9 × O(C=O)*C*H_3) ppm; HRMS (ESI$^+$) *m*/*z*: [M + NH_4]$^+$ calcd for $C_{32}H_{48}NO_{21}^+$, 782.2713; found, 782.2719.

2',3',4',6'-Tetra-*O*-acetyl-α-D-galactopyranosyl-(1'→8)-1,3,4,6,7-penta-*O*-acetyl-2-deoxy-α-D-*glycero*-D-*gulo*-octopyranose (5-*anti*-β): Compound **2-*anti*** (154 mg, 0.202 mmol) was reacted accordingly as described for the conversion of **2-*syn***, leading to a colorless highly viscous oil. Separation of the resulting mixture of ring size and anomeric configuration was achieved via silica gel chromatography (heptane/ethyl acetate 1:1, v/v) to give compound **5-*anti*-β** (62 mg, 0.081 mmol, 40%) as colorless oil. R_f = 0.5 (heptane/ethyl acetate 1:2, v/v); $[\alpha]_D^{20}$ +36.7 (*c* 1.0, dichloromethane); ^{1}H NMR (600.25 MHz, $CDCl_3$, 25 °C) δ 5.674 (dd, $^3J_{1,2a}$ = 10.1 Hz, $^3J_{1,2b}$ = 2.2 Hz, 1H, H-1), 5.539 (dd, $^3J_{4',3'}$ = 3.5 Hz, $^3J_{4',5'}$ = 1.0 Hz, 1H, H-4'), 5.524 (dd, $^3J_{4,3}$ = 3.0 Hz, $^3J_{4,5}$ = 1.0 Hz, 1H, H-4), 5.511 (dd, $^3J_{3',2'}$ = 10.8 Hz, $^3J_{3',4'}$ = 3.5 Hz, 1H, H-3'), 5.494 (dd, $^3J_{6,5}$ = 8.5 Hz, $^3J_{6,7}$ = 1.9 Hz, 1H, H-6), 5.353 (ddd, $^3J_{3,2a}$ = 12.6 Hz, $^3J_{3,2b}$ = 5.0 Hz, $^3J_{3,4}$ = 3.0 Hz, 1H, H-3), 5.156 (d, $^3J_{1',2'}$ = 4.0 Hz, 1H, H-1'), 5.095 (dd, $^3J_{2',3'}$ = 10.8 Hz, $^3J_{2',1'}$ = 4.0 Hz, 1H, H-2'), 4.988 (ddd, $^3J_{7,8b}$ = 9.7 Hz, $^3J_{7,8a}$ = 5.3 Hz, $^3J_{7,6}$ = 1.9 Hz, 1H, H-7), 4.312 (ddd, $^3J_{5',6'a}$ = 6.8 Hz, $^3J_{5',6'b}$ = 6.0 Hz, $^3J_{5',4'}$ = 1.0 Hz, 1H, H-5'), 4.232 (dd, $^3J_{5,6}$ = 8.5 Hz, $^3J_{5,4}$ = 1.0 Hz, 1H, H-5), 4.124 (dd, $^2J_{6'a,6'b}$ = 11.7 Hz, $^3J_{6'a,5'}$ = 6.8 Hz, 1H, H-6'a), 4.114 (dd, $^2J_{6'b,6'a}$ = 11.7 Hz, $^3J_{6'b,5'}$ = 6.0 Hz, 1H, H-6'b), 3.819 (dd, $^2J_{8a,\ 8b}$ = 8.7 Hz, $^3J_{8a,7}$ = 5.3 Hz, 1H, H-8a), 3.656 (dd, $^3J_{8b,7}$ = 9.7 Hz, $^2J_{8b,8a}$ = 8.7 Hz, 1H, H-8b), 2.256, 2.185, 2.153 (3s, 9H, OAc), 2.105 (ddd, $^2J_{2a,2b}$ = 14.3 Hz, $^3J_{2a,3}$ = 12.6 Hz, $^3J_{2a,1}$ = 10.1 Hz, 1H, H-2a), 2.088, 2.064, 2.056 (3s, 9H, OAc),

1.980 (ddd, $^2J_{2b,2a}$ = 14.3 Hz, $^3J_{2b,3}$ = 5.0 Hz, $^3J_{2b,1}$ = 2.2 Hz, 1H, H-2b), 1.975, 1.975, 1.959 (3s, 9H, OAc) ppm; ^{13}C NMR (150.93 MHz, $CDCl_3$, 25 °C) δ 171.07, 170.54, 170.44, 170.02, 169.96, 169.88, 169.56, 169.34, 168.96 (9 × O(*C*=O)CH_3), 97.02 (C-1'), 91.46 (C-1), 73.48 (C-5), 71.33 (C-6), 68.99 (C-2'), 68.49 (C-4'), 68.43 (C-3), 68.11 (C-7), 67.22 (C-3'), 67.15 (C-5'), 65.88 (C-8), 64.90 (C-4), 61.68 (C-6'), 30.31 (C-2), 20.96, 20.88, 20.77, 20.73, 20.71, 20.69, 20.66, 20.64, 20.58 (9 × O(C=O)*C*H_3) ppm; HRMS (ESI$^+$) *m*/*z*: $[M + NH_4]^+$ calcd for $C_{32}H_{48}NO_{21}^+$, 782.2713; found, 782.2720.

Supporting Information

Supporting information features copies of ^{1}H NMR, ^{13}C NMR spectra and mass analysis data of all compounds, as well as X-ray data of compound **2-*syn***.

Supporting Information File 1

General instructions, NMR spectra, mass analysis data and X-ray data.
[https://www.beilstein-journals.org/bjoc/content/supplementary/1860-5397-15-238-S1.pdf]

Supporting Information File 2

Cif-report of compound **2-*syn***.
[https://www.beilstein-journals.org/bjoc/content/supplementary/1860-5397-15-238-S2.pdf]

Supporting Information File 3

Crystallographic information file of compound **2-*syn***.
[https://www.beilstein-journals.org/bjoc/content/supplementary/1860-5397-15-238-S3.cif]

Acknowledgements

We would like to thank the NMR center for NMR analysis, the mass spectrometry center for mass analysis and A. Roller for X-ray crystallographic analysis. We also thank T. Wrodnigg for critical comments on the manuscript.

ORCID® iDs

Christian Denner - https://orcid.org/0000-0001-5100-5854
Manuel Gintner - https://orcid.org/0000-0001-8503-3335
Hanspeter Kählig - https://orcid.org/0000-0002-3898-6501

References

1. Kozikowski, A. P.; Sorgi, K. L.; Wang, B. C.; Xu, Z.-b. *Tetrahedron Lett.* **1983,** *24,* 1563–1566. doi:10.1016/s0040-4039(00)81710-4
2. Schmid, W.; Whitesides, G. M. *J. Am. Chem. Soc.* **1991,** *113,* 6674–6675. doi:10.1021/ja00017a049
3. Li, C. J.; Chan, T. H. *Tetrahedron Lett.* **1991,** *32,* 7017–7020. doi:10.1016/0040-4039(91)85028-4
4. Chan, T. H.; Li, C. J. *J. Chem. Soc., Chem. Commun.* **1992,** 747–748. doi:10.1039/c39920000747
5. Chan, T. H.; Isaac, M. B. *Pure Appl. Chem.* **1996,** *68,* 919–924. doi:10.1351/pac199668040919
6. Paquette, L. A.; Mitzel, T. M. *Tetrahedron Lett.* **1995,** *36,* 6863–6866. doi:10.1016/00404-0399(50)1439o-
7. Bernardelli, P.; Paquette, L. A. *J. Org. Chem.* **1997,** *62,* 8284–8285. doi:10.1021/jo9716800
8. Fischer, M.; Schmölzer, C.; Nowikow, C.; Schmid, W. *Eur. J. Org. Chem.* **2011,** 1645–1651. doi:10.1002/ejoc.201001443
9. Balla, E.; Zamyatina, A.; Hofinger, A.; Kosma, P. *Carbohydr. Res.* **2007,** *342,* 2537–2545. doi:10.1016/j.carres.2007.07.022
10. Schmölzer, C.; Fischer, M.; Schmid, W. *Eur. J. Org. Chem.* **2010,** 4886–4892. doi:10.1002/ejoc.201000623
11. Prenner, R. H.; Schmid, W. *Monatsh. Chem.* **1996,** *127,* 1045–1050. doi:10.1007/bf00807577
12. Gordon, D. M.; Whitesides, G. M. *J. Org. Chem.* **1993,** *58,* 7937–7938. doi:10.1021/jo00079a050
13. Gintner, M.; Yoneda, Y.; Schmölzer, C.; Denner, C.; Kählig, H.; Schmid, W. *Carbohydr. Res.* **2019,** *474,* 34–42. doi:10.1016/j.carres.2019.01.009
14. Prenner, R. H.; Binder, W. H.; Schmid, W. *Liebigs Ann. Chem.* **1994,** 73–78. doi:10.1002/jlac.199419940113
15. Kim, E.; Gordon, D. M.; Schmid, W.; Whitesides, G. M. *J. Org. Chem.* **1993,** *58,* 5500–5507. doi:10.1021/jo00072a038
16. Albler, C.; Hollaus, R.; Kählig, H.; Schmid, W. *Beilstein J. Org. Chem.* **2014,** *10,* 2230–2234. doi:10.3762/bjoc.10.231
17. Binder, W. H.; Prenner, R. H.; Schmid, W. *Tetrahedron* **1994,** *50,* 749–758. doi:10.1016/s0040-4020(01)80790-0
18. Gintner, M.; Denner, C.; Schmölzer, C.; Fischer, M.; Frühauf, P.; Kählig, H.; Schmid, W. *Monatsh. Chem.* **2019,** *150,* 849–860. doi:10.1007/s00706-019-02438-y

License and Terms

BEILSTEIN JOURNAL OF ORGANIC CHEMISTRY

Supporting Information

for

Indium-mediated C-allylation of melibiose

Christian Denner, Manuel Gintner, Hanspeter Kählig and Walther Schmid

Beilstein J. Org. Chem. **2019,** *15,* 2458–2464. doi:10.3762/bjoc.15.238

General instructions, NMR spectra, mass analysis data and X-ray data

Table of Contents

General instructions: ^{1}H and ^{13}C NMR spectra were recorded on a Bruker AV III 600. Chemical shifts (δ) are reported in parts per million (ppm) and spectra were calibrated using solvent signal of $CDCl_3$. Signal multiplicity is indicated by one or more of the following: s (singlet); d (doublet); t (triplet); q (quartet). NMR analysis was assisted by the spin simulation software DAISY (part of Bruker Top Spin software). High resolution mass spectra (HRMS) were recorded on a Bruker maXis UHR-TOF spectrometer in ESI mode. Optical rotations were measured on a Schmidt-Haensch Digital Polarimeter Unipol L 2000. Ozonolysis was performed operating an Anseros COM-AD-04 ozone generator. Column chromatography was performed using Macherey-Nagel silica gel 60 (0.04–0.063 mm, 240–400 mesh). TLC monitoring was carried out on precoated Merck silica gel 60 F_{254} glass plates. Compounds were visualized by treatment with a Mo–$Ce(SO_4)_2$ complex solution (48 g $(NH_4)_6Mo_7O_{24}$ and 2 g $CeSO_4$ in 1 dm^3 10% H_2SO_4) followed by heating. Filtrations over celite were performed with Celite® S by Sigma-Aldrich®. Solvents were distilled, if necessary, prior to use. Reagents were purchased from commercial suppliers and were used without further purification.

2’,3’,4’,6’-Tetra-*O*-acetyl-α-D-galactopyranosyl-(1’→1)-2,3,4,5,6-penta-*O*-acetyl-7,8,9-trideoxy-D-*glycero*-L-*gulo*-8,9-nonenitol (**2-*syn***)

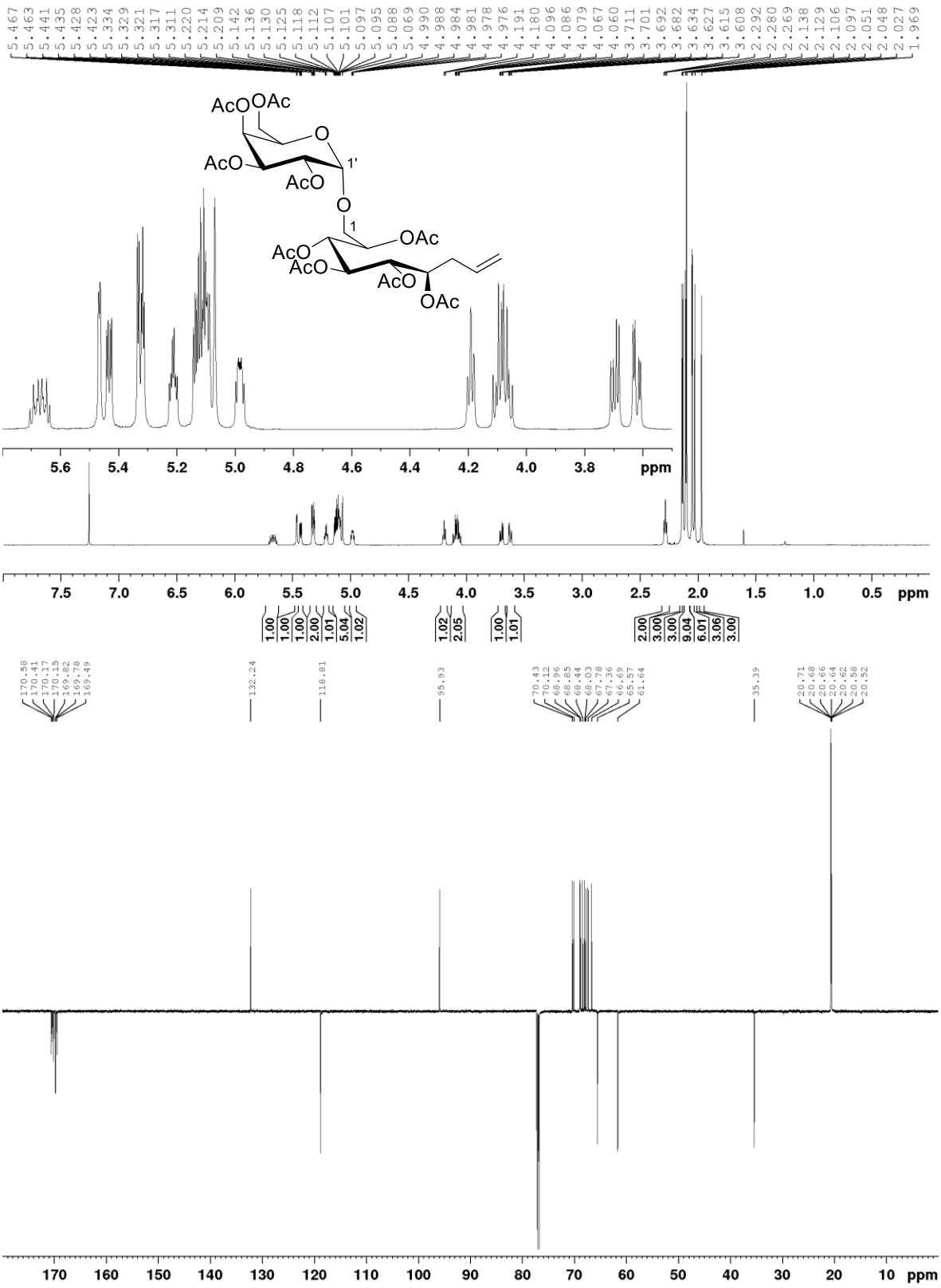

S3

2’,3’,4’,6’-Tetra-*O*-acetyl-α-D-galactopyranosyl-(1’→1)-2,3,4,5,6-penta-*O*-acetyl-7,8,9-trideoxy-L-*glycero*-L-*gulo*-8,9-nonenitol (**2-*anti***)

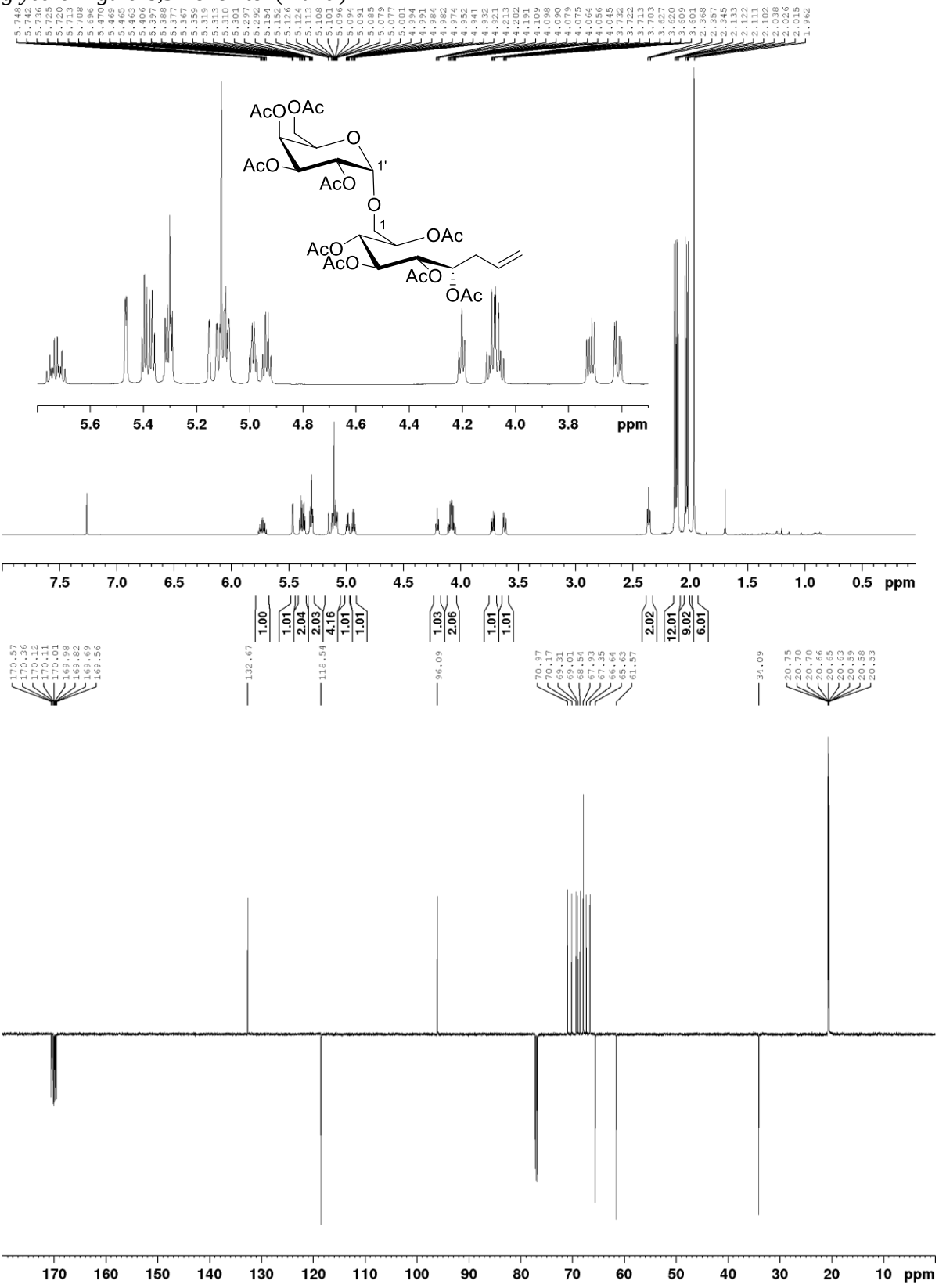

2’,3’,4’,6’-Tetra-*O*-acetyl-α-D-galactopyranosyl-(1’→8)-1,3,4,6,7-penta-*O*-acetyl-2-deoxy-α-D-*glycero*-D-*ido*-octopyranose (**5-*syn*-β**)

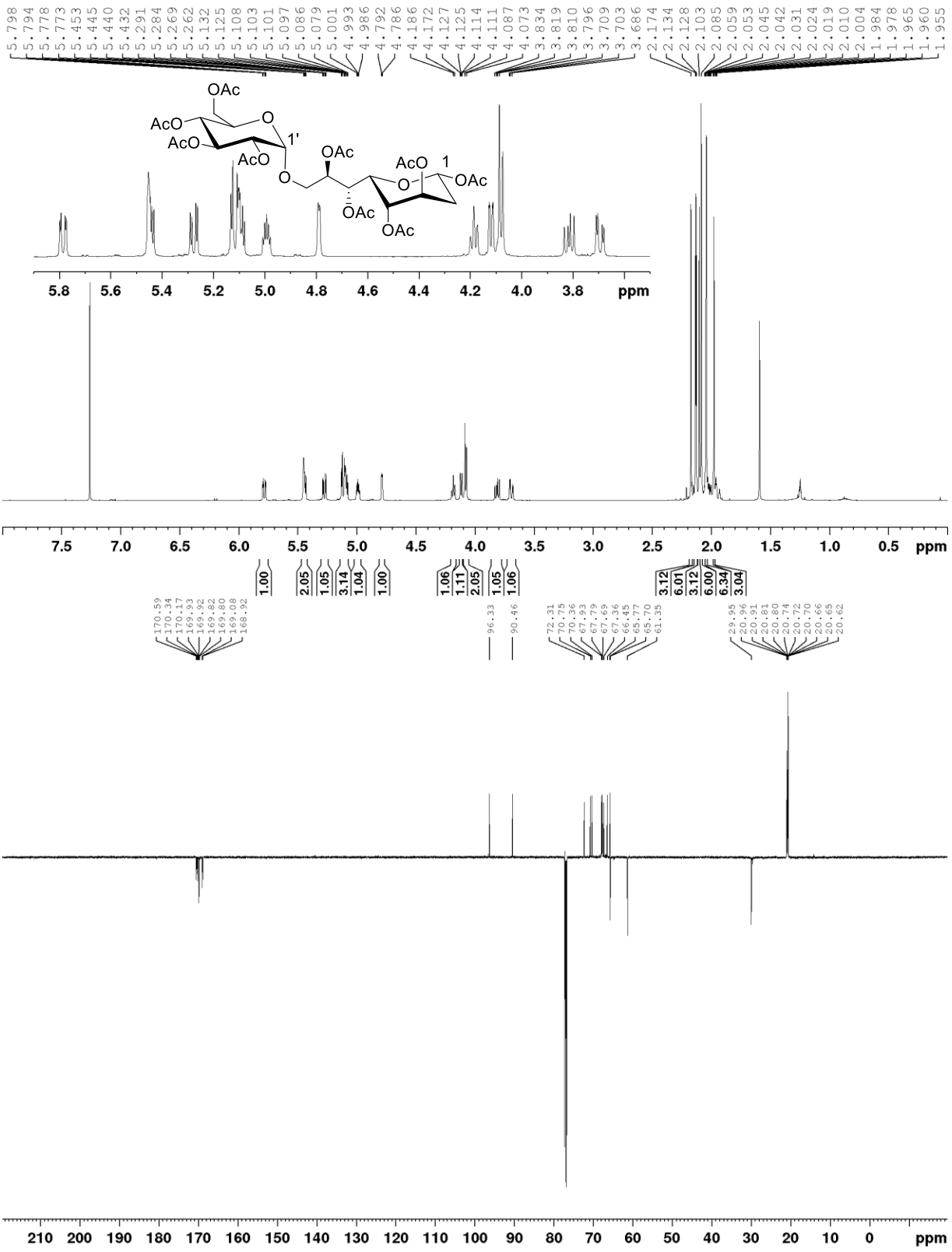

2’,3’,4’,6’-Tetra-*O*-acetyl-α-D-galactopyranosyl-(1’→8)-1,3,4,6,7-penta-*O*-acetyl-2-deoxy-α-D-*glycero*-D-*gulo*-octopyranose (**5-*anti*-β**)

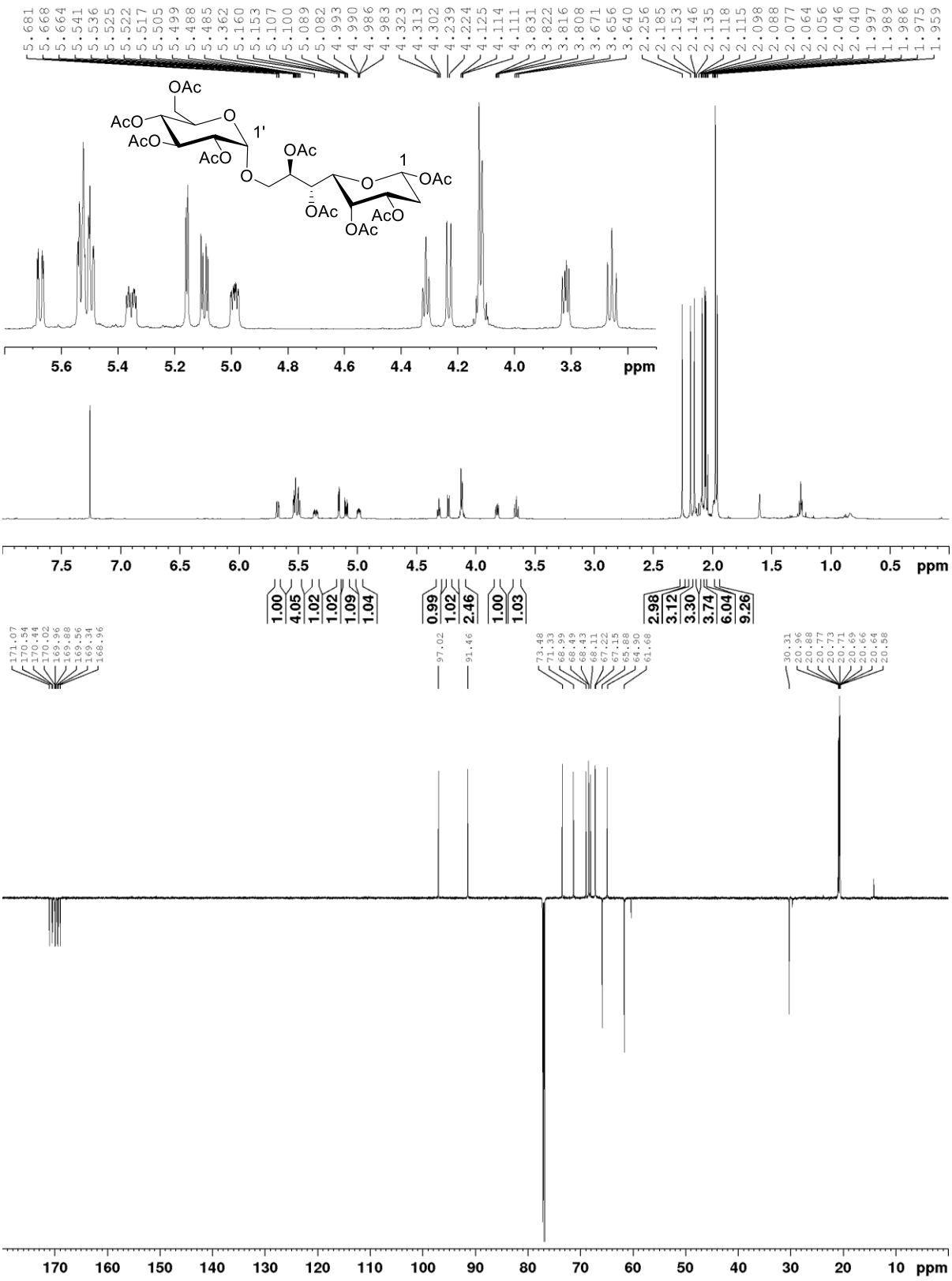

2’,3’,4’,6’-Tetra-*O*-acetyl-α-D-galactopyranosyl-(1’→1)-2,3,4,5,6-penta-*O*-acetyl-7,8,9-trideoxy-D-*glycero*-L-*gulo*-8,9-nonenitol (**2-*syn***)

HRMS (ESI$^+$) m/z = 785.2473 [M+Na]$^+$ calcd. for $C_{33}H_{46}O_{20}Na^+$: 785.2475.

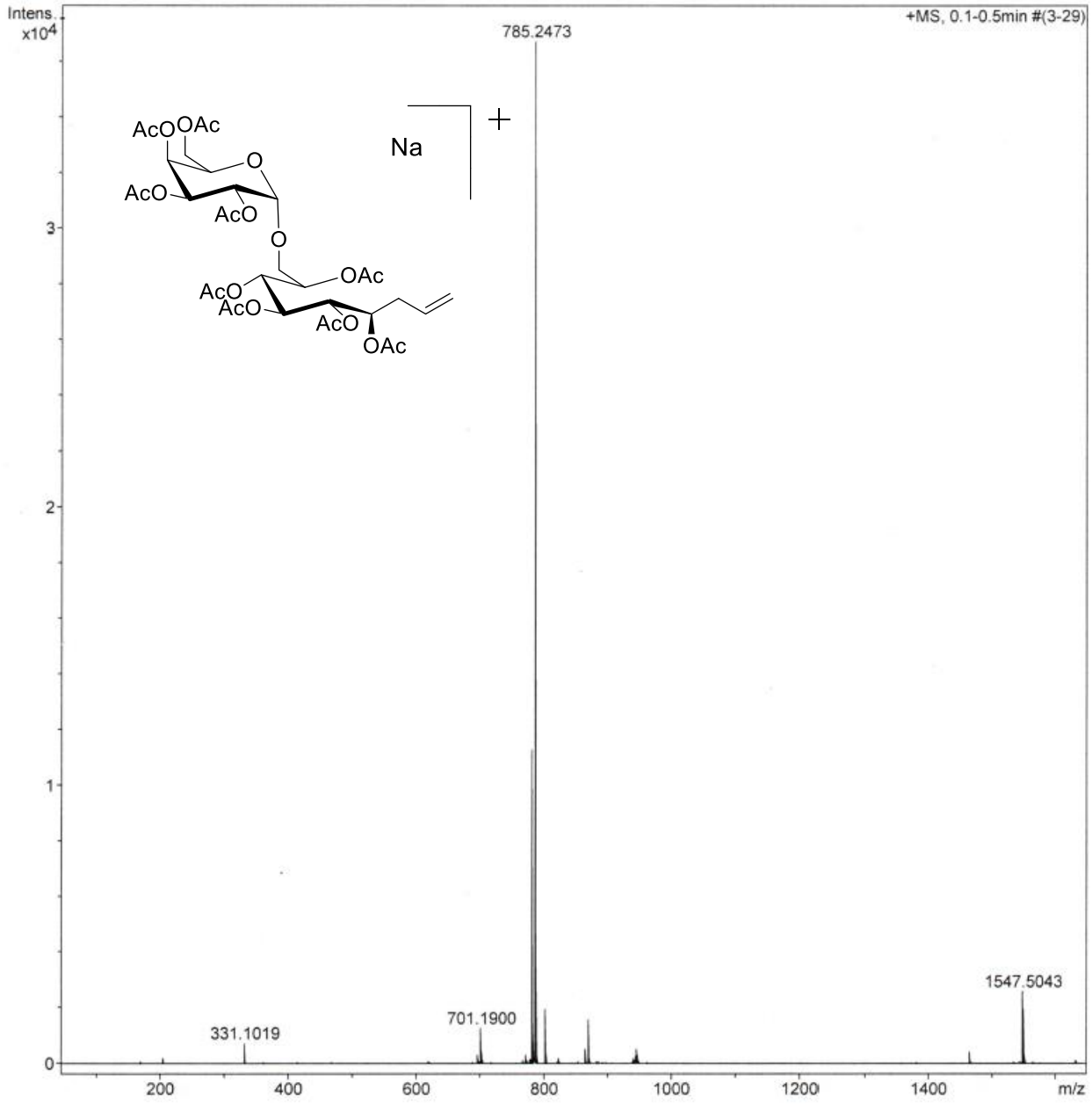

2’,3’,4’,6’-Tetra-*O*-acetyl-α-D-galactopyranosyl-(1’→1)-2,3,4,5,6-penta-*O*-acetyl-7,8,9-trideoxy-L-*glycero*-L-*gulo*-8,9-nonenitol (**2-*anti***)

HRMS (ESI$^+$) m/z = 785.2479 $[M+Na]^+$ calcd. for $C_{33}H_{46}O_{20}Na^+$: 785.2475.

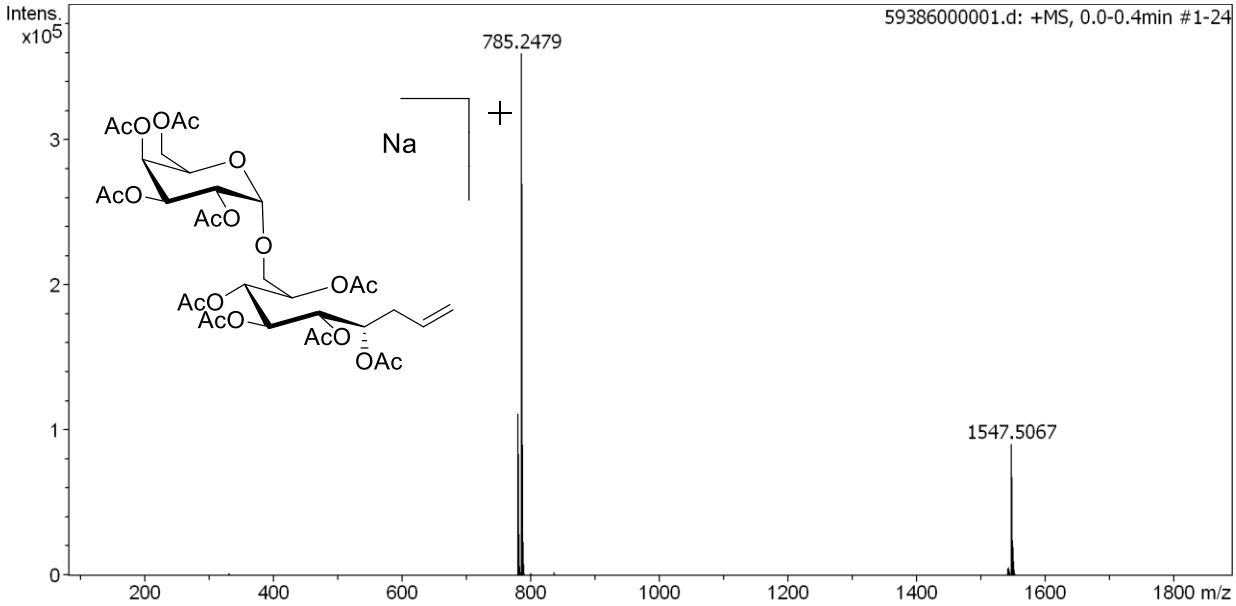

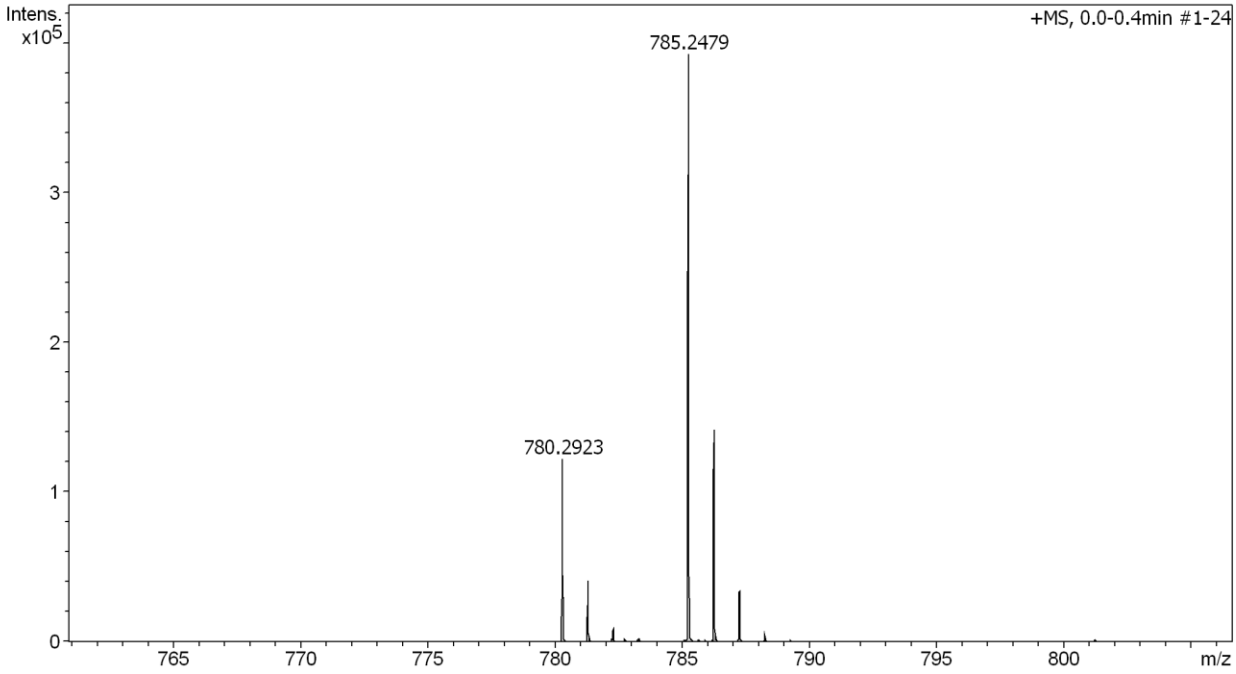

2’,3’,4’,6’-Tetra-*O*-acetyl-α-D-galactopyranosyl-(1’→8)-1,3,4,6,7-penta-*O*-acetyl-2-deoxy-α-D-*glycero*-D-*ido*-octopyranose (**5-*syn*-β**)

HRMS (ESI$^+$) m/z = 782.2719 [M+ NH_4]$^+$ calcd. for $C_{32}H_{48}NO_{21}^+$: 782.2713.

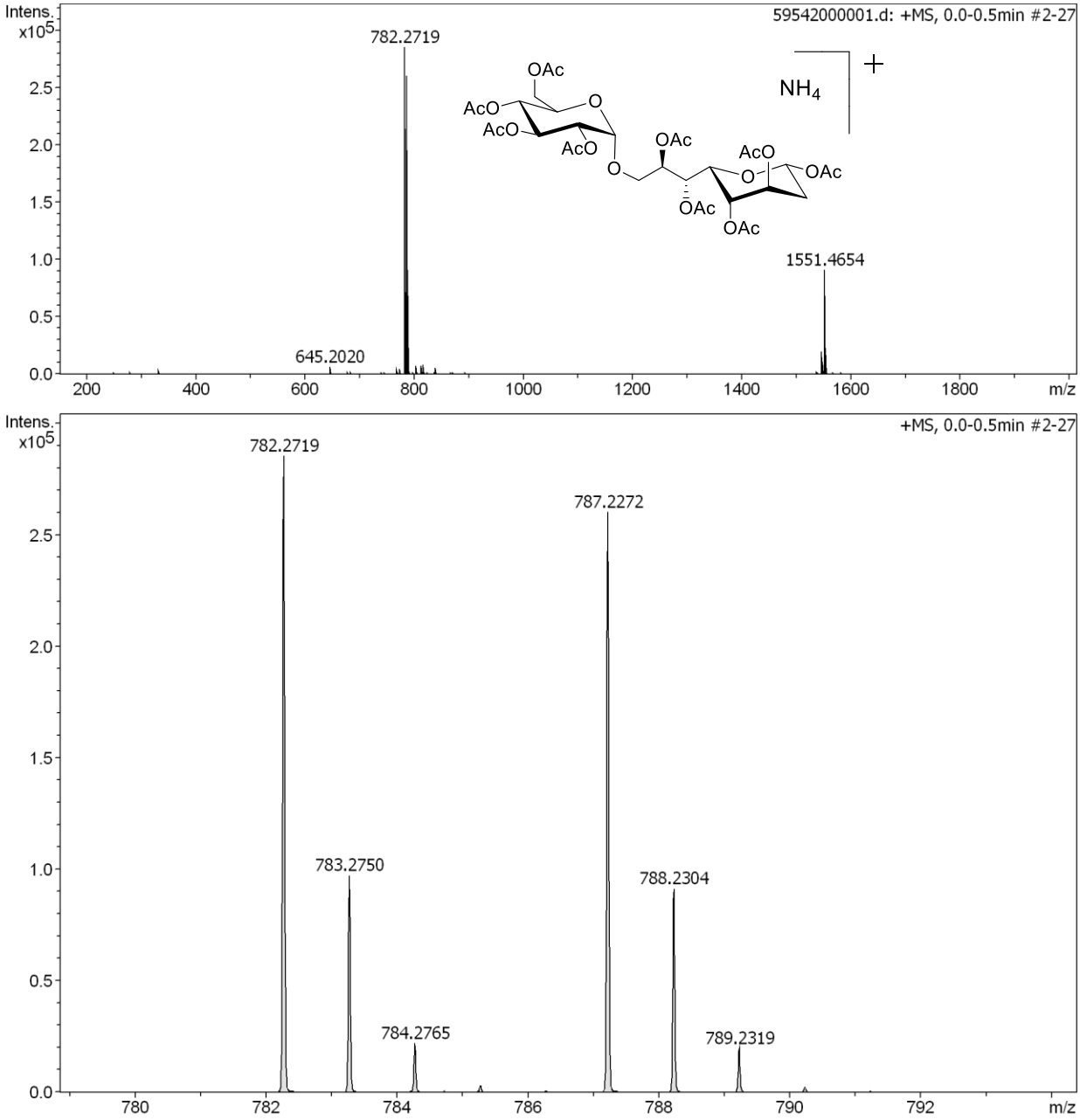

2’,3’,4’,6’-Tetra-*O*-acetyl-α-D-galactopyranosyl-(1’→8)-1,3,4,6,7-penta-*O*-acetyl-2-deoxy-α-D-*glycero*-D-*gulo*-octopyranose (**5-*anti*-β**)

HRMS (ESI$^+$) m/z = 782.2720 $[M+NH_4]^+$ calcd. for $C_{32}H_{48}NO_{21}^+$: 782.2713.

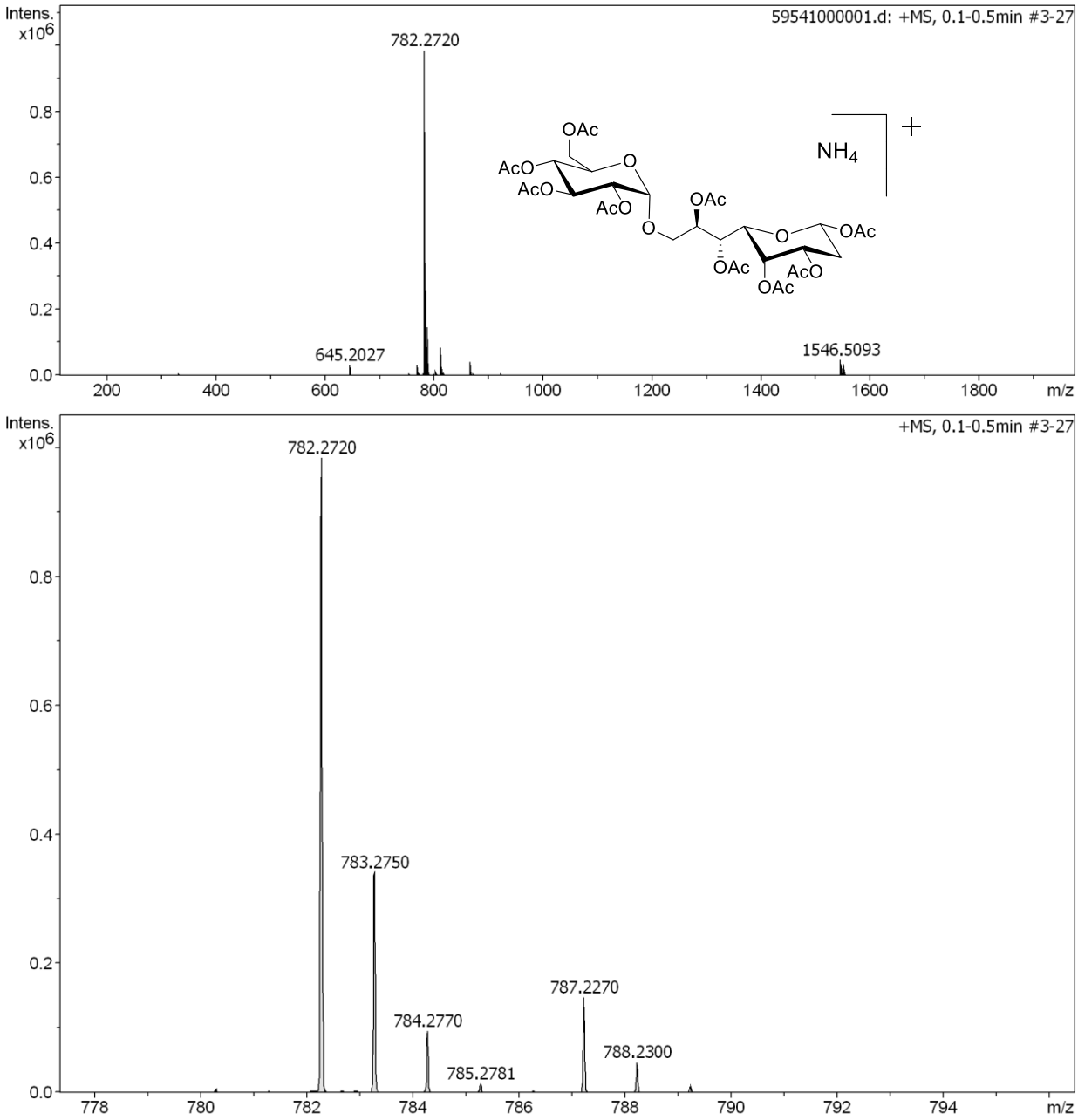

X-ray analysis

The X-ray intensity data were measured on Bruker D8 Venture diffractometer equipped with multilayer monochromator, Mo Kα INCOATEC micro focus sealed tube and Oxford cooling system. The structure was solved by *charge flipping* and refined by *full-matrix least-squares techniques*. Non-hydrogen atoms were refined with *anisotropic displacement parameters*. Hydrogen atoms were inserted at calculated positions and refined with riding model. The following software was used: *Bruker SAINT software package*[i] using a narrow-frame algorithm for frame integration, *SADABS*[ii] for absorption correction, *OLEX2*[iii] for structure solution, molecular diagrams and graphical user-interface, *Shelxle*[iv] for refinement and graphical user-interface, *SHELXL-2015*[v] for refinement, *Platon*[vi] for symmetry check. Experimental data and CCDC-Codes Experimental data and CCDC-Code (Available online: http://www.ccdc.cam.ac.uk/conts/retrieving.html) can be found in Table S1. Crystal data, data collection parameters, and structure refinement details are given in Tables S2 and S3. Crystal structure is visualized in Figure S1.

Table S1 Experimental parameter and CCDC-Code.

Sample	Machine	Source	Temp.	Detector Distance	Time/ Frame	#Frames	Frame width	CCDC
	Bruker		[K]	[mm]	[s]		[°]	
2-syn	D8	Mo	100	37	8	6216	0.500	1922520

2-syn

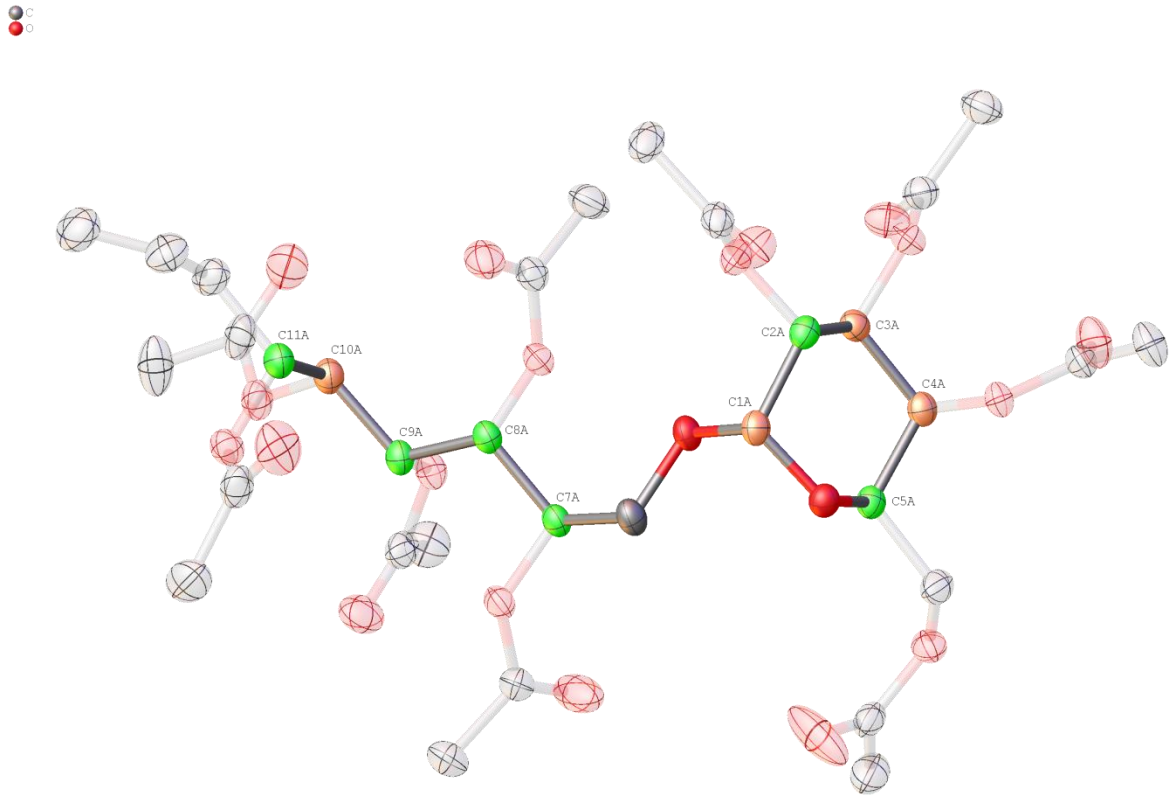

Figure S1 Crystal structure of [**2-syn**], drawn with 50% displacement ellipsoid. Backbone highlighted, side chains translucent. The green carbons are in R conformation, the orange ones are S. Chirality is proofed by reference molecule and AD. The bond precision for C–C single bonds is 0.0033 Å. Second independent molecule in the AU, Hydrogen Atoms and Disorder omitted for clarity. Main residue disorder is 9%.

Table S2 Sample and crystal data [**2-syn**].

Chemical formula	C33H46O20	**Crystal system**	monoclinic	
Formula weight [g/mol]	762.7	**Space group**	*P21*	
Temperature [K]	100	**Z**	4	
Measurement method	\f and \w scans	**Volume [Å^3]**	3800.8(3)	
Radiation (Wavelength [Å])	MoKα (λ = 0.71073)	**Unit cell dimensions [Å] and [°]**	14.1418(6)	90
Crystal size / [mm^3]	0.35 × 0.23 × 0.211		9.0704(3)	91.8306(15)
Crystal habit	clear colourless block		29.6461(12)	90
Density (calculated) / [g/cm^3]	1.333	**Absorption coefficient / [mm^{-1}]**	0.111	
Abs. correction Tmin	0.7191	**Abs. correction Tmax**	0.746	
Abs. correction type	multiscan	**F(000) [e$^-$]**	1616	

Table S3 Data collection and structure refinement[**2-syn**]..

Index ranges	$-19 \leq h \leq 19$, $-12 \leq k \leq 12$, $-41 \leq l \leq 41$	**Theta range for data collection [°]**	4.124 to 60.124	
Reflections number	489568	**Data / restraints / parameters**	22249/5/1051	
Refinement method	Least squares	**Final R indices**	all data	R1 = 0.0483, wR2 = 0.1031
Function minimized	$\Sigma\, w(F_o^2 - F_c^2)^2$		$I>2\sigma(I)$	R1 = 0.0384, wR2 = 0.0925
Goodness-of-fit on F^2	1.093	**Weighting scheme**	$w=1/[\sigma^2(F_o^2)+(0.0403P)^2+1.2026P]$	
Largest diff. peak and hole [e $Å^{-3}$]	0.47/-0.25		where $P=(F_o^2+2F_c^2)/3$	

[i] Bruker SAINT v8.38B Copyright © 2005-2019 Bruker AXS
[ii] Sheldrick, G. M. (1996). *SADABS*. University of Göttingen, Germany.
[iii] Dolomanov, O.V.; Bourhis, L.J.; Gildea, R.J; Howard, J.A.K.; Puschmann, H. OLEX2, (2009), *J. Appl. Cryst.* **2009,** *42,* 339-341
[iv] Huebschle, C. B.; Sheldrick, G. M.; Dittrich, B. ShelXle: a Qt graphical user interface for SHELXL, *J. Appl. Cryst.* **2011,** *44,* 1281-1284
[v] Sheldrick, G. M. (2015). *SHELXL* v 2016/4 University of Göttingen, Germany.
[vi] Spek, A. L. *Acta Cryst.* **2009,** *D65,* 148-155.

2.2 Publication II

Indium-mediated allylation of disaccharides

Christian Denner, Manuel Gintner, Hanspeter Kählig, Tanja M. Wrodnigg, Walther Schmid

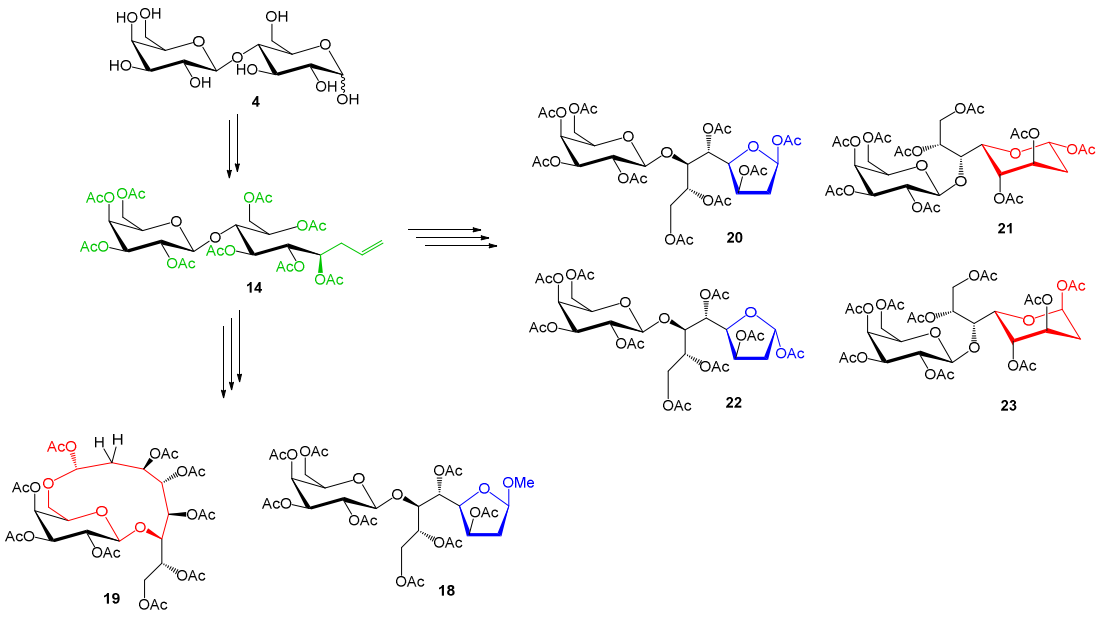

Carbohydrate Research, **2020**, 498, 108170.

Within this work, as the first author I developed, conducted and optimized the reaction sequence as well as the purification procedures. Subsequently, I prepared the analytical samples and either tested them myself or gave them to the corresponding center for measurements (NMR and MS). Furthermore, I performed most of the structural elucidation of main and side products. I am the corresponding author of this publication.

Carbohydrate Research 498 (2020) 108170

Contents lists available at ScienceDirect

Carbohydrate Research

journal homepage: www.elsevier.com/locate/carres

Indium-mediated allylation of disaccharides☆

Christian Denner [a,*], Manuel Gintner [a], Hanspeter Kählig [a], Tanja M. Wrodnigg [b], Walther Schmid [a,†]

[a] Institute of Organic Chemistry, University of Vienna, Währinger Straße 38, A-1090, Vienna, Austria
[b] Glycogroup, Institute of Chemistry and Technology for Biobased Systems, Graz University of Technology, Stremayrgasse 9, A-8010, Graz, Austria

ARTICLE INFO

Keywords:
Indium-mediated allylation
Ozonolysis
Disaccharide
C–C bond formation

ABSTRACT

The indium-mediated allylation followed by ozonolysis has been applied for the elongation of different disaccharides such as cellobiose, lactose and maltose. This reaction sequence and per-*O*-acetylation produced the expected mixture of α/β-pyranoid as well as α/β-furanoid isomers. The main product in all cases adopted the β-pyranose form and could be isolated and fully characterized with the help of NMR-spin simulations. Thorough investigation of the side products throughout optimization of the conditions for the ozonolysis resulted in the discovery of a novel 12 membered bridged disaccharide.

1. Introduction

Elongation of carbohydrate structures is an important research goal in synthetic carbohydrate chemistry, especially for the synthesis of sugars that exceed the most commonly seen chain lengths of five and six carbon backbones. Such carbohydrates are present in a wide variety of organisms and have proven to be important in many different areas of life and medicine. One prominent example is the compound class of sialic acids (e.g. *N*-Acetylneuraminic acid **1**, Fig. 1), with a nine-carbon backbone, which are present on cell walls and are important for cell-cell interactions as well as cell-cell communication events and have been intensely studied in the context of cancer and human-bacterial interactions [1–4]. Heptoses, such as Sedoheptulose (**2**, Fig. 1), are present in the pentose phosphate pathway and on lipopolysaccharides and have been targeted as potential therapeutic and analytical drugs [5,6]. Lincomycin and Clindamycin (**3**, Fig. 1) are octoses that are used as antibiotics and clindamycin is mentioned on the world health organization's list of essential medicines [7–9].

In this context, the investigation of concise possibilities to synthesize complex carbohydrate structures from easily accessible and cheap starting materials is an important research area [10,11]. The indium-mediated allylation (IMA) presents a perfect tool for this synthetic challenge in carbohydrate chemistry because it allows the use of simple as well as unprotected carbohydrate based starting materials. Furthermore, the stereochemistry can be controlled with the help of one modification next to the anomeric center [12–14]. Therefore, our group and many others could show the versatility of the IMA in the synthesis of elongated carbohydrates [15–17]. In a proof a concept study, we have successfully employed the IMA on melibiose, a disaccharidic substrate [18]. In this work we want to expand the IMA on common disaccharides in a broader context.

2. Results and discussion

Lactose (**4**), maltose (**5**) as well as cellobiose (**6**) were used in the indium-mediated allylation with allyl-bromide followed by an ozonolysis protocol to synthesize the respective elongated disaccharides. Per-*O*-acetylation was used for purification of the resulting product mixtures (Scheme 1).

The reaction conditions for the allylation reaction involved the investigation of different metals, such as indium and zinc, variations in the reaction temperature as well as solvent systems, which has been optimized with melibiose as starting material as described in our previous work [18]. The conditions of choice turned out to be the employment of 4 equivalents of indium in an ethanol/water mixture (4/1) and 6 equivalents of allyl bromide stirring at 65 °C, for approx. 6 h. After conventional work up and per-*O*-acetylation with acetic anhydride, pyridine and 4-Dimethylaminopyridine (DMAP), yields from 80 to 92% over two steps could be achieved when applied on lactose (**4**), maltose (**5**) as well as cellobiose (**6**) as starting materials (Table 1).

☆ C.D. dedicates this contribution to his mentor and friend, the late Univ.-Prof. Dr. Mag. Walther Schmid.

* Corresponding author.
E-mail address: christian.denner@univie.ac.at (C. Denner).

† Deceased, Dec 2017.

https://doi.org/10.1016/j.carres.2020.108170
Received 7 July 2020; Received in revised form 24 September 2020; Accepted 30 September 2020
Available online 8 October 2020

The diastereomeric ratio of the elongated disaccharides varied between 80:20 to 90:10 but showed no significant dependence on reaction conditions employed. In all cases the main product was purified by column chromatography and characterized by NMR. In case of cellobiose (**6**) we were able to prove the expected *syn* configuration of the newly introduced stereo center by IMA, position C-4, to given position C-5 of the main product (**15**) [CCDC 2010237] by x-ray crystallography (Scheme 2).

The purified per-*O*-acetylated main products (**14**), (**15**) and (**16**) were subjected to the ozonolysis protocol as follows: first deprotection took place under Zemplén conditions in 2–4 h determined by TLC, the resulting solution was diluted with dichloromethane cooled to −78 °C and directly employed to ozonolysis. Thereafter, a per-*O*-acetylation step had to follow for purification and thorough analysis of the obtained compounds. With lactose (**4**) our first attempts did not give the desired fully acetylated compounds **13** straight away but the corresponding elongated carbohydrate **18** with *O*-methylation at the anomeric position. This was probably caused by highly acidic conditions in the workup after the ozonolysis step. Additionally, a 12 membered bridged bicyclic carbohydrate compound **19** was formed (Scheme 3). From this reaction mixture, the major product, compound **18**, could be isolated and its structure clearly determined by NMR analysis (B in Fig. 2). Compound **19** could only be obtained as an inseparable 1:1 mixture with compound **18**. Comparing the ^{13}C NMR spectra of pure compound **18** (B in Fig. 2) against the mixture (A in Fig. 2) clearly identified the signals of compound **19** (red signals in A Fig. 2). Continuing with 2D NMR experiments the structure of compound **19** could be thoroughly elucidated even in this mixture. As a final proof, a ^{1}H NMR spectrum was calculated for the mixture with the help of spin simulations (Daisy, TopSpin software, Bruker BioSpin). This is clearly and completely superimposable with the experimental one (Fig. 3). Attempts to find conditions favoring the formation of compound **19** have not been successful.

To avoid this undesired methylation of the anomeric center the ozonolysis reaction was optimized through shorter reaction times, which resulted in a significantly less pronounced pH drop. Thereafter, no further *O*-methylation took place. Still with these optimized reaction conditions the resulting mixture after per-*O*-acetylation contained four different disaccharides, α/β-pyranose and α/β-furanose (Scheme 4). All those products naturally belong to the same unprotected carbohydrate but due to the complexity of the equilibrium, elucidation and conformation of the structure at this stage was not possible. Additionally, due to the polarity of unprotected disaccharides, clean products could not be obtained without an additional acetylation step. For the elongation of lactose (**4**), Scheme 4 shows the four resulting carbohydrates **20**, **21**, **22** and **23**, respectively.

The ratios of the obtained compound mixture, α- and β-furanose as well as α- and β-pyranose, were strongly dependent on the respective starting material but no effect from reaction conditions could be observed. Separation of all obtained isomers could not be achieved, therefore, a complete analysis was not possible. Nonetheless, in all cases purification of the main product adopting the β-pyranose conformation of the elongated sugar unit, (**21**), (**24**) as well as (**25**), and structural elucidation has been achieved by NMR-spectroscopy with the help of spin simulations (Scheme 5). Overall yields were found between 50 and 70% over three steps, the main product could be isolated in up to 52% yield in case of maltose (**5**) as starting material (Table 2).

3. Conclusion

In summary, disaccharides lactose (**4**), maltose (**5**) as well as cellobiose (**6**) have, for the first time, been exploited to an indium-mediated allylation - ozonolysis reaction sequence for chain elongation at the reducing end. Preparative overall yields are fair with good to excellent yields of 80–92% in the elongation step. The resulting per-*O*-acetylated carbohydrates adopted α/β-pyranose and α/β-furanose conformation, whereas the β-pyranose form, **21**, **24**, **25** proved to be the main product in all cases, in yields of 38, 52, 35% for lactose, maltose and cellobiose, respectively. An interesting novel 12 membered bridged disaccharide **19** has been identified during optimization of the conditions for the ozonolysis reaction sequence employing lactose as starting material. Full elucidation of the NMR spectra, with the help of spin simulations, has been achieved.

4. Experimental

4.1. General procedure for indium-mediated allylation reaction (IMA)

The corresponding disaccharide (200 mg, 0.555 mmol) was added to a solution of allyl bromide (3.47 mmol, 0.3 mL, 420 mg, 6 equiv.) and indium powder (2.22 mmol, 255 mg, 4 equiv.) in 20 cm^3 ethanol/water (4:1, v/v). The suspension was heated to 65 °C and stirred for 6 h, until no further conversion of the starting material has been observed, indicated by TLC analysis (1-butanol/acetone/water 5:4:1, v/v/v). The reaction mixture was filtered over a ped of celite which was subsequently rinsed with ethanol (10 cm^3). The filtrate was concentrated under reduced pressure yielding a colorless oil. The oil was taken up in pyridine (10 cm^3), acetic anhydride (10 cm^3) and a catalytic amount of DMAP were added at 0 °C and the reaction mixture was stirred for 3 h while the solution was allowed to come to room temperature (rt). After a single spot was detected by TLC analysis (heptane/ethyl acetate 1:2, v/v) the reaction mixture was diluted with toluene and the solvents evaporated under reduced pressure. The residue was taken up in ethyl acetate (15 cm^3) and filtered over a bed of celite which was subsequently rinsed with ethyl acetate (15 cm^3). The resulting filtrate was then washed successively with water (2 × 30 cm^3) and brine (30 cm^3). The organic layer was dried over $MgSO_4$, filtered and the solvent was evaporated under reduced pressure leading to a colorless highly viscous oil. Separation of the resulting compound mixture was achieved via silica gel column chromatography (cyclohexane/ethyl acetate 1:1, v/v).

4.2. General procedure for ozonolysis

The respective allylated disaccharide was dissolved in methanol (15 cm^3) and the solution was treated with a catalytic amount of NaOMe until a pH of approx. 9 was reached. The solution was stirred at rt for 3 h, until reaction monitoring via TLC analysis (1-butanol/acetone/H_2O

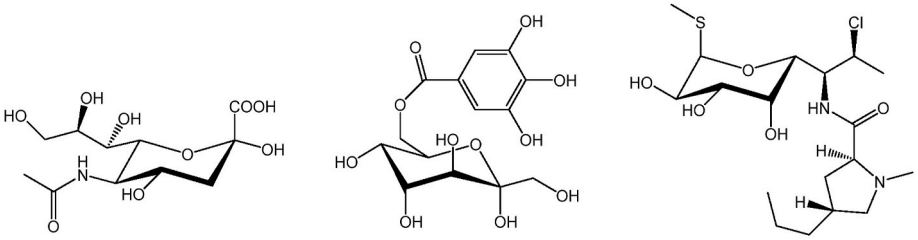

Fig. 1. Typical representatives of higher carbohydrate structures 1–3.

5:4:1, v/v/v) showed complete conversion of the starting material. The solution was diluted with dichloromethane (15 cm^3) (resulting in a mixture of dichloromethane/MeOH, 1:1, v/v) and cooled to – 78 °C. Ozone was led trough the reaction mixture via a gas inlet tube for 1 s/mg. The mixture was then purged with air for 15 min, PPh_3 (2 equiv) was added and stirring continued at rt overnight. The solvents were removed under reduced pressure and the residue was taken up in dichloromethane (20 cm^3) and water (20 cm^3). The aqueous phase was washed with dichloromethane (3 × 10 cm^3). The water was removed under reduced pressure to give a light-yellow oil. The residue was taken up in pyridine (10 cm^3), acetic anhydride (10 cm^3) and a catalytic amount of DMAP was added at 0 °C and the reaction mixture was stirred for 3 h while the solution was allowed to come to room temperature (rt), until a single spot was detected by TLC analysis (heptane/ethyl acetate 1:2, v/v). The reaction mixture was diluted with toluene and the solvents evaporated under reduced pressure. The residue was separated between water and ethyl acetate and the aqueous phase was extracted with ethyl acetate (3 × 5 mL), the combined organic layers were washed subsequently with water (10 cm^3), brine (10 cm^3) and dried over $MgSO_4$. After filtration the solvent was removed under reduced pressure leaving a colorless highly viscous oil. Separation of the resulting mixture was achieved via silica gel column chromatography (cyclohexane/ethyl acetate 1:1, v/v).

4.3. 2′,3′,4′,6′-Tetra-O-acetyl-β-D-galactopyranosyl-(1′→3)-1,2,4,5,6-penta-O-acetyl-7,8,9-trideoxy-D-glycero-L-gulo-8,9-nonenitol (14)

Lactose (**4**, 203 mg, 0.563 mmol) was reacted according to the general allylation procedure, to give compound **9** (387 mg, 0.507 mmol, 90%, *syn/anti* 80:20) as colorless oil. Analytical data for (**14**): R_f = 0.52 (heptane/ethyl acetate 1:2, v/v); $[\alpha]_D^{20}$ +23.5 (c 1.0, dichloromethane); ^{1}H NMR (600.25 MHz, $CDCl_3$, 25 °C): δ = 5.696 (dddd, $^3J_{8,9a}$ = 17.1 Hz, $^3J_{8,9b}$ = 10.1 Hz, $^3J_{8,7b}$ = 7.5 Hz, $^3J_{8,7a}$ = 6.5 Hz, 1H, H-8), 5.459 (dd, $^3J_{5,4}$ = 8.7 Hz, $^3J_{5,6}$ = 2.8 Hz, 1H, H-5), 5.442 (ddd, $^3J_{6,7b}$ = 8.6 Hz, $^3J_{6,7a}$ = 4.5 Hz, $^3J_{6,5}$ = 2.8 Hz, 1H, H-6), 5.382 (dd, $^3J_{4',3'}$ = 3.5 Hz, $^3J_{4',5'}$ = 1.2 Hz, 1H, H-4′), 5.306 (dd, $^3J_{4,5}$ = 8.7 Hz, $^3J_{4,3}$ = 2.4 Hz, 1H, H-4), 5.190 (dd, $^3J_{2',3'}$ = 10.3 Hz, $^3J_{2',1'}$ = 8.0 Hz, 1H, H-2′), 5.092 (dddd, $^3J_{9a,8}$ = 17.1 Hz, $^4J_{9a,7a}$ = 1.8 Hz, $^2J_{9a,9b}$ = 1.6 Hz, $^4J_{9a,7b}$ = 1.2 Hz, 1H, H-9a), 5.064 (dddd, $^3J_{9b,8}$ = 10.1 Hz, $^2J_{9b,9a}$ = 1.6 Hz, $^4J_{9b,7a}$ = 1.4 Hz, $^4J_{9b,7b}$ = 1.0 Hz, 1H, H-9b), 5.008 (dd, $^3J_{3',2'}$ = 10.3 Hz, $^3J_{3',4'}$ = 3.5 Hz, H-3′), 4.892 (ddd, $^3J_{2,3}$ = 6.6 Hz, $^3J_{2,1b}$ = 5.4 Hz, $^3J_{2,1a}$ = 2.4 Hz, 1H, H-2), 4.695 (d, $^3J_{1',2'}$ = 8.0 Hz, 1H, H-1′), 4.561 (dd, $^2J_{1a,1b}$ = 12.6 Hz, $^3J_{1a,2}$ = 2.4 Hz, 1H, H-1a), 4.192 (dd, $^2J_{6'a,6'b}$ = 11.2 Hz, $^3J_{6'a,5'}$ = 7.1 Hz, 1H, H-6'a), 4.189 (dd, $^3J_{3,2}$ = 6.6 Hz, $^3J_{3,4}$ = 2.4 Hz, 1H, H-3), 4.152 (dd, $^2J_{6'b,6'a}$ = 11.2 Hz, $^3J_{6'b,5'}$ = 6.3 Hz, 1H, H-6'b), 4.021 (dd, $^2J_{1b,1a}$ = 12.6 Hz, $^3J_{1b,2}$ = 5.4 Hz, 1H, H-1b), 3.947 (ddd, $^3J_{5',6'a}$ = 7.1 Hz, $^3J_{5',6'b}$ = 6.3 Hz, $^3J_{5',4'}$ = 1.2 Hz, H-5′), 2.290 (ddddd, $^2J_{7a,7b}$ = 14.4 Hz, $^3J_{7a,8}$ = 6.5 Hz, $^3J_{7a,6}$ = 4.5 Hz, $^4J_{7a,9a}$ = 1.8 Hz, $^4J_{7a,9b}$ = 1.4 Hz, 1H, H-7a), 2.271 (ddddd, $^2J_{7b,7a}$ = 14.4 Hz, $^3J_{7b,6}$ = 8.6 Hz, $^3J_{7b,8}$ = 7.5 Hz, $^4J_{7b,9a}$ = 1.2 Hz, $^4J_{7b,9b}$ = 1.0 Hz, 1H, H-7b), 2.181, 2.088, 2.086, 2.069, 2.066, 2.041, 2.032, 2.029, 1.977 (9s, 27H, 9 × OAc) ppm; ^{13}C NMR (150.93 MHz, $CDCl_3$, 25 °C) δ = 170.45, 170.40, 170.38, 170.27, 170.14, 169.99, 169.74, 169.62, 168.99 (9 × O(C=O)CH_3), 132.30 (C-8), 118.66 (C-9), 100.63 (C-1′), 74.06 (C-3), 71.61 (C-5), 71.25 (C-5′), 71.11 (C-3′), 70.66 (C-2), 69.82 (C-6), 69.55 (C-4), 69.14 (C-2′), 66.74 (C-4′), 61.18 (C-1), 60.94 (C-6′), 35.66 (C-7), 20.82, 20.79, 20.71, 20.68, 20.66, 20.63, 20.63, 20.61, 20.55 (9 × O(C=O)CH_3) ppm; HRMS (ESI^+) *m/z*: $[M + NH_4]^+$ calcd. for $C_{33}H_{50}NO_{20}^+$, 780.2922; found, 780.2927.

Table 1
Yields and diastereomeric ratio of the allylation sequence of disaccharides.

Starting material	Allylation sequence, yield, 2 steps	Diastereomeric ratio *syn/anti*
Lactose (**4**)	compound **9**, 90%	80:20
Cellobiose (**6**)	compound **10**, 80%	84:16
Maltose (**5**)	compound **11**, 92%	90:10
Melibiose [18]	compound **26**, 98%	78:22

4.4. 2′,3′,4′,6′-Tetra-O-acetyl-β-D-glucopyranosyl-(1′→3)-1,2,4,5,6-penta-O-acetyl-7,8,9-trideoxy-D-glycero-L-gulo-8,9-nonenitol (15)

Cellobiose (**6**, 200 mg, 0.555 mmol) was reacted according to the general allylation procedure, to give compound **11** (340 mg, 0.446 mmol, 80%, *syn/anti* 84:16) as colorless oil. Analytical data for (**15**): R_f = 0.54 (heptane/ethyl acetate 1:2, v/v); $[\alpha]_D^{20}$ +11.6 (c 1.0, dichloromethane); mp 123–125 °C (methanol used for crystallization); ^{1}H NMR (600.25 MHz, $CDCl_3$, 25 °C) δ = 5.629 (dddd, $^3J_{8,9a}$ = 16.8 Hz, $^3J_{8,9b}$ = 10.1 Hz, $^3J_{8,7b}$ = 7.5 Hz, $^3J_{8,7a}$ = 6.5 Hz, 1H, H-8), 5.514 (ddd, $^3J_{6,7b}$ = 9.0 Hz, $^3J_{6,7a}$ = 4.2 Hz, $^3J_{6,5}$ = 2.7 Hz, 1H, H-6), 5.441 (dd, $^3J_{5,4}$ = 8.9 Hz, $^3J_{5,6}$ = 2.7 Hz, 1H, H-5), 5.298 (dd, $^3J_{4,5}$ = 8.9 Hz, $^3J_{4,3}$ = 2.2 Hz, 1H, H-4), 5.199 (dd, $^3J_{3',2'}$ = 9.5 Hz, $^3J_{3',4'}$ = 9.5 Hz, H-3′), 5.138 (dd, $^3J_{4',5'}$ = 10.1 Hz, $^3J_{4',3'}$ = 9.5 Hz, 1H, H-4′), 5.054 (dddd, $^3J_{9a,8}$ = 16.8 Hz,

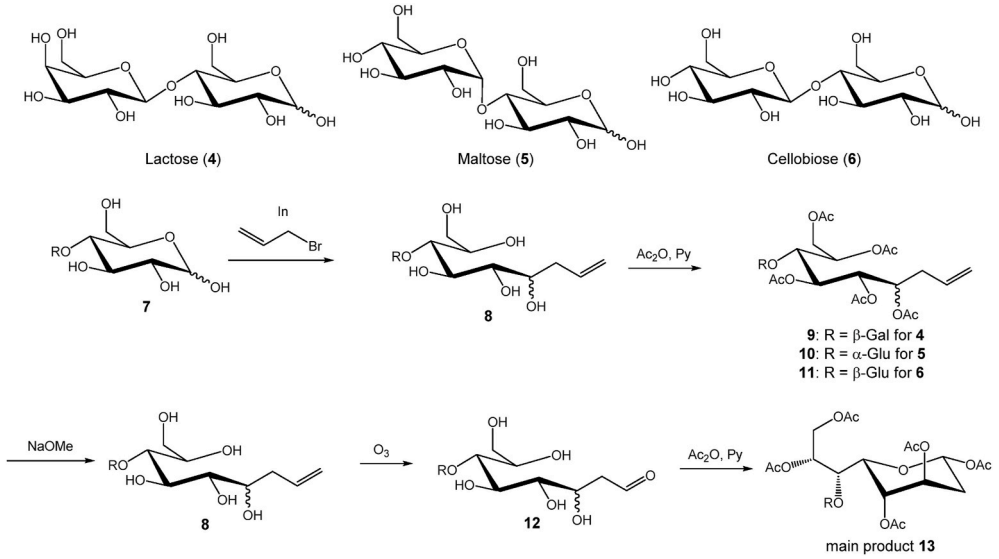

Scheme 1. General elongation sequence, IMA and ozonolysis, for disaccharidic starting materials, lactose (**4**, R = β-Gal in compounds **7**–**13**), maltose (**5**, R = α-Glu in compounds **7**–**13**) as well as cellobiose (**6**, R = β-Glu in compounds **7**–**13**).

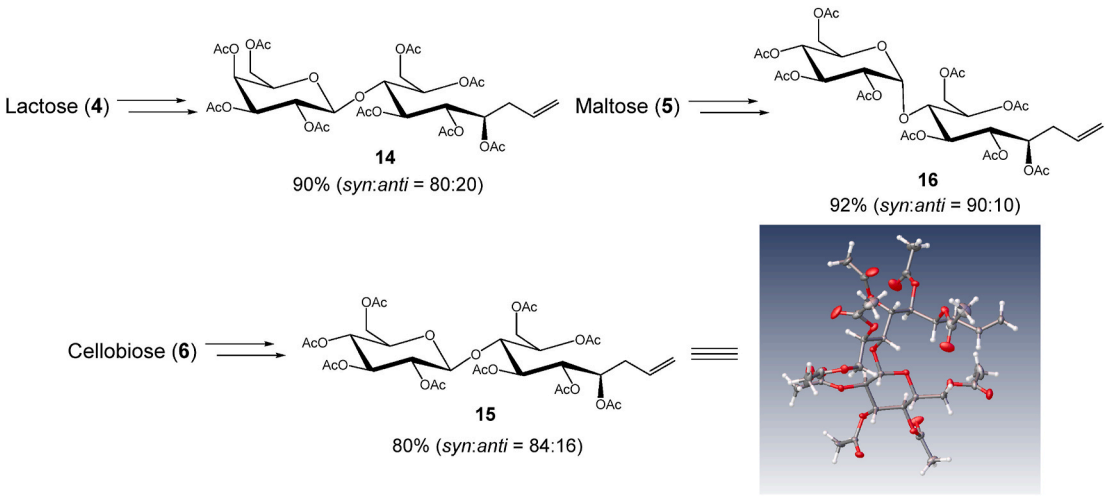

Scheme 2. Products of the allylation sequence and X-ray structure for the allylation of cellobiose (**6**) [CCDC 2010237].

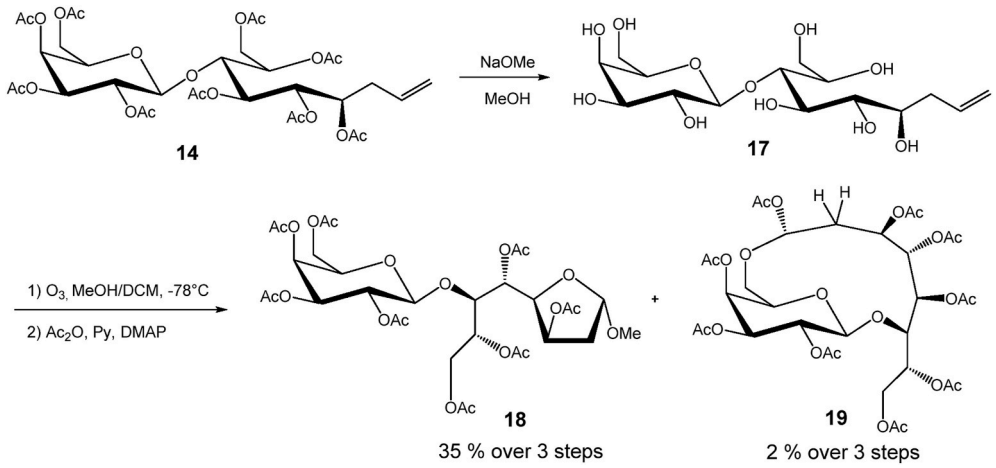

Scheme 3. Fist attempts of ozonolysis sequence and unexpected side products in the elongation of lactose (**4**).

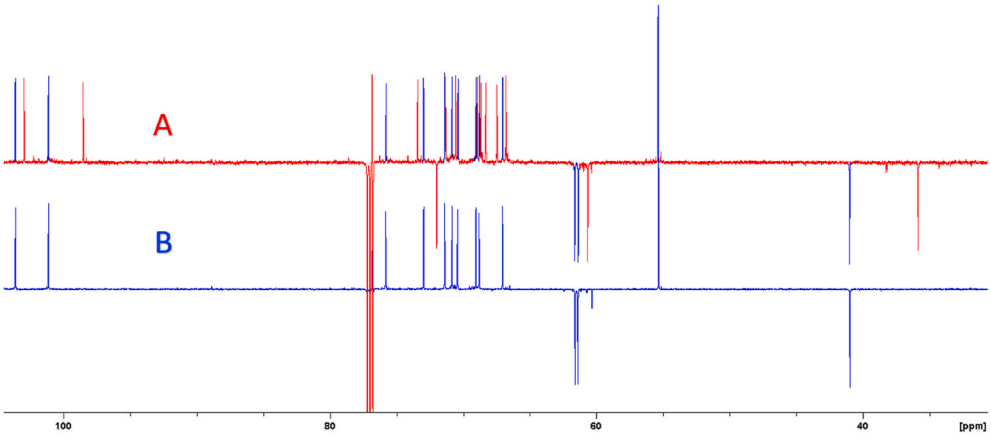

Fig. 2. A: top, ^{13}C NMR of the mixture of compounds **18** and **19** (blue: signals for compound **18**; red signals for compound **19**. B: bottom, ^{13}C NMR of pure compound **18**. (For interpretation of the references to color in this figure legend, the reader is referred to the Web version of this article.)

$^{4}J_{9a,7a} = 1.5$ Hz, $^{2}J_{9a,9b} = 1.5$ Hz, $^{4}J_{9a,7b} = 1.0$ Hz, 1H, H-9a), 5.041 (dd, $^{3}J_{2',3'} = 9.5$ Hz, $^{3}J_{2',1'} = 8.0$ Hz, 1H, H-2′), 5.038 (dddd, $^{3}J_{9b,8} = 10.1$ Hz, $^{2}J_{9b,9a} = 1.5$ Hz, $^{4}J_{9b,7b} = 1.5$ Hz, $^{4}J_{9b,7a} = 1.0$ Hz, 1H, H-9b), 4.871 (ddd, $^{3}J_{2,3} = 6.8$ Hz, $^{3}J_{2,1b} = 5.2$ Hz, $^{3}J_{2,1a} = 2.4$ Hz, 1H, H-2), 4.753 (d, $^{3}J_{1',2'} = 8.0$ Hz, 1H, H-1′), 4.604 (dd, $^{2}J_{1a,1b} = 12.6$ Hz, $^{3}J_{1a,2} = 2.4$ Hz, 1H, H-1a), 4.379 (dd, $^{2}J_{6'a,6'b} = 12.6$ Hz, $^{3}J_{6'a,5'} = 4.0$ Hz, 1H, H-6'a), 4.185 (dd, $^{3}J_{3,2} = 6.8$ Hz, $^{3}J_{3,4} = 2.2$ Hz, 1H, H-3), 4.159 (dd, $^{2}J_{6'b,6'a} = 12.6$ Hz, $^{3}J_{6'b,5'} = 2.2$ Hz, 1H, H-6'b), 3.996 (dd, $^{2}J_{1b,1a} = 12.6$ Hz, $^{3}J_{1b,2} = 5.2$ Hz, 1H, H-1b), 3.727 (ddd, $^{3}J_{5',4'} = 10.1$ Hz, $^{3}J_{5',6'a} = 4.0$ Hz, $^{3}J_{5',6'b} = 2.2$ Hz, H-5′), 2.265 (ddddd, $^{2}J_{7a,7b} = 14.4$ Hz, $^{3}J_{7a,8} = 6.5$ Hz,

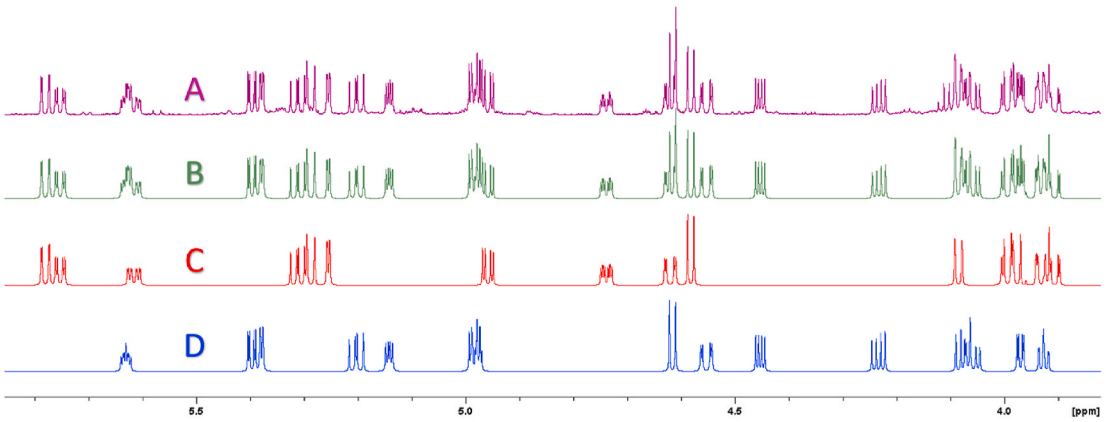

Fig. 3. Expanded region of the ^{1}H NMR of the mixture of compounds **18** and **19** (A: experimental spectrum, B: sum of the calculated spectra of compound **18** and **19**, C: calculated spectrum of compound **19**, D: calculated spectrum of compound **18**).

$^{3}J_{7a,6}$ = 4.2 Hz, $^{4}J_{7a,9a}$ = 1.5 Hz, $^{4}J_{7a,9b}$ = 1.0 Hz, 1H, H-7a), 2.246 (ddddd, $^{2}J_{7b,7a}$ = 14.4 Hz, $^{3}J_{7b,6}$ = 9.0 Hz, $^{3}J_{7b,8}$ = 7.5 Hz, $^{4}J_{7b,9b}$ = 1.5 Hz, $^{4}J_{7b,9a}$ = 1.0 Hz, 1H, H-7b), 2.096, 2.092, 2.092, 2.065, 2.063, 2.031, 2.031 2.021, 2.005 (9s, 27H, 9 × OAc) ppm; ^{13}C NMR (150.93 MHz, $CDCl_3$, 25 °C) δ = 170.69, 170.58, 170.34, 170.30, 169.97, 169.58, 169.57, 169.26, 169.01 (9 × O(C═O)CH_3), 132.34 (C-8), 118.48 (C-9), 100.26 (C-1′), 74.05 (C-3), 73.04 (C-3′), 72.36 (C-5′), 71.69 (C-2′), 71.56 (C-5), 70.55 (C-2), 69.69 (C-6), 69.34 (C-4), 67.59 (C-4′), 61.16 (C-6′), 61.04 (C-1), 35.61 (C-7), 20.79, 20.76, 20.62, 20.62, 20.58, 20.58, 20.58, 20.58, 20.53 (9 × O(C═O)CH_3) ppm; HRMS (ESI+) *m/z*: $[M + Na]^+$ calcd. for $C_{33}H_{46}O_{20}Na^+$, 785.2475; found, 785.2476. CCDC 2010237 contains the supplementary crystallographic data for compound **15**. These data can be obtained from The Cambridge Crystallographic Data Centre, http://www.ccdc.cam.ac.uk/data_request/cif.

4.5. 2′,3′,4′,6′-Tetra-O-acetyl-α-D-glucopyranosyl-(1′→3)-1,2,4,5,6-penta-O-acetyl-7,8,9-trideoxy-D-glycero-L-gulo-8,9-nonenitol (16)

Maltose (**5**, 208 mg, 0.577 mmol) was reacted according to the general allylation procedure, to give compound **10** (398 mg, 0.522 mmol, 92%, *syn/anti* 90:10) as colorless oil. Analytical data for (**16**): R_f = 0.54 (heptane/ethyl acetate 1:2, v/v); $[\alpha]_D^{20}$ +84.2 (*c* 1.0, dichloromethane); ^{1}H NMR (600.25 MHz, $CDCl_3$, 25 °C) δ = 5.682 (dddd, $^{3}J_{8,9a}$ = 16.8 Hz, $^{3}J_{8,9b}$ = 10.1 Hz, $^{3}J_{8,7b}$ = 8.2 Hz, $^{3}J_{8,7a}$ = 6.0 Hz, 1H, H-8), 5.385 (dd, $^{3}J_{4,3}$ = 5.7 Hz, $^{3}J_{4,5}$ = 5.0 Hz, 1H, H-4), 5.377 (dd, $^{3}J_{3',2'}$ = 10.4 Hz, $^{3}J_{3',4'}$ = 9.5 Hz, H-3′), 5.307 (dd, $^{3}J_{5,6}$ = 5.6 Hz, $^{3}J_{5,4}$ = 5.0 Hz, 1H, H-5), 5.266 (d, $^{3}J_{1',2'}$ = 3.9 Hz, 1H, H-1′), 5.099 (dddd, $^{3}J_{9a,8}$ = 16.8 Hz, $^{2}J_{9a,9b}$ = 1.3 Hz, $^{4}J_{9a,7a}$ = 1.2 Hz, $^{4}J_{9a,7b}$ = 1.0 Hz, 1H, H-9a), 5.094 (ddd, $^{3}J_{6,7b}$ = 9.0 Hz, $^{3}J_{6,5}$ = 5.6 Hz, $^{3}J_{6,7a}$ = 4.0 Hz, 1H, H-6), 5.086 (ddd, $^{3}J_{2,1b}$ = 6.5 Hz, $^{3}J_{2,3}$ = 3.7 Hz, $^{3}J_{2,1a}$ = 3.3 Hz, 1H, H-2), 5.074 (dd, $^{3}J_{4',5'}$ = 10.3 Hz, $^{3}J_{4',3'}$ = 9.5 Hz, 1H, H-4′), 5.071 (dddd, $^{3}J_{9b,8}$ = 10.1 Hz, $^{4}J_{9b,7a}$ = 1.5 Hz, $^{2}J_{9b,9a}$ = 1.3 Hz, $^{4}J_{9b,7b}$ = 1.0 Hz, 1H, H-9b), 4.927 (dd, $^{3}J_{2',3'}$ = 10.4 Hz, $^{3}J_{2',1'}$ = 3.9 Hz, 1H, H-2′), 4.554 (dd, $^{2}J_{1a,1b}$ = 12.4 Hz, $^{3}J_{1a,2}$ = 3.3 Hz, 1H, H-1a), 4.307 (dd, $^{2}J_{6'a,6'b}$ = 12.4 Hz, $^{3}J_{6'a,5'}$ = 4.3 Hz, 1H, H-6'a), 4.192 (ddd, $^{3}J_{5',4'}$ = 10.3 Hz, $^{3}J_{5',6'a}$ = 4.3 Hz, $^{3}J_{5',6'b}$ = 2.1 Hz, H-5′), 4.146 (dd, $^{2}J_{1b,1a}$ = 12.4 Hz, $^{3}J_{1b,2}$ = 6.5 Hz, 1H, H-1b), 4.074 (dd, $^{2}J_{6'b,6'a}$ = 12.4 Hz, $^{3}J_{6'b,5'}$ = 2.1 Hz, 1H, H-6'b), 4.043 (dd, $^{3}J_{3,4}$ = 5.7 Hz, $^{3}J_{3,2}$ = 3.7 Hz, 1H, H-3), 2.389 (ddddd, $^{2}J_{7a,7b}$ = 14.8 Hz, $^{3}J_{7a,8}$ = 6.0 Hz, $^{3}J_{7a,6}$ = 4.0 Hz, $^{4}J_{7a,9b}$ = 1.5 Hz, $^{4}J_{7a,9a}$ = 1.2 Hz, 1H, H-7a), 2.282 (ddddd, $^{2}J_{7b,7a}$ = 14.8 Hz, $^{3}J_{7b,6}$ = 9.0 Hz, $^{3}J_{7b,8}$ = 8.2 Hz, $^{4}J_{7b,9a}$ = 1.0 Hz, $^{4}J_{7b,9b}$ = 1.0 Hz, 1H, H-7b), 2.106, 2.097, 2.079, 2.079, 2.069, 2.056, 2.033, 2.022, 1.988 (9s, 27H, 9 × OAc) ppm; ^{13}C NMR (150.93 MHz, $CDCl_3$, 25 °C) δ = 170.54, 170.39, 170.36, 170.11, 169.84, 169.82, 169.7,6 169.51, 169.46 (9 × O(C═O)CH_3), 132.06 (C-8), 118.94 (C-9), 96.39 (C-1′), 75.48 (C-3), 71.39 (C-5), 71.29 (C-6), 70.53 (C-2′), 70.42 (C-4), 70.06 (C-2), 69.66 (C-3′), 68.18 (C-5′), 68.01 (C-4′), 61.74 (C-1), 61.53 (C-6′), 35.37 (C-7), 20.90, 20.74, 20.70, 20.63, 20.63, 20.59, 20.57, 20.57, 20.55 (9 × O(C═O)CH_3) ppm; HRMS (ESI^+) *m/z*: $[M + NH_4]^+$ calcd. for $C_{33}H_{50}NO_{20}^+$, 780.2922; found, 780.2922.

4.6. 2′,3′,4′,6′-Tetra-O-acetyl-β-D-galactopyranosyl-(1′→6)-3,4,7,8-penta-O-acetyl-2-deoxy-1-O-methyl-β-D-glycero-D-ido-octofuranose (18)

Compound **14** (150 mg, 0.197 mmol) was dissolved in methanol (10 cm^3) and the solution was treated with a catalytic amount of NaOMe until a pH of approx. 9 was reached. The solution was stirred at rt for 8 h, until reaction monitoring via TLC analysis (1-butanol/acetone/H_2O 5:4:1, v/v/v) showed complete conversion of the starting material. The solution was diluted with dichloromethane (15 cm^3) (resulting in a mixture of dichloromethane/MeOH, 1:1, v/v) and cooled to − 78 °C. Ozone was led trough the reaction mixture via a gas inlet tube for 10min (4 s/mg). The mixture was then purged with air for 15 min, PPh_3 (2 equiv) was added and stirring continued at rt overnight. The solvents were removed under reduced pressure and the residue was taken up in dichloromethane (15 cm^3) and water (15 cm^3). The aqueous phase was washed with dichloromethane (3 × 10 cm^3). The water was removed

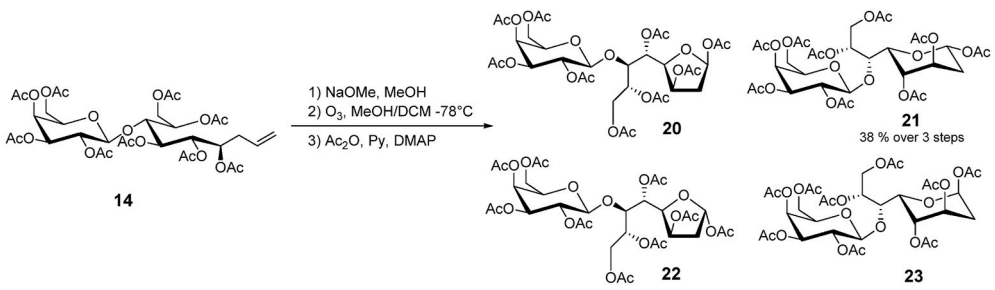

Scheme 4. Products after the ozonolysis sequence of compound **14**, ^{13}C spectra of the compound mixture in the electronic supporting information.

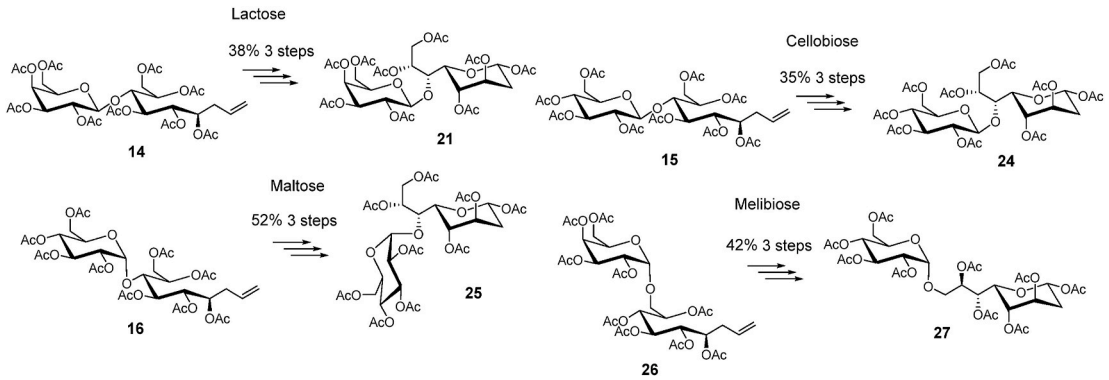

Scheme 5. Main products of the elongation of disaccharides **4**, **5**, **6**, melibiose for comparison.

under reduced pressure to give a light-yellow oil. The residue was taken up in pyridine (10 cm^3), acetic anhydride (10 cm^3) and a catalytic amount of DMAP was added at 0 °C and the reaction mixture was stirred for 3 h while the solution was allowed to come to room temperature (rt), until a single spot was detected by TLC analysis (heptane/ethyl acetate 1:2, v/v). The reaction mixture was diluted with toluene and the solvents evaporated under reduced pressure. The residue was separated between water and ethyl acetate and the aqueous phase was extracted with ethyl acetate (3 × 5 mL), the combined organic layers were washed subsequently with water (10 cm^3), brine (10 cm^3) and dried over $MgSO_4$. After filtration the solvent was removed under reduced pressure leaving a colorless highly viscous oil. Separation of the resulting mixture was achieved via silica gel column chromatography (cyclohexane/ethyl acetate 1:1, v/v) which gives compound **18** (50 mg, 0.068 mmol, 35%) as colorless oil. R_f = 0.40 (heptane/ethyl acetate 1:2, v/v); $[\alpha]_D^{20}$ +37.0 (c 1.0, dichloromethane); ^{1}H NMR (600.25 MHz, $CDCl_3$, 25 °C) δ = 5.637 (ddd, $^3J_{3,2a}$ = 6.4 Hz, $^3J_{3,4}$ = 4.0 Hz, $^3J_{3,2b}$ = 2.4 Hz, 1H, H-3), 5.404 (dd, $^3J_{5,4}$ = 8.0 Hz, $^3J_{5,6}$ = 2.3 Hz, 1H, H-5), 5.385 (dd, $^3J_{4',3'}$ = 3.5 Hz, $^3J_{4',5'}$ = 1.1 Hz, 1H, H-4′), 5.209 (dd, $^3J_{2',3'}$ = 10.4 Hz, $^3J_{2',1'}$ = 8.0 Hz, 1H, H-2′), 5.148 (dd, $^3J_{1,2b}$ = 5.7 Hz, $^3J_{1,2a}$ = 3.0 Hz, 1H, H-1), 4.989 (dd, $^3J_{3',2'}$ = 10.4 Hz, $^3J_{3',4'}$ = 3.5 Hz, 1H, H-3′), 4.986 (ddd, $^3J_{7,6}$ = 6.7 Hz, $^3J_{7,8b}$ = 5.3 Hz, $^3J_{7,8a}$ = 2.3 Hz, 1H, H-7), 4.620 (d, $^3J_{1',2'}$ = 8.0 Hz, 1H, H-1′), 4.560 (dd, $^2J_{8a,8b}$ = 12.5 Hz, $^3J_{8a,7}$ = 2.3 Hz, 1H, H-8a), 4.459 (dd, $^3J_{4,5}$ = 8.0 Hz, $^3J_{4,3}$ = 4.0 Hz, 1H, H-4), 4.238 (dd, $^2J_{6'a,6'b}$ = 11.6 Hz, $^3J_{6'a,5'}$ = 5.8 Hz, 1H, H-6'a), 4.083 (dd, $^2J_{6'b,6'a}$ = 11.6 Hz, $^3J_{6'b,5'}$ = 6.7 Hz, 1H, H-6'b), 4.064 (dd, $^2J_{8b,8a}$ = 12.5 Hz, $^3J_{8b,7}$ = 5.3 Hz, 1H, H-8b), 3.976 (dd, $^3J_{6,7}$ = 6.7 Hz, $^3J_{6,5}$ = 2.3 Hz, 1H, H-6), 3.930 (ddd, $^3J_{5',6'}$ = 6.7 Hz, $^3J_{5',6'a}$ = 5.8 Hz, $^3J_{5',4'}$ = 1.1 Hz, 1H, H-5′), 3.336 (s, 3H, OMe), 2.234 (ddd, $^2J_{2a,2b}$ = 14.8 Hz, $^3J_{2a,3}$ = 6.4 Hz, $^3J_{2a,1}$ = 3.0 Hz, 1H, H-2a), 2.182 (ddd, $^2J_{2b,2a}$ = 14.8 Hz, $^3J_{2b,1}$ = 5.7 Hz, $^3J_{2b,3}$ = 2.4 Hz, 1H, H-2b), 2.175, 2.103, 2.091, 2.081, 2.066, 2.058, 2.054, 1.987 (8s, 24H, OAc) ppm; ^{13}C NMR (150.93 MHz, $CDCl_3$, 25 °C) δ = 170.47, 170.32, 170.21, 170.18, 170.16, 170.03, 169.60, 169.13 (8 × O(C═O)CH_3), 103.62 (C-1), 101.15 (C-1′),76.82 (C-4), 75.83 (C-6), 72.98 (C-3), 71.40 (C-5′), 70.85 (C-3′), 70.43 (C-7), 69.06 (C-5), 68.81 (C-2′), 67.05 (C-4′), 61.61 (C-6′), 61.39 (C-8), 55.34 (OCH_3), 40.97 (C-2), 20.84, 20.84, 20.84, 20.65, 20.64, 20.64, 20.55, 20.47 (8 × O(C═O)CH_3) ppm; HRMS (ESI+) *m/z*: $[M + Na]^+$ calcd. for $C_{31}H_{44}O_{20}Na^+$, 759.2318; found, 759.2317.

*4.7. (1S,3R,4S,5S,6R,8R,11R,12S,13S,14R)-3-((R)-1,2-diacetoxyethyl)-2,9,15-trioxabicyclo[9.3.1]pentadecane-4,5,6,8,12,13,14-heptayl heptaacetate (**19**)*

Compound **14** (200 mg, 0.263 mmol) was dissolved in methanol (10 cm^3) and the solution was treated with a catalytic amount of NaOMe until a pH of approx. 9 was reached. The solution was stirred at rt for 5 h, until reaction monitoring via TLC analysis (1-butanol/acetone/H_2O 5:4:1, v/v/v) showed complete conversion of the starting material. The solution was diluted with dichloromethane (15 cm^3) (resulting in a mixture of dichloromethane/MeOH, 1:1, v/v) and cooled to – 78 °C. Ozone was led trough the reaction mixture via a gas inlet tube for 10min (3 s/mg). The mixture was then purged with air for 15 min, PPh_3 (2 equiv) was added and stirring continued at rt overnight. The solvents were removed under reduced pressure and the residue was taken up in dichloromethane (15 cm^3) and water (15 cm^3). The aqueous phase was washed with dichloromethane (3 × 10 cm^3). The water was removed under reduced pressure to give a light-yellow oil. The residue was taken up in pyridine (10 cm^3), acetic anhydride (10 cm^3) and a catalytic amount of DMAP was added at 0 °C and the reaction mixture was stirred for 3 h while the solution was allowed to come to room temperature (rt), until a single spot was detected by TLC analysis (heptane/ethyl acetate 1:2, v/v). The reaction mixture was diluted with toluene and the solvents evaporated under reduced pressure. The residue was separated between water and ethyl acetate and the aqueous phase was extracted with ethyl acetate (3 × 5 mL), the combined organic layers were washed subsequently with water (10 cm^3), brine (10 cm^3) and dried over $MgSO_4$. After filtration the solvent was removed under reduced pressure leaving a colorless highly viscous oil. Separation of the resulting mixture was achieved via silica gel column chromatography (cyclohexane/ethyl acetate 1:1, v/v) which gives compound **18** (67 mg, 0.091 mmol, 35%) as colorless oil (Analytical data see 4.6) and compound **19** (4 mg, 0.005 mmol, 2%) as colorless oil. R_f = 0.40 (heptane/ethyl acetate 1:2, v/v); ^{1}H NMR (600.25 MHz, $CDCl_3$, 25 °C) δ = 5.781 (dd, $^3J_{4,5}$ = 9.8 Hz, $^3J_{4,3}$ = 1.4 Hz, 1H, H-4), 5.753 (dd, $^3J_{1,2a}$ = 10.2 Hz, $^3J_{1,2b}$ = 2.2 Hz, 1H, H-1), 5.616 (ddd, $^3J_{3,2b}$ = 11.3 Hz, $^3J_{3,2a}$ = 3.9 Hz, $^3J_{3,4}$ = 1.4 Hz, 1H, H-3), 5.312 (dd, $^3J_{2',3'}$ = 10.4 Hz, $^3J_{2',1'}$ = 8.1 Hz, 1H, H-2′), 5.288 (dd, $^3J_{5,4}$ = 9.8 Hz, $^3J_{5,6}$ = 0.8 Hz, 1H, H-5), 5.255 (dd, $^3J_{4',3'}$ = 3.5 Hz, $^3J_{4',5'}$ = 1.0 Hz, 1H, H-4′), 4.959 (dd, $^3J_{3',2'}$ = 10.4 Hz, $^3J_{3',4'}$ = 3.5 Hz, 1H, H-3′), 4.739 (ddd, $^3J_{7,6}$ = 9.4 Hz, $^3J_{7,8b}$ = 3.3 Hz, $^3J_{7,8a}$ = 2.2 Hz, 1H, H-7), 4.620 (dd, $^2J_{8a,8b}$ = 12.4 Hz, $^3J_{8a,7}$ = 2.2 Hz, 1H, H-8a), 4.582 (d, $^3J_{1',2'}$ = 8.1 Hz, 1H, H-1′), 4.085 (dd, $^3J_{6,7}$ = 9.4 Hz, $^3J_{6,5}$ = 0.8 Hz, 1H, H-6), 3.994 (dd, $^2J_{8b,8a}$ = 12.4 Hz, $^3J_{8b,7}$ = 3.3 Hz, 1H, H-8b), 3.983 (dd, $^2J_{6'a,6'b}$ = 12.6 Hz, $^3J_{6'a,5'}$ = 10.3 Hz, 1H, H-6'a), 3.933 (ddd, $^3J_{5',6'a}$ = 10.3 Hz, $^3J_{5',6'b}$ = 2.6 Hz, $^3J_{5',4'}$ = 1.0 Hz, 1H, H-5′), 3.908 (dd, $^2J_{6'b,6'a}$ = 12.6 Hz, $^3J_{6'b,5'}$ = 2.6 Hz, 1H, H-6'b), 2.208, 2.140, 2.127, 2.080, 2.056, 2.038, 2.015, 2.015, 1.964 (9s, 27H, OAc), 1.917 (ddd, $^2J_{2a,2b}$ = 13.6 Hz, $^3J_{2a,1}$ = 10.2 Hz, $^3J_{2a,3}$ = 3.9 Hz, 1H, H-2a), 1.880 (ddd, $^2J_{2b,2a}$ = 13.6 Hz, $^3J_{2b,3}$ = 11.3 Hz, $^3J_{2b,1}$ = 2.2 Hz, 1H, H-2b) ppm; ^{13}C NMR

Table 2
Yields of the ozonolysis sequence, melibiose for comparison [18].[a] compound mixture of α- and β-furanose as well as α- and β-pyranose forms.

Starting material	Ozonolysis sequence, yields, 3 steps[a]	Main product, yield
Lactose (**4**)	64%	compound **21**, 38%
Cellobiose (**6**)	50%	compound **24**, 35%
Maltose (**5**)	70%	compound **25**, 52%
Melibiose [18]	72%	compound **27**, 42%

(150.93 MHz, $CDCl_3$, 25 °C) δ = 170.52, 170.52, 170.23, 170.14, 170.12, 170.08, 169.86, 169.49, 168.98 (9 × O(C=O)CH_3), 102.98 (C-1′), 98.55 (C-1), 68.32 (C-5), 76.85 (C-6), 68.94 (C-7), 71.34 (C-3′), 68.68 (C-2′), 66.81 (C-4′), 73.44 (C-5′), 67.47 (C-3), 70.57 (C-4), 60.66 (C-8), 72.00 (C-6′), 35.86 (C-2), 21.12, 20.74, 20.73, 20.69, 20.69, 20.69, 20.59, 20.52, 20.48 (9 × O(C=O)CH_3) ppm; HRMS (ESI+) *m/z*: $[M + Na]^+$ calcd. for $C_{32}H_{44}O_{21}Na^+$, 787.2268; found, 787.2263.

4.8. 2′,3′,4′,6′-Tetra-O-acetyl-β-D-galactopyranosyl-(1′→6)-1,3,4,7,8-penta-O-acetyl-2-deoxy-β-D-glycero-D-ido-octopyranose (21)

Compound **14** (189 mg, 0.248 mmol) was reacted according to the general ozonolysis procedure, to give compound **21** (73 mg, 0.095 mmol, 38%) as colorless oil. R_f = 0.36 (heptane/ethyl acetate 1:2, v/v); $[\alpha]_D^{20}$ +15.2 (c 1.0, dichloromethane); ^{1}H NMR (600.25 MHz, $CDCl_3$, 25 °C) δ = 5.854 (dd, $^3J_{1,2a}$ = 10.4 Hz, $^3J_{1,2b}$ = 2.3 Hz, 1H, H-1), 5.365 (dd, $^3J_{4',3'}$ = 3.5 Hz, $^3J_{4',5'}$ = 1.2 Hz, 1H, H-4′), 5.167 (ddd, $^3J_{7,8b}$ = 7.1 Hz, $^3J_{7,6}$ = 4.1 Hz, $^3J_{7,8a}$ = 3.0 Hz, 1H, H-7), 5.151 (dd, $^3J_{2',3'}$ = 10.4 Hz, $^3J_{2',1'}$ = 7.9 Hz, 1H, H-2′), 5.100 (ddd, $^3J_{3,4}$ = 3.5 Hz, $^3J_{3,2a}$ = 2.9 Hz, $^3J_{3,2b}$ = 2.9 Hz, 1H, H-3), 4.992 (dd, $^3J_{3',2'}$ = 10.4 Hz, $^3J_{3',4'}$ = 3.5 Hz, 1H, H-3′), 4.920 (dd, $^3J_{4,3}$ = 3.5 Hz, $^3J_{4,5}$ = 1.1 Hz, 1H, H-4), 4.589 (d, $^3J_{1',2'}$ = 7.9 Hz, 1H, H-1′), 4.448 (dd, $^2J_{8a,8b}$ = 12.4 Hz, $^3J_{8a,7}$ = 3.0 Hz, 1H, H-8a), 4.253 (dd, $^3J_{5,6}$ = 5.8 Hz, $^3J_{5,4}$ = 1.1 Hz, 1H, H-5), 4.123 (dd, $^2J_{6'a,6'b}$ = 11.3 Hz, $^3J_{6'a,5'}$ = 6.4 Hz, 1H, H-6'a), 4.117 (dd, $^3J_{6,5}$ = 5.8 Hz, $^3J_{6,7}$ = 4.1 Hz, 1H, H-6), 4.096 (dd, $^2J_{8b,8a}$ = 12.4 Hz, $^3J_{8b,7}$ = 7.1 Hz, 1H, H-8b), 4.077 (dd, $^2J_{6'b,6'a}$ = 11.3 Hz, $^3J_{6'b,5'}$ = 7.6 Hz, 1H, H-6'b), 3.866 (ddd, $^3J_{5',6'b}$ = 7.6 Hz, $^3J_{5',6'a}$ = 6.4 Hz, $^3J_{5',4'}$ = 1.2 Hz, 1H, H-5′), 2.195, 2.168, 2.114, 2.110, 2.080, 2.072, 2.057, 2.046 (8s, 24H, OAc), 2.001 (ddd, $^2J_{2a,2b}$ = 14.5 Hz, $^3J_{2a,3}$ = 2.9 Hz, $^3J_{2a,1}$ = 2.3 Hz, 1H, H-2a), 1.979 (1s, 3H, OAc), 1.952 (ddd, $^2J_{2b,2a}$ = 14.5 Hz, $^3J_{2b,1}$ = 10.4 Hz, $^3J_{2b,3}$ = 2.9 Hz, 1H, H-2b) ppm; ^{13}C NMR (150.93 MHz, $CDCl_3$, 25 °C) δ = 170.35, 170.33, 170.16, 170.16, 169.69, 169.67, 169.26, 168.99, 168.95 (9 × O(C=O)CH_3), 101.87 (C-1′), 90.90 (C-1), 78.99 (C-6), 73.05 (C-5), 71.55 (C-7), 70.93 (C-3′), 70.67 (C-5′), 69.03 (C-2′), 67.70 (C-3), 66.75 (C-4′), 65.86 (C-4), 61.89 (C-8), 60.82 (C-6′), 30.02 (C-2), 21.02, 21.00, 20.92, 20.89, 20.78, 20.73, 20.65, 20.61, 20.55 (9 × O(C=O)CH_3) ppm; HRMS (ESI+) *m/z*: $[M + Na]^+$ calcd. for $C_{32}H_{44}O_{21}Na^+$, 787.2268; found, 787.2269.

4.9. 2′,3′,4′,6′-Tetra-O-acetyl-β-D-glucopyranosyl-(1′→6)-1,3,4,7,8-penta-O-acetyl-2-deoxy-β-D-glycero-D-ido-octopyranose (24)

Compound **15** (140 mg, 0.184 mmol) was reacted according to the general ozonolysis procedure, to give compound **24** (49 mg, 0.064 mmol, 35%) as colorless oil. R_f = 0.39 (heptane/ethyl acetate 1:2, v/v); $[\alpha]_D^{20}$ +4.6 (c 0.5, dichloromethane); ^{1}H NMR (600.25 MHz, $CDCl_3$, 25 °C) δ = 5.859 (dd, $^3J_{1,2a}$ = 9.7 Hz, $^3J_{1,2b}$ = 3.0 Hz, 1H, H-1), 5.174 (dd, $^3J_{3',2'}$ = 9.6 Hz, $^3J_{3',4'}$ = 9.5 Hz, 1H, H-3′), 5.173 (ddd, $^3J_{7,8a}$ = 7.2 Hz, $^3J_{7,6}$ = 3.8 Hz, $^3J_{7,8b}$ = 3.2 Hz, 1H, H-7), 5.096 (ddd, $^3J_{3,4}$ = 3.5 Hz, $^3J_{3,2a}$ = 3.0 Hz, $^3J_{3,2b}$ = 3.0 Hz, 1H, H-3), 5.069 (dd, $^3J_{4',5'}$ = 9.9 Hz, $^3J_{4',3'}$ = 9.5 Hz, 1H, H-4′), 4.941 (dd, $^3J_{2',3'}$ = 9.6 Hz, $^3J_{2',1'}$ = 7.9 Hz, 1H, H-2′), 4.904 (dd, $^3J_{4,3}$ = 3.5 Hz, $^3J_{4,5}$ = 1.1 Hz, 1H, H-4), 4.684 (d, $^3J_{1',2'}$ = 7.9 Hz, 1H, H-1′), 4.405 (dd, $^2J_{8a,8b}$ = 12.3 Hz, $^3J_{8a,7}$ = 3.2 Hz, 1H, H-8a), 4.262 (dd, $^3J_{5,6}$ = 6.3 Hz, $^3J_{5,4}$ = 1.1 Hz, 1H, H-5), 4.233 (dd, $^2J_{6'a,6'b}$ = 12.2 Hz, $^3J_{6'a,5'}$ = 4.8 Hz, 1H, H-6'a), 4.136 (dd, $^3J_{6,5}$ = 6.3 Hz, $^3J_{6,7}$ = 3.8 Hz, 1H, H-6), 4.110 (dd, $^2J_{6'b,6'a}$ = 12.2 Hz, $^3J_{6'b,5'}$ = 2.7 Hz, 1H, H-6'b), 4.085 (dd, $^2J_{8b,8a}$ = 12.3 Hz, $^3J_{8b,7}$ = 7.2 Hz, 1H, H-8b), 3.671 (ddd, $^3J_{5',4'}$ = 9.9 Hz, $^3J_{5',6'a}$ = 4.8 Hz, $^3J_{5',6'b}$ = 2.7 Hz, 1H, H-5′), 2.169, 2.106, 2.106, 2.092, 2.063, 2.063, 2.054, 2.016 (8s, 24H, OAc), 2.001 (ddd, $^2J_{2a,2b}$ = 14.5 Hz, $^3J_{2a,1}$ = 9.7 Hz, $^3J_{2a,3}$ = 3.0 Hz, 1H, H-2a), 2.000 (1s, 3H, OAc), 1.956 (ddd, $^2J_{2b,2a}$ = 14.5 Hz, $^3J_{2b,3}$ = 3.0 Hz, $^3J_{2b,1}$ = 3.0 Hz, 1H, H-2b) ppm; ^{13}C NMR (150.93 MHz, $CDCl_3$, 25 °C) δ = 170.63, 170.35, 170.30, 169.66, 169.63, 169.32, 169.19, 169.00, 168.91 (9 × O(C=O)CH_3), 101.07 (C-1′), 90.85 (C-1), 78.71 (C-6), 73.27 (C-5), 72.80 (C-7), 71.85 (C-5′), 71.57 (C-2′), 71.46 (C-3′), 68.35 (C-4′), 67.61 (C-3), 65.71 (C-4), 62.13 (C-6′), 61.95 (C-8), 30.04 (C-2), 20.98, 20.97, 20.90, 20.88, 20.75, 20.68, 20.63, 20.59, 20.57 (9 × O(C=O)CH_3) ppm; HRMS (ESI+) *m/z*: $[M + Na]^+$ calcd. for $C_{32}H_{44}O_{21}Na^+$, 787.2268; found, 787.2266.

4.10. 2′,3′,4′,6′-Tetra-O-acetyl-α-D-glucopyranosyl-(1′→6)-1,3,4,7,8-penta-O-acetyl-2-deoxy-β-D-glycero-D-ido-octopyranose (25)

Compound **16** (230 mg, 0.302 mmol) was reacted according to the general ozonolysis procedure, to give compound **25** (119 mg, 156 mmol, 52%) as colorless oil. R_f = 0.45 (heptane/ethyl acetate 1:2, v/v); $[\alpha]_D^{20}$ +83.2 (c 1.0, dichloromethane); ^{1}H NMR (600.25 MHz, $CDCl_3$, 25 °C) δ = 5.810 (dd, $^3J_{1,2b}$ = 10.4 Hz, $^3J_{1,2a}$ = 2.3 Hz, 1H, H-1), 5.491 (d, $^3J_{1',2'}$ = 3.8 Hz, 1H, H-1′), 5.365 (dd, $^3J_{3',2'}$ = 10.5 Hz, $^3J_{3',4'}$ = 9.5 Hz, 1H, H-3′), 5.107 (ddd, $^3J_{3,4}$ = 3.2 Hz, $^3J_{3,2a}$ = 3.0 Hz, $^3J_{3,2b}$ = 3.0 Hz, 1H, H-3), 5.063 (dd, $^3J_{4',5'}$ = 9.9 Hz, $^3J_{4',3'}$ = 9.5 Hz, 1H, H-4′), 4.956 (dd, $^3J_{2',3'}$ = 10.5 Hz, $^3J_{2',1'}$ = 3.8 Hz, 1H, H-2′), 4.905 (ddd, $^3J_{7,8a}$ = 8.0 Hz, $^3J_{7,8b}$ = 3.2 Hz, $^3J_{7,6}$ = 1.5 Hz, 1H, H-7), 4.859 (dd, $^3J_{4,3}$ = 3.2 Hz, $^3J_{4,5}$ = 1.2 Hz, 1H, H-4), 4.490 (dd, $^2J_{8a,8b}$ = 12.5 Hz, $^3J_{8a,7}$ = 3.2 Hz, 1H, H-8a), 4.297 (dd, $^2J_{6'a,6'b}$ = 12.3 Hz, $^3J_{6'a,5'}$ = 4.2 Hz, 1H, H-6'a), 4.274 (ddd, $^3J_{5',4'}$ = 9.9 Hz, $^3J_{5',6'a}$ = 4.2 Hz, $^3J_{5',6'b}$ = 2.4 Hz, 1H, H-5′), 4.215 (dd, $^3J_{5,6}$ = 8.5 Hz, $^3J_{5,4}$ = 1.2 Hz, 1H, H-5), 4.209 (dd, $^2J_{8b,8a}$ = 12.5 Hz, $^3J_{8b,7}$ = 8.0 Hz, 1H, H-8b), 4.181 (dd, $^3J_{6,5}$ = 8.5 Hz, $^3J_{6,7}$ = 1.5 Hz, 1H, H-6), 3.963 (dd, $^2J_{6'b,6'a}$ = 12.3 Hz, $^3J_{6'b,5'}$ = 2.4 Hz, 1H, H-6'b), 2.150, 2.131, 2.068, 2.068, 2.068, 2.060, 2.046, 2.021, 1.984 (9s, 27H, OAc), 1.935 (ddd, $^2J_{2a,2b}$ = 14.5 Hz, $^3J_{2a,3}$ = 3.0 Hz, $^3J_{2a,1}$ = 2.3 Hz, 1H, H-2a), 1.916 (ddd, $^2J_{2b,2a}$ = 14.5 Hz, $^3J_{2b,1}$ = 10.4 Hz, $^3J_{2b,3}$ = 3.0 Hz, 1H, H-2b) ppm; ^{13}C NMR (150.93 MHz, $CDCl_3$, 25 °C) δ = 170.57, 170.51, 170.01, 169.88, 169.88, 169.43, 169.41, 168.94, 168.87 (9 × O(C=O)CH_3), 95.71 (C-1′), 90.42 (C-1), 76.01 (C-5), 74.98 (C-6), 70.71 (C-7), 69.82 (C-3′), 69.46 (C-2′), 68.38 (C-4′), 67.36 (C-5′), 67.25 (C-3), 65.05 (C-4), 61.76 (C-8), 61.67 (C-6′), 30.08 (C-2), 20.98, 20.89, 20.81, 20.76, 20.72, 20.60, 20.60, 20.60, 20.60 (9 × O(C=O)CH_3) ppm; HRMS (ESI+) *m/z*: $[M + Na]^+$ calcd. for $C_{32}H_{44}O_{21}Na^+$, 787.2268; found, 787.2268.

Declaration of competing interest

The authors declare that they have no known competing financial interests or personal relationships that could have appeared to influence the work reported in this paper.

Acknowledgments

We would like to thank the NMR center for NMR analysis, the mass spectrometry center for mass analysis and A. Roller for X-ray crystallographic analysis.

Appendix A. Supplementary data

Supplementary data to this article can be found online at https://doi.org/10.1016/j.carres.2020.108170.

References

[1] R. Schauer, Achievements and challenges of sialic acid research, Glycoconj. J. 17 (2000) 485–499, https://doi.org/10.1023/A:1011062223612.
[2] X. Chen, A. Varki, Advances in the biology and chemistry of sialic acids, ACS Chem. Biol. 5 (2010) 163–176, https://doi.org/10.1021/cb900266r.
[3] A. Varki, P. Gagneux, Multifarious roles of sialic acids in immunity, Ann. N. Y. Acad. Sci. 1253 (2012) 16–36, https://doi.org/10.1111/j.1749-6632.2012.06517.x.
[4] V. Padler-Karavani, Aiming at the sweet side of cancer: aberrant glycosylation as possible target for personalized-medicine, Canc. Lett. 352 (2014) 102–112, https://doi.org/10.1016/j.canlet.2013.10.005.
[5] C. Nagy, A. Haschemi, Sedoheptulose kinase regulates cellular carbohydrate metabolism by sedoheptulose 7-phosphate supply, Biochem. Soc. Trans. 41 (2013) 674–680, https://doi.org/10.1042/BST20120354.
[6] T. Yokozawa, K.S. Kang, C.H. Park, J.S. Noh, N. Yamabe, N. Shibahara, T. Tanaka, Bioactive constituents of Corni Fructus: the therapeutic use of morroniside, loganin, and 7-O-galloyl-D-sedoheptulose as renoprotective agents in type 2 diabetes, Drug Discov. Ther. 4 (2010) 223–234.

[7] S.A. Zacchinoa, E. Butassia, M. Di Libertoa, M. Raimondib, A. Postigoa, M. Sortino, Plant phenolics and terpenoids as adjuvants of antibacterial and antifungal drugs, Phytomedicine 37 (2017) 27–48, https://doi.org/10.1016/j.phymed.2017.10.018.
[8] J. Spížek, T. Řezanka, Lincosamides: chemical structure, biosynthesis, mechanism of action, resistance, and applications, Biochem. Pharmacol. 133 (2017) 20–28, https://doi.org/10.1016/j.bcp.2016.12.001.
[9] World Health Organization, Breastfeeding and maternal medication recommendations for drugs in the eleventh WHO model list of essential drugs. https://apps.who.int/iris/bitstream/handle/10665/62435/55732.pdf, 2002. (Accessed 6 July 2020).
[10] W. Schmid, G.M. Whitesides, Carbon-carbon bond formation in aqueous ethanol: diastereoselective transformation of unprotected carbohydrates to higher carbon sugars using allyl bromide and tin metal, J. Am. Chem. Soc. 113 (1991) 6674–6675, https://doi.org/10.1021/ja00017a049.
[11] M. Gintner, Y. Yoneda, C. Schmölzer, C. Denner, H. Kählig, W. Schmid, A versatile de novo synthesis of legionaminic acid and 4-epi-legionaminic acid starting from d-serine, Carbohydr. Res. 474 (2019) 34–42, https://doi.org/10.1016/j.carres.2019.01.009.
[12] C.J. Li, T.H. Chan, Organometallic reactions in aqueous media with indium, Tetrahedron Lett. 32 (1991) 7017–7020, https://doi.org/10.1016/0040-4039(91)85028-4.
[13] L.A. Paquette, T.M. Mitzel, Chelation control associated with organometallic addition reactions in water. The high stereoselectivity offered by α- and β-hydroxyl substituents obviates the need for protecting groups, Tetrahedron Lett. 36 (1995) 6863–6866, https://doi.org/10.1016/0040-4039(95)01439-O.
[14] M. Gintner, C. Denner, C. Schmölzer, M. Fischer, P. Frühauf, H. Kählig, W. Schmid, Synthesis of 3-deoxy-2-uloses via the indium-mediated allylation reaction, Monatsh. Chem. 150 (2019) 849–860, https://doi.org/10.1007/s00706-019-02438-y.
[15] T.H. Chan, C.J. Li, A concise chemical synthesis of (+)-3-deoxy-d-glycero-d-galacto-nonulosonic acid KDN, J. Chem. Soc. Chem. Commun. (1992) 747–748, https://doi.org/10.1039/C39920000747.
[16] E. Balla, A. Zamyatina, A. Hofinger, P. Kosma, Synthesis of a deoxy analogue of ADP l-glycero-d-manno-heptose, Carbohydr. Res. 342 (2007) 2537–2545, https://doi.org/10.1016/j.carres.2007.07.022.
[17] C. Stanetty, I.R. Baxendale, Large-Scale Synthesis of Crystalline 1,2,3,4,6,7-Hexa-O-acetyl-l-glycero-α-d-manno-heptopyranose, Eur. J. Org Chem. (2015) 2718–2726, https://doi.org/10.1002/ejoc.201500024.
[18] C. Denner, M. Gintner, H. Kählig, W. Schmid, Indium-mediated C-allylation of melibiose, Beilstein J. Org. Chem. 15 (2019) 2458–2464, https://doi.org/10.3762/bjoc.15.238.

Supporting Information

for

Indium-mediated allylation of disaccharides

Christian Denner, Manuel Gintner, Hanspeter Kählig, Tanja M. Wrodnigg, Walther Schmid

General instructions, NMR spectra, mass analysis data and X-ray data

Table of Contents

General Instructions: ^{1}H and ^{13}C NMR spectra were recorded on a Bruker AV III 600. Chemical shifts (δ) are reported in parts per million (ppm) and spectra were calibrated using solvent signal of $CDCl_3$. Signal multiplicity is indicated by one or more of the following: s (singlet); d (doublet); t (triplet); q (quartet). NMR analysis was assisted by the spin simulation software DAISY (part of Bruker Top Spin software). High resolution mass spectra (HRMS) were recorded on a Bruker maXis UHR-TOF spectrometer in ESI mode. Optical rotations were measured on a Schmidt-Haensch Digital Polarimeter Unipol L 2000. Ozonolysis was performed operating an Anseros COM-AD-04 ozone generator. Column chromatography was performed using Macherey-Nagel silica gel 60 (0.04–0.063 mm, 240–400 mesh). TLC monitoring was carried out on precoated Merck silica gel 60 F_{254} glass plates. Compounds were visualized by treatment with a Mo–$Ce(SO_4)_2$ complex solution (48 g $(NH_4)_6Mo_7O_{24}$ and 2 g $CeSO_4$ in 1 dm^3 10% H_2SO_4) followed by heating. Filtrations over celite were performed with Celite® S by Sigma-Aldrich®. Reagents were purchased from commercial suppliers and were used without further purification.

2’,3’,4’,6’-Tetra-*O*-acetyl-β-D-galactopyranosyl-(1’→3)-1,2,4,5,6-penta-*O*-acetyl-7,8,9-trideoxy-D-*glycero*-L-*gulo*-8,9-nonenitol (**14**)

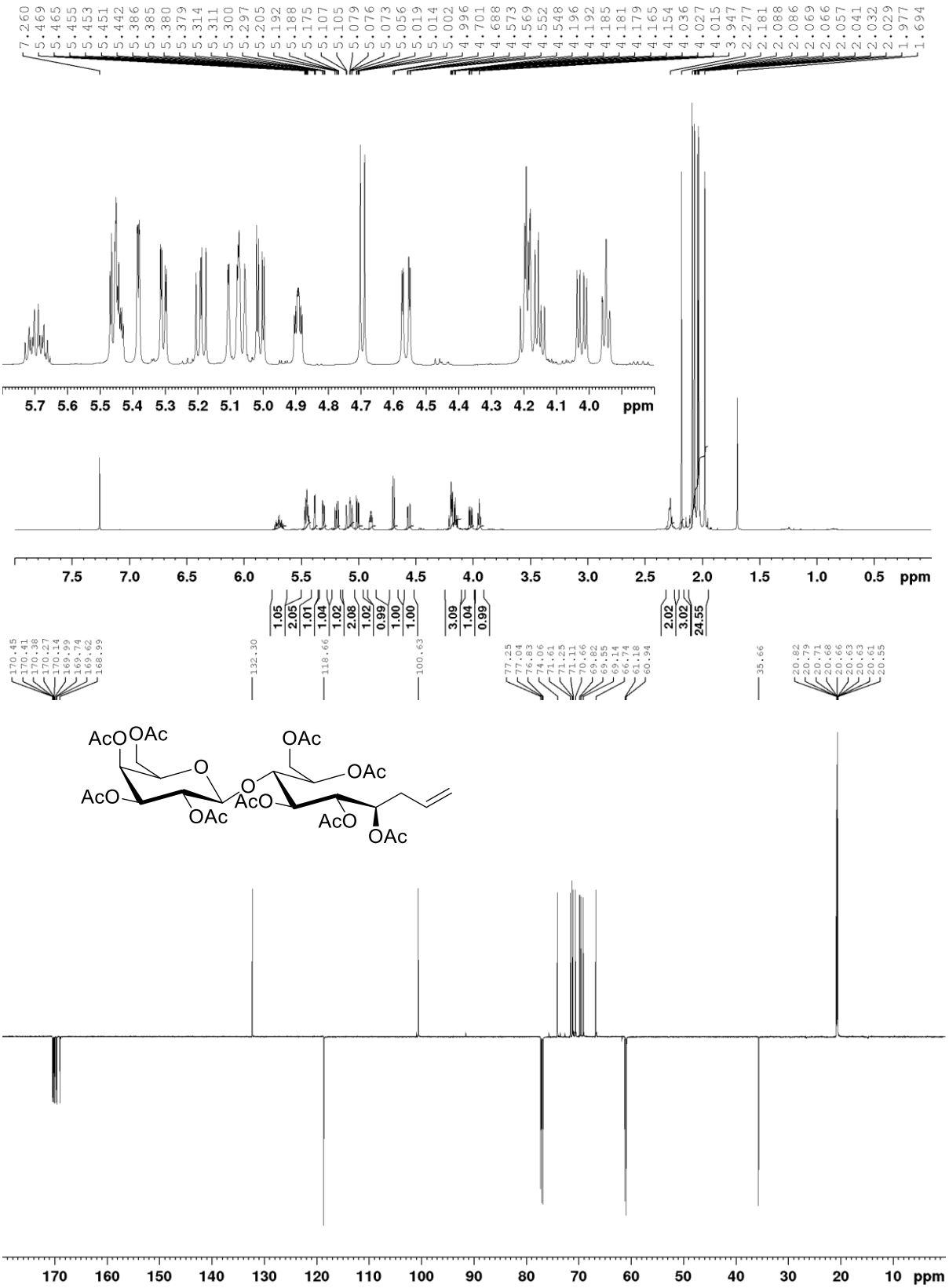

2’,3’,4’,6’-Tetra-*O*-acetyl-β-D-glucopyranosyl-(1’→3)-1,2,4,5,6-penta-*O*-acetyl-7,8,9-trideoxy-D-*glycero*-L-*gulo*-8,9-nonenitol (**15**)

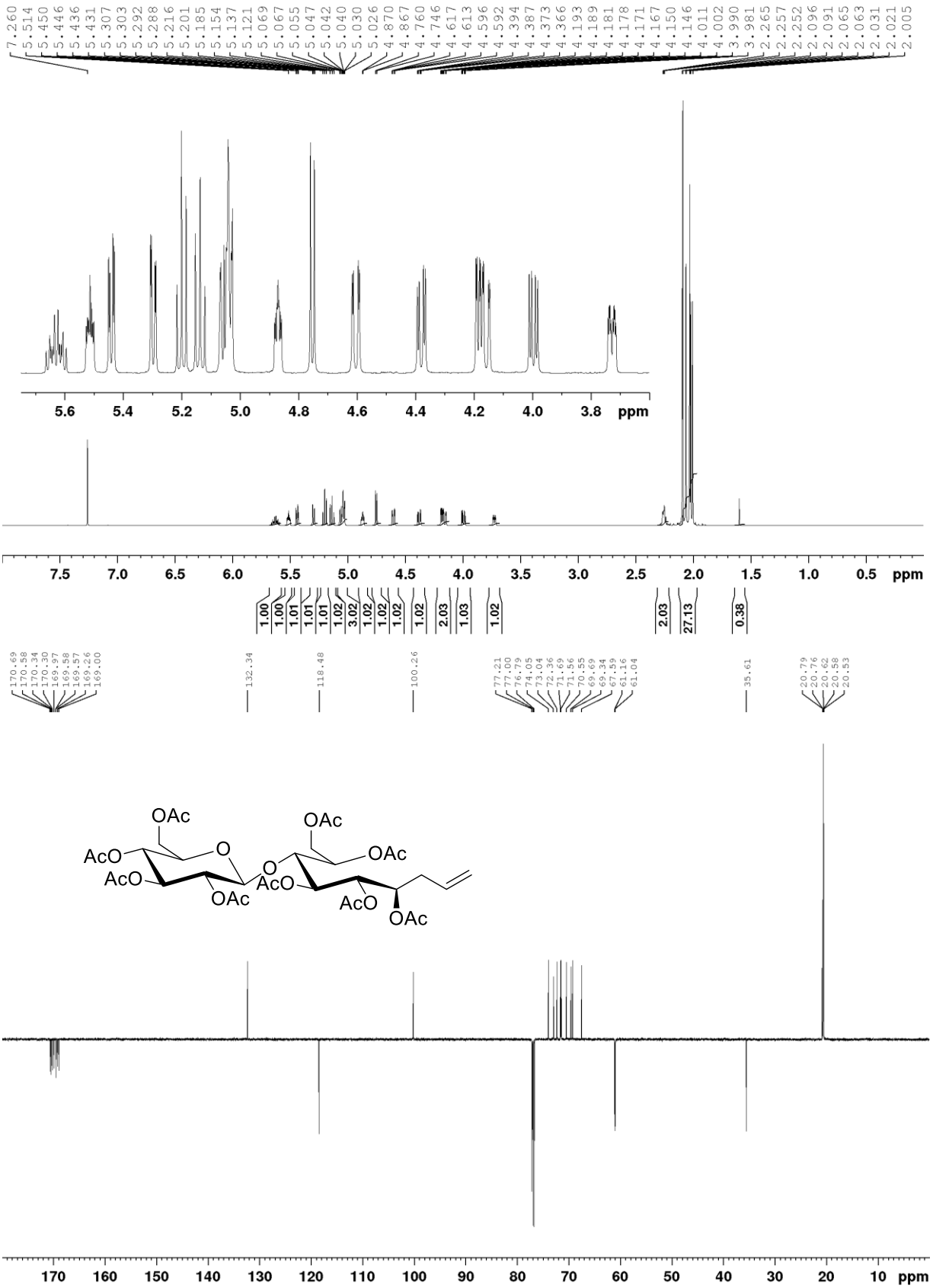

2’,3’,4’,6’-Tetra-*O*-acetyl-α-D-glucopyranosyl-(1’→3)-1,2,4,5,6-penta-*O*-acetyl-7,8,9-trideoxy-D-*glycero*-L-*gulo*-8,9-nonenitol (**16**)

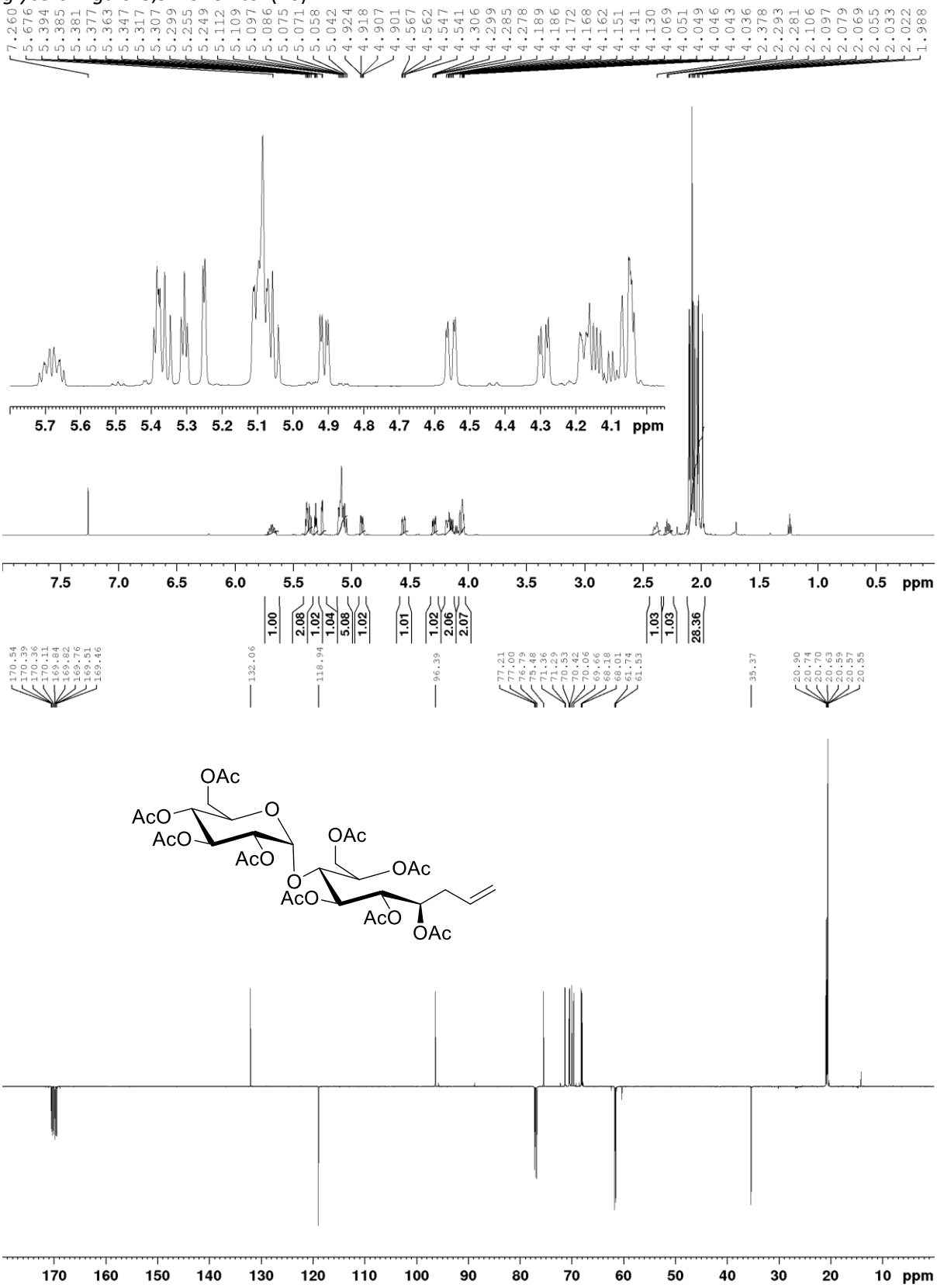

2’,3’,4’,6’-Tetra-*O*-acetyl-β-D-galactopyranosyl-(1’→6)-3,4,7,8-penta-*O*-acetyl-2-deoxy-1-*O*-methyl-β-D-*glycero*-D-*ido*-octofuranose (**18**)

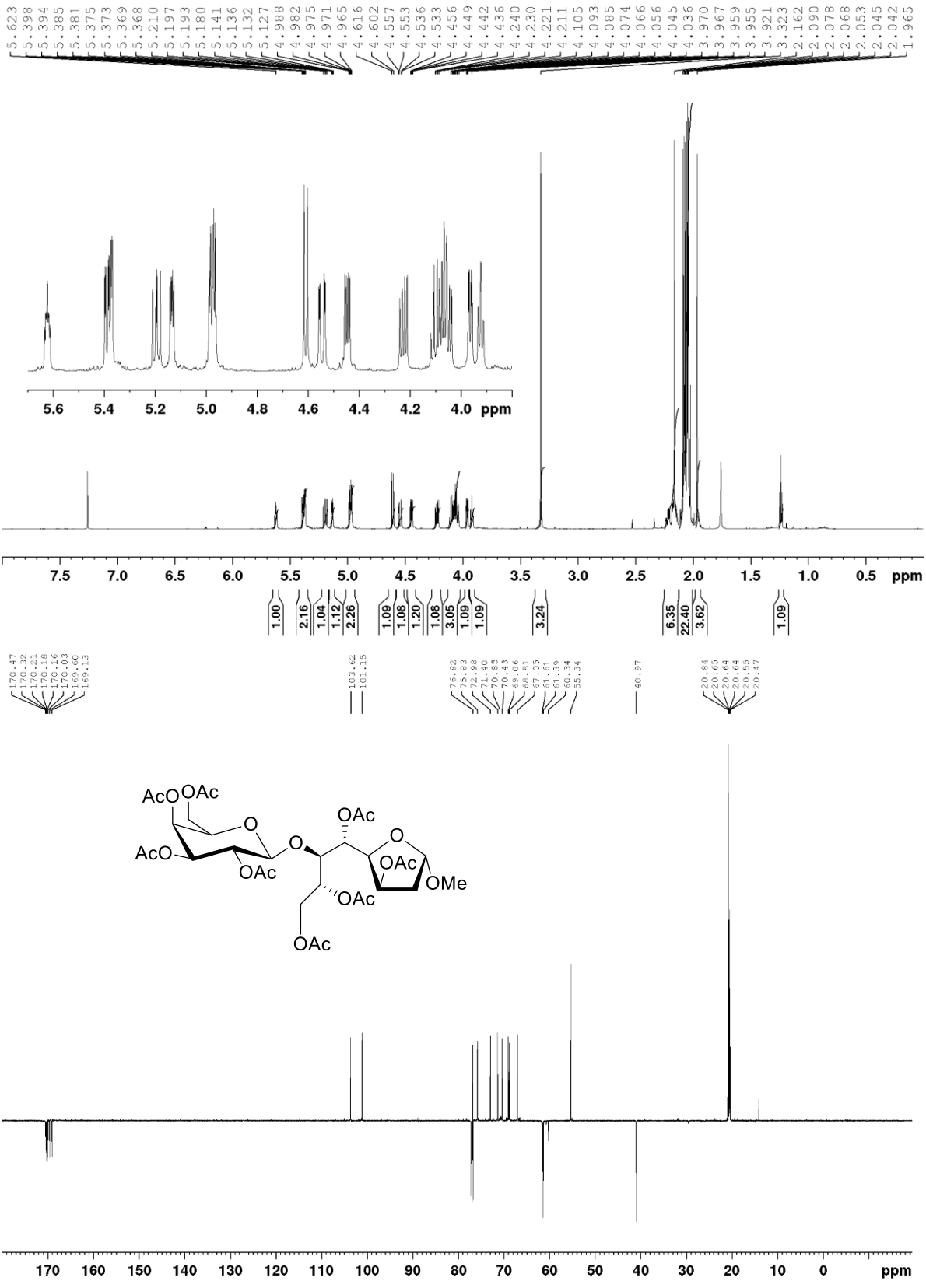

2’,3’,4’,6’-Tetra-*O*-acetyl-β-D-galactopyranosyl-(1’→6)-3,4,7,8-penta-*O*-acetyl-2-deoxy-1-*O*-methyl-β-D-*glycero*-D-*ido*-octofuranose (**18**)

(1*S*,3*R*,4*S*,5*S*,6*R*,8*R*,11*R*,12*S*,13*S*,14*R*)-3-((*R*)-1,2-diacetoxyethyl)-2,9,15-trioxabicyclo[9.3.1]pentadecane-4,5,6,8,12,13,14-heptayl heptaacetate (**19**)

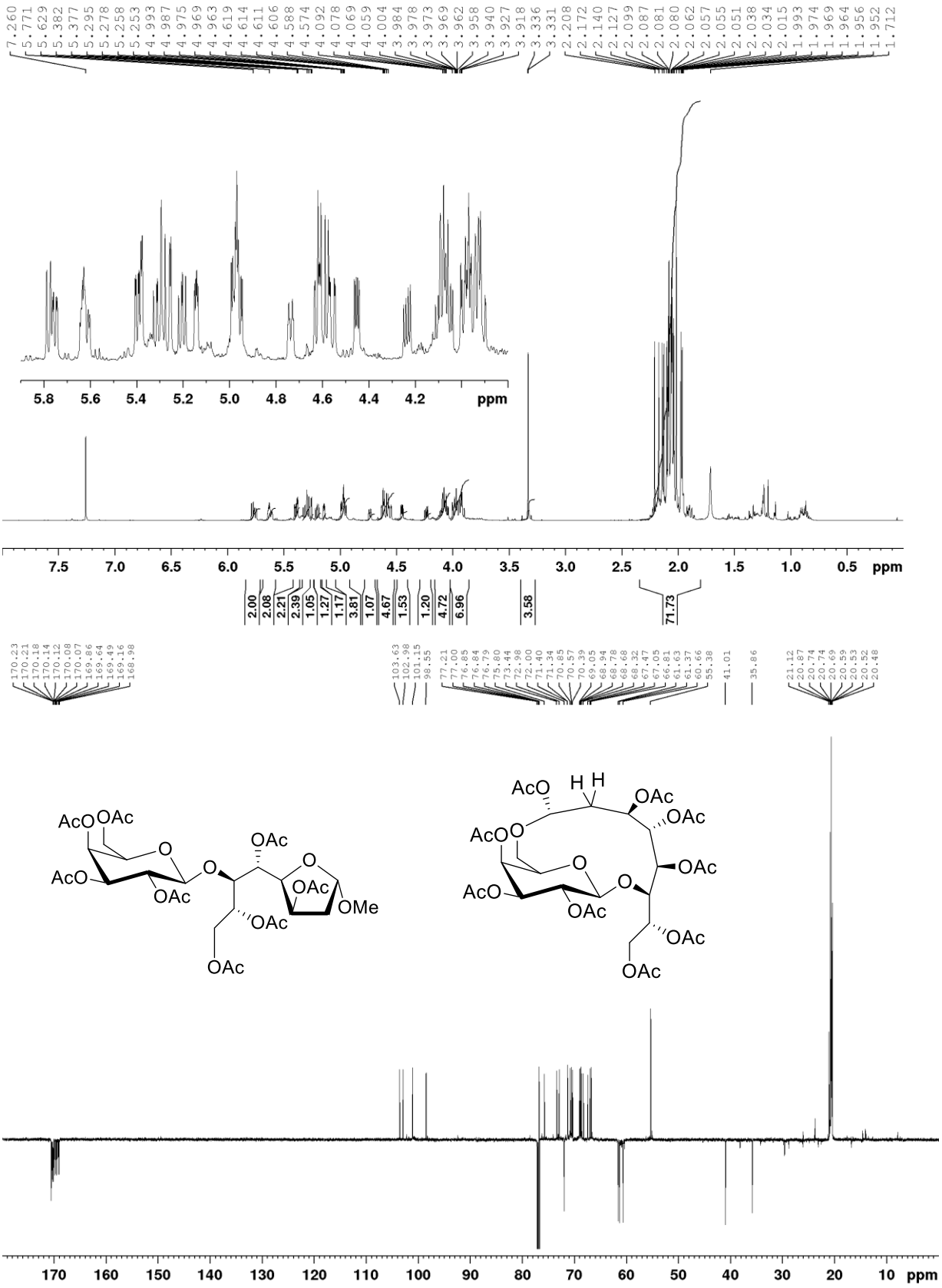

2’,3’,4’,6’-Tetra-*O*-acetyl-β-D-galactopyranosyl-(1’→6)-1,3,4,7,8-penta-*O*-acetyl-2-deoxy-β-D-*glycero*-D-*ido*-octopyranose (**21**)

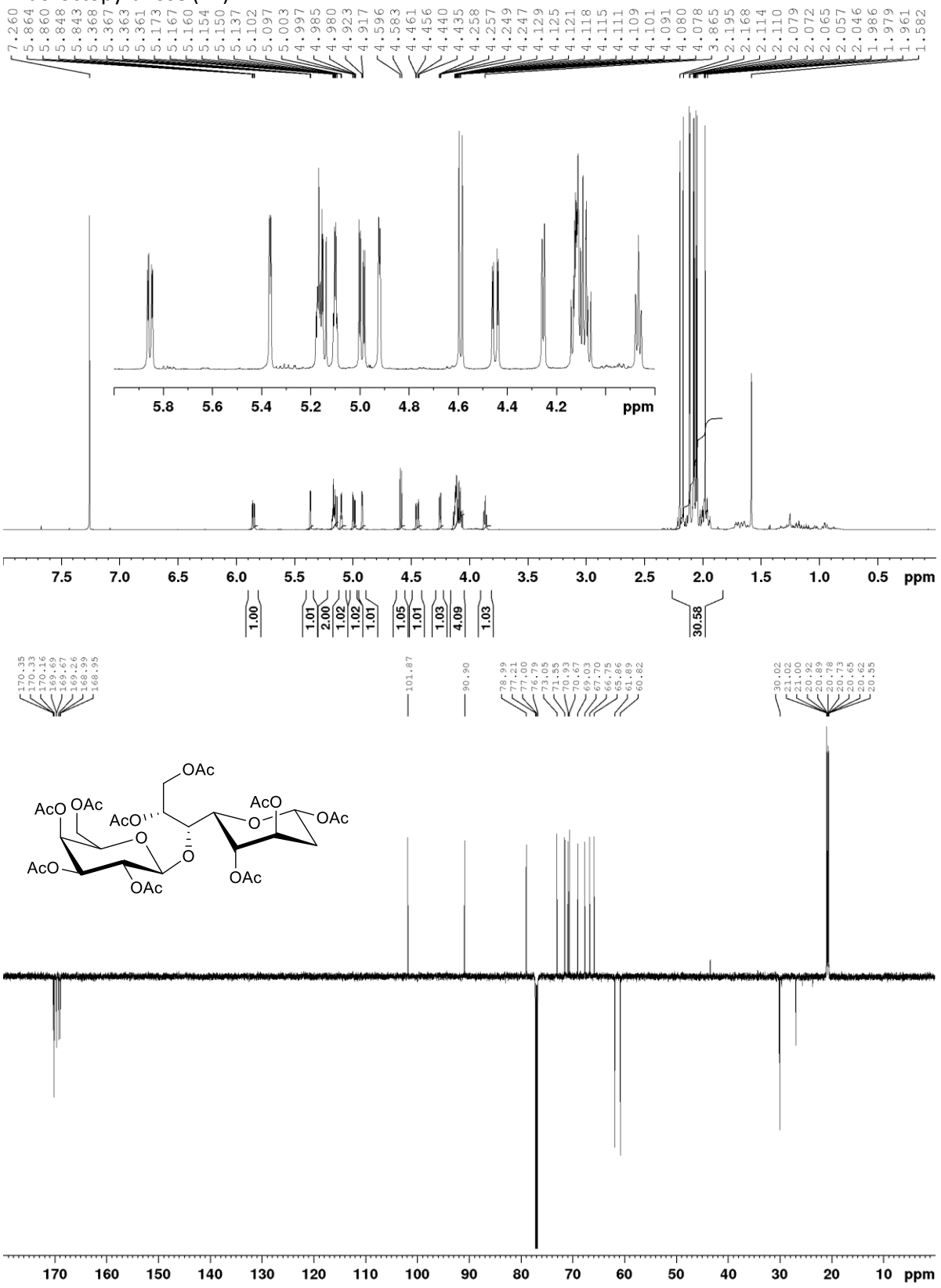

2’,3’,4’,6’-Tetra-*O*-acetyl-β-D-galactopyranosyl-(1’→6)-1,3,4,7,8-penta-*O*-acetyl-2-deoxy-β-D-*glycero*-D-*ido*-octopyranose (**21**)

Expanded region of the ^{13}C NMR of the resulting compound mixture after ozonolysis

A: ^{13}C NMR of the resulting compound mixture in red position C-1, in blue position C-2.

B: ^{13}C NMR of pure compound **21**

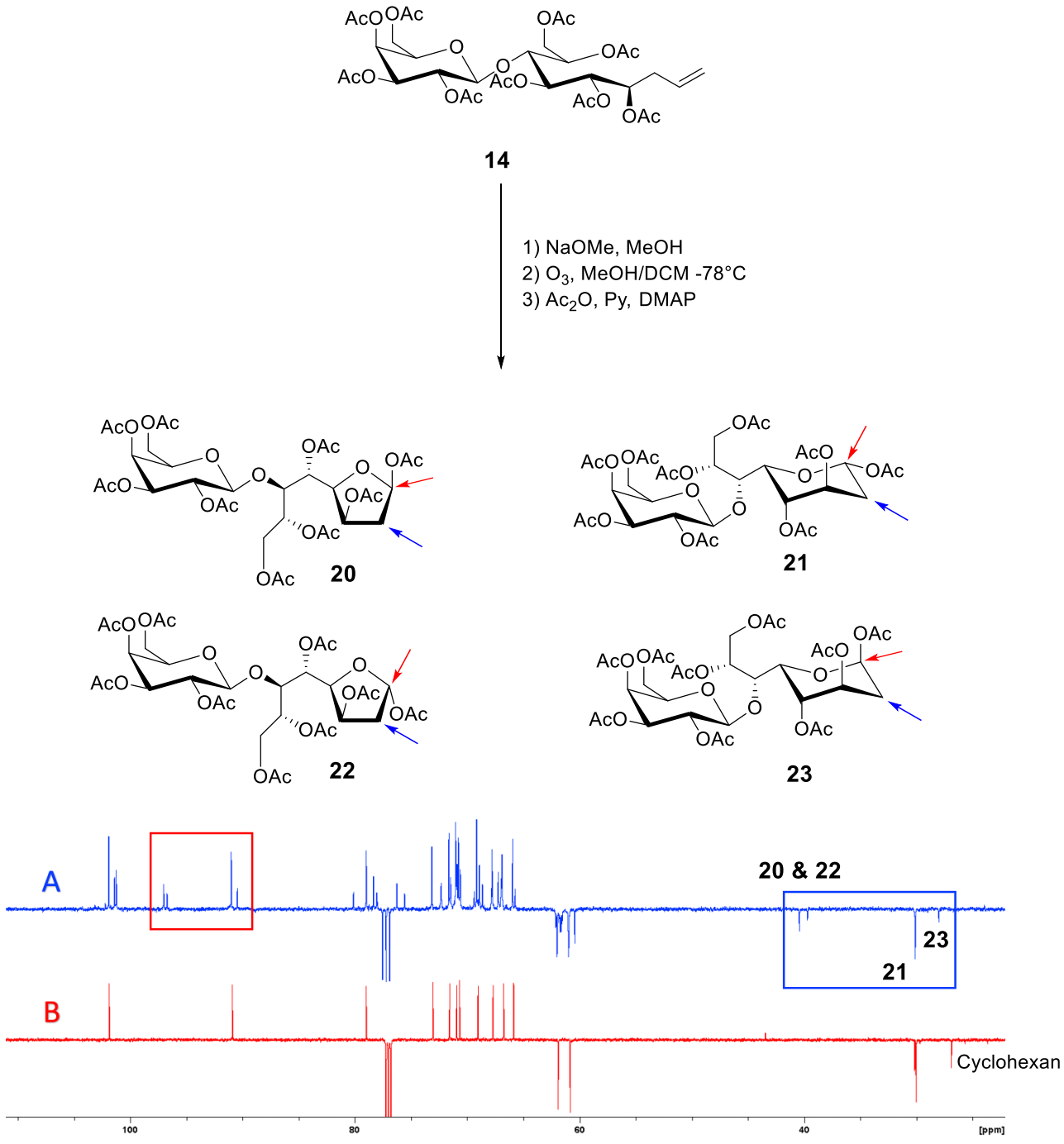

2’,3’,4’,6’-Tetra-*O*-acetyl-β-D-glucopyranosyl-(1’→6)-1,3,4,7,8-penta-*O*-acetyl-2-deoxy-β-D-*glycero*-D-*ido*-octopyranose (**24**)

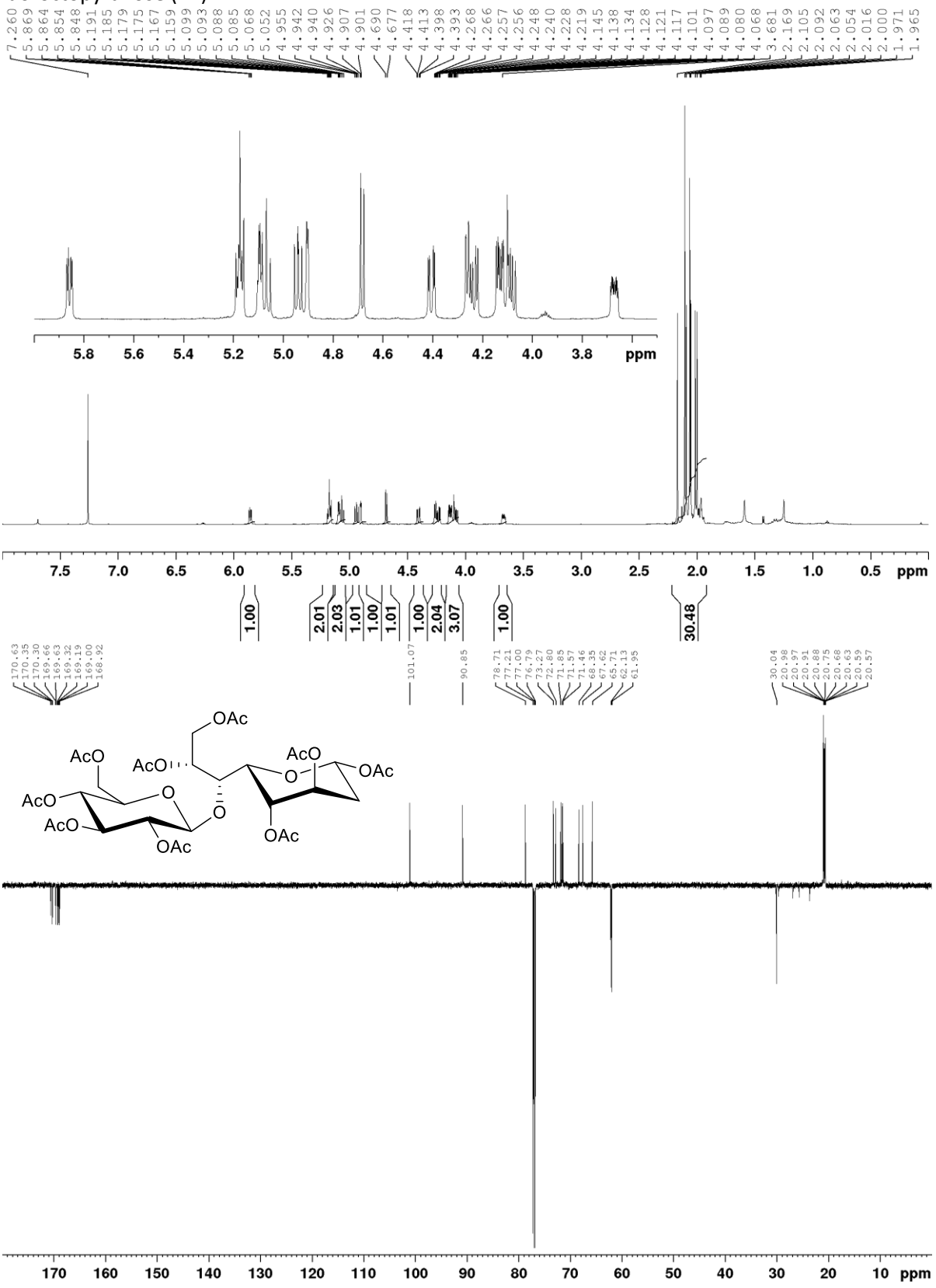

2’,3’,4’,6’-Tetra-*O*-acetyl-α-D-glucopyranosyl-(1’→6)-1,3,4,7,8-penta-*O*-acetyl-2-deoxy-β-D-*glycero*-D-*ido*-octopyranose (**25**)

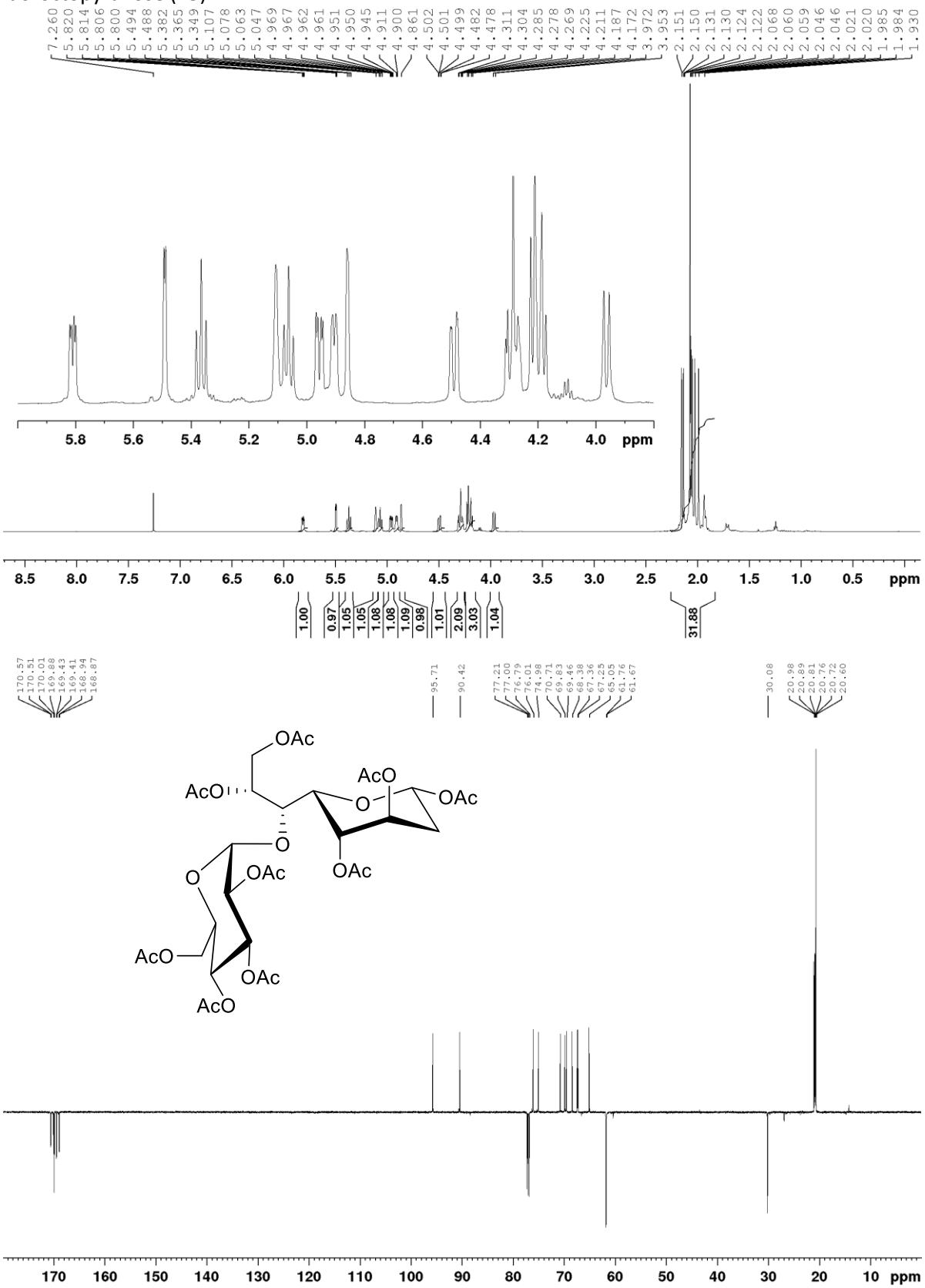

2’,3’,4’,6’-Tetra-*O*-acetyl-β-D-galactopyranosyl-(1’→3)-1,2,4,5,6-penta-*O*-acetyl-7,8,9-trideoxy-D-*glycero*-L-*gulo*-8,9-nonenitol (**14**)

HRMS (ESI$^+$) *m/z*: [M + NH_4]$^+$ calcd. for $C_{33}H_{50}NO_{20}^+$, 780.2922; found, 780.2927.

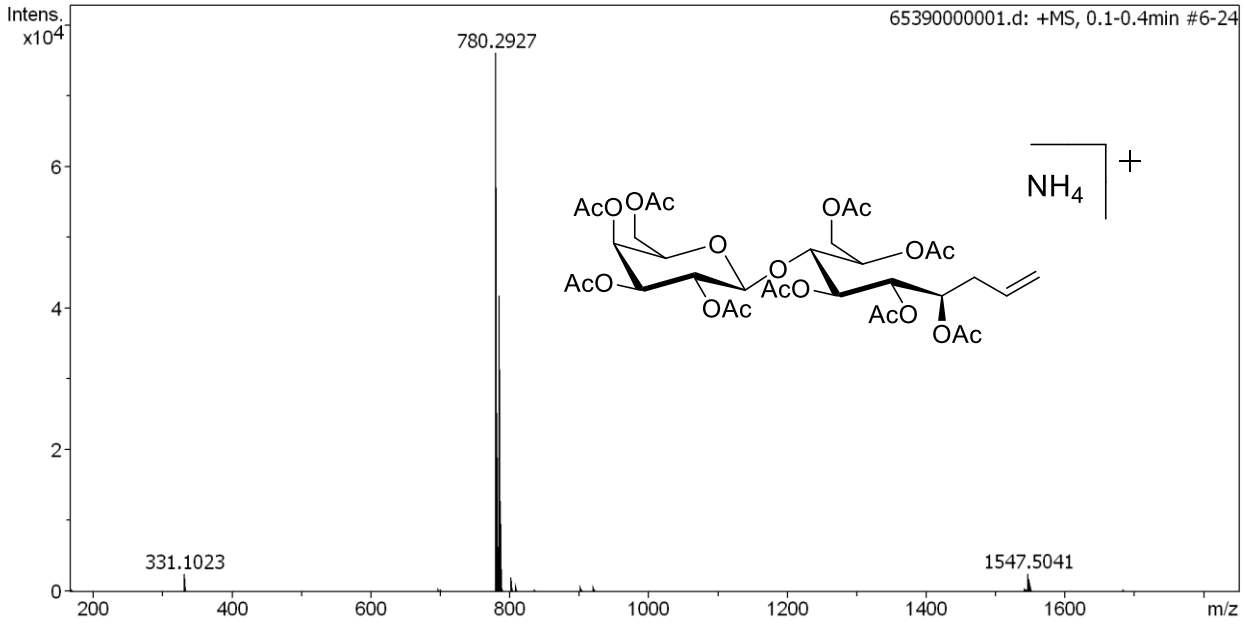

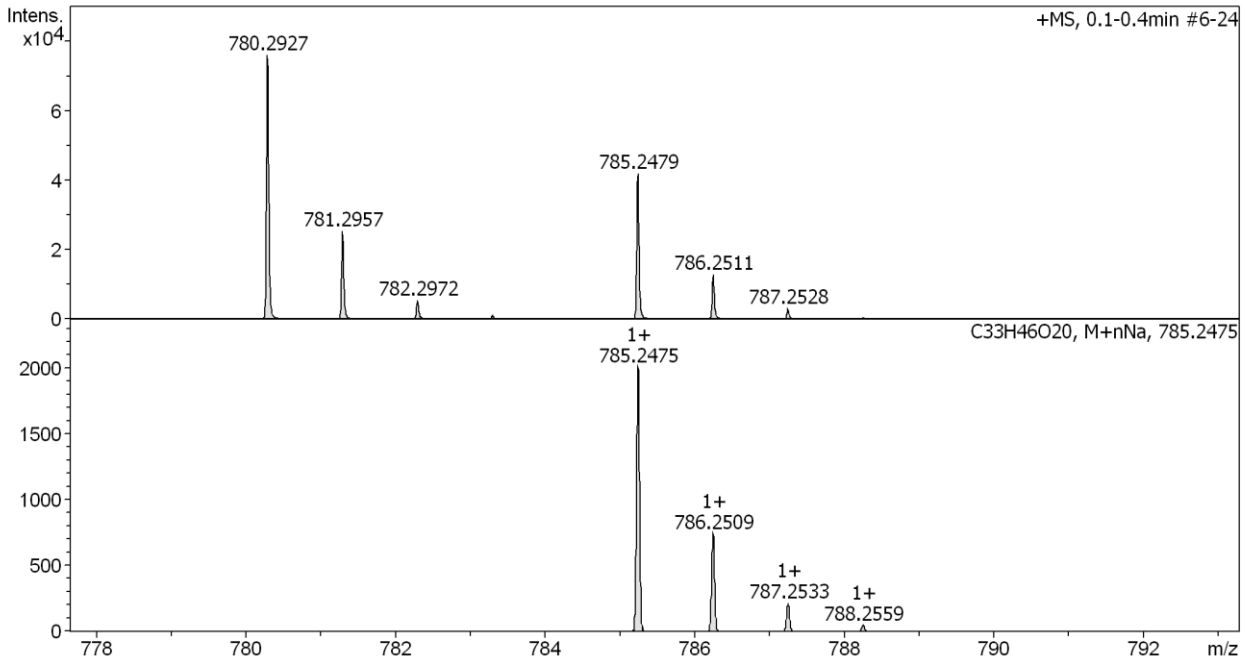

2’,3’,4’,6’-Tetra-*O*-acetyl-β-D-glucopyranosyl-(1’→3)-1,2,4,5,6-penta-*O*-acetyl-7,8,9-trideoxy-D-*glycero*-L-*gulo*-8,9-nonenitol (**15**)

HRMS (ESI+) m/z: $[M + Na]^+$ calcd. for $C_{33}H_{46}O_{20}Na^+$, 785.2475; found, 785.2476.

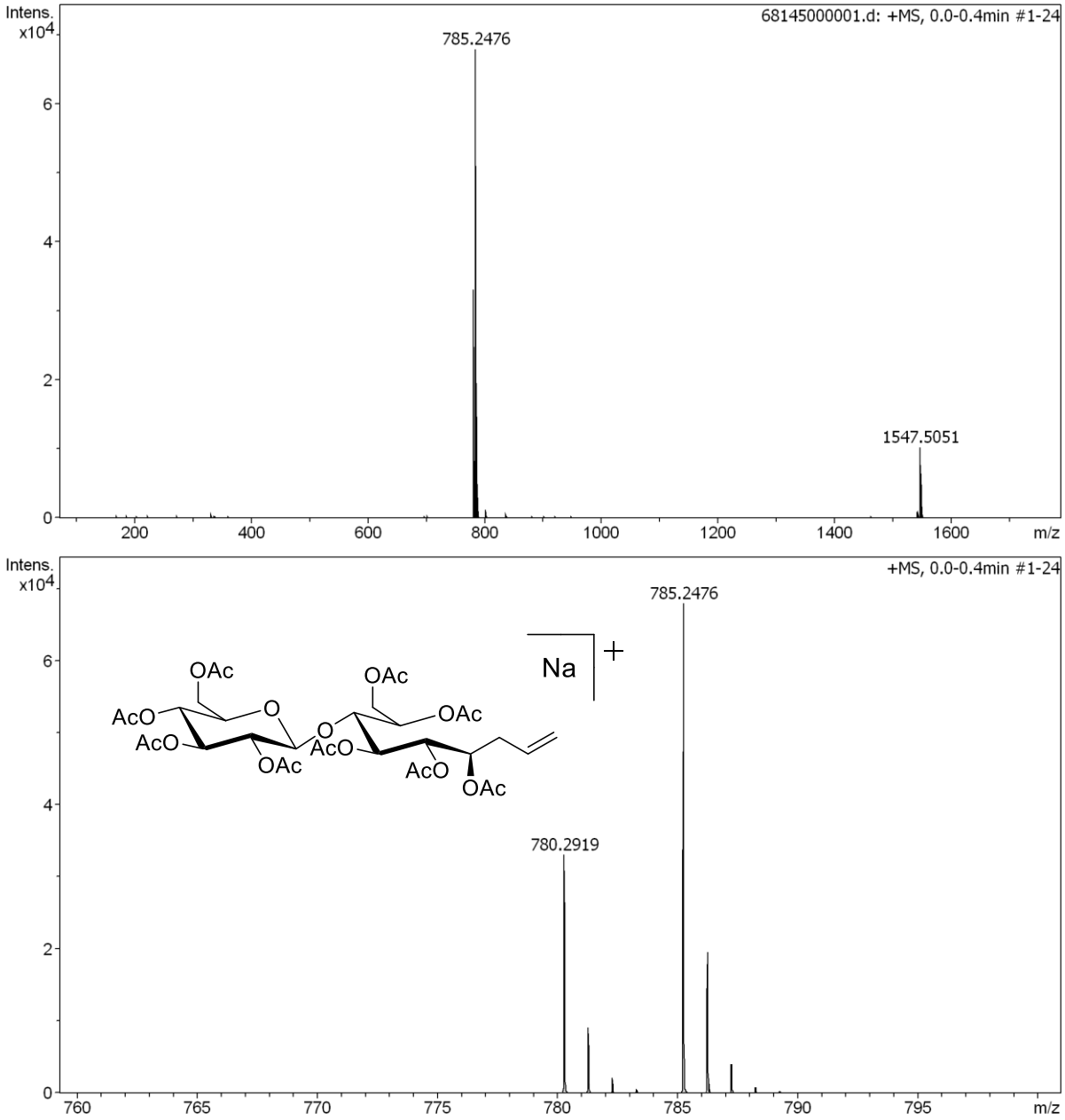

2’,3’,4’,6’-Tetra-*O*-acetyl-α-D-glucopyranosyl-(1’→3)-1,2,4,5,6-penta-*O*-acetyl-7,8,9-trideoxy-D-*glycero*-L-*gulo*-8,9-nonenitol (**16**)

HRMS (ESI$^+$) *m/z*: [M + NH_4]$^+$ calcd. for $C_{33}H_{50}NO_{20}^+$, 780.2922; found, 780.2922.

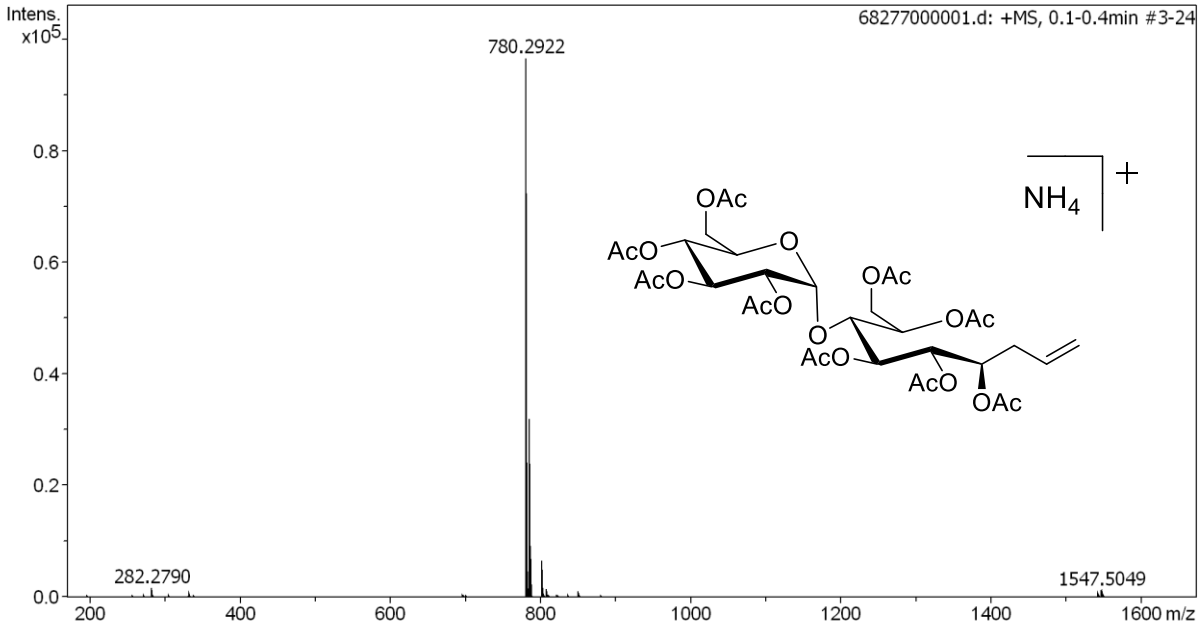

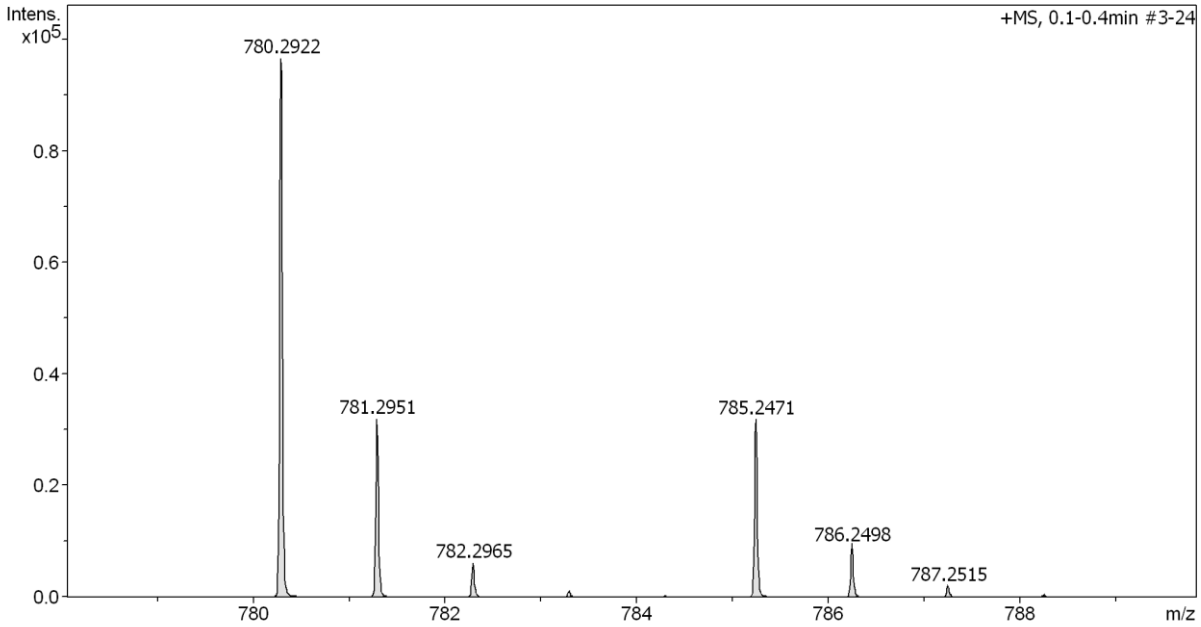

2’,3’,4’,6’-Tetra-*O*-acetyl-β-D-galactopyranosyl-(1’→6)-3,4,7,8-penta-*O*-acetyl-2-deoxy-1-*O*-methyl-β-D-*glycero*-D-*ido*-octofuranose (**18**)

HRMS (ESI+) m/z: $[M + Na]^+$ calcd. for $C_{31}H_{44}O_{20}Na^+$, 759.2318; found, 759.2317.

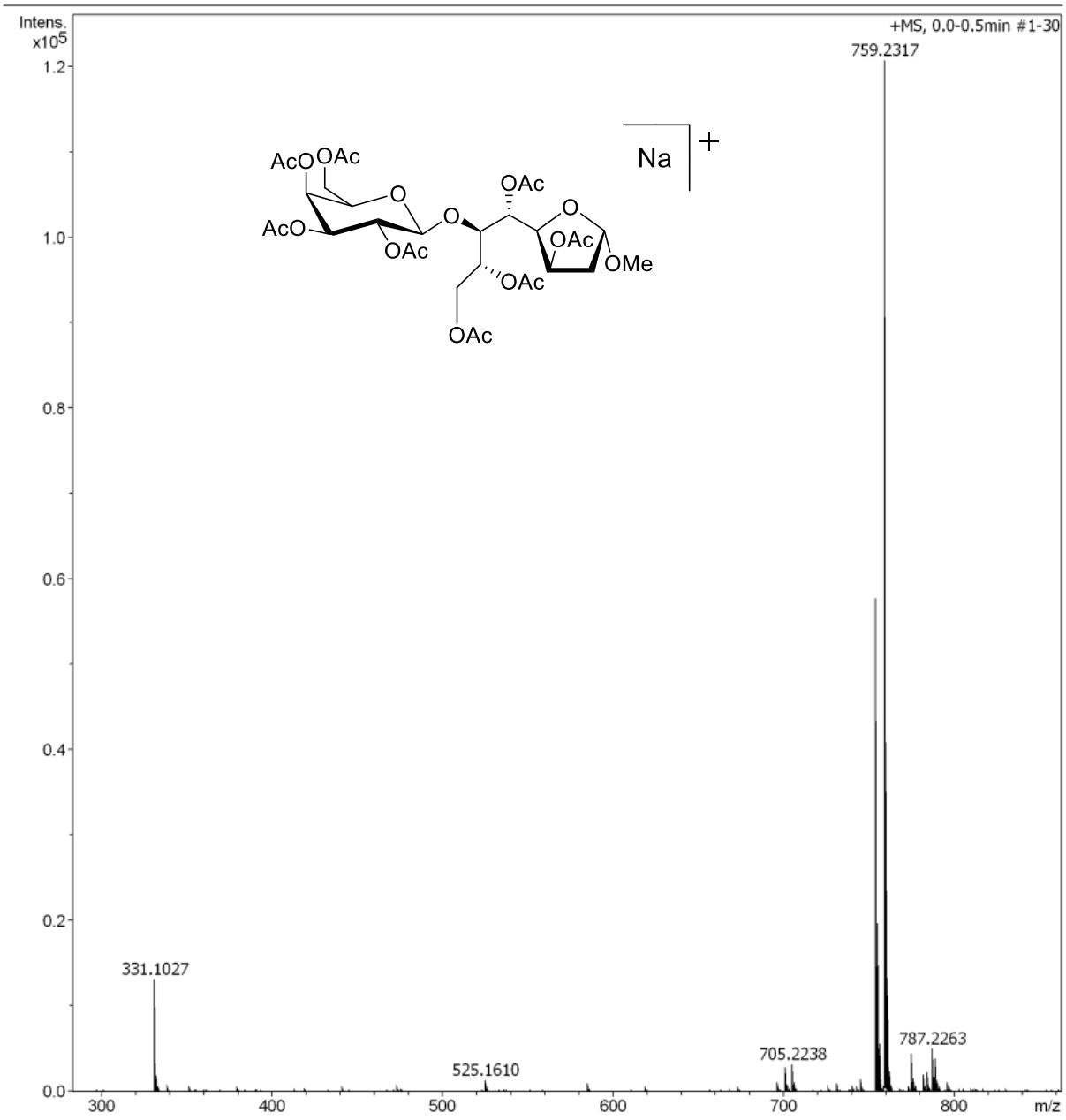

(1*S*,3*R*,4*S*,5*S*,6*R*,8*R*,11*R*,12*S*,13*S*,14*R*)-3-((*R*)-1,2-diacetoxyethyl)-2,9,15-trioxabicyclo[9.3.1]pentadecane-4,5,6,8,12,13,14-heptayl heptaacetate (**19**)

HRMS (ESI+) m/z: $[M + Na]^+$ calcd. for $C_{32}H_{44}O_{21}Na^+$, 787.2268; found, 787.2263.

2',3',4',6'-Tetra-*O*-acetyl-β-D-galactopyranosyl-(1'→6)-3,4,7,8-penta-*O*-acetyl-2-deoxy-1-*O*-methyl-β-D-*glycero*-D-*ido*-octofuranose (**18**)

HRMS (ESI+) m/z: $[M + Na]^+$ calcd. for $C_{31}H_{44}O_{20}Na^+$, 759.2318; found, 759.2314.

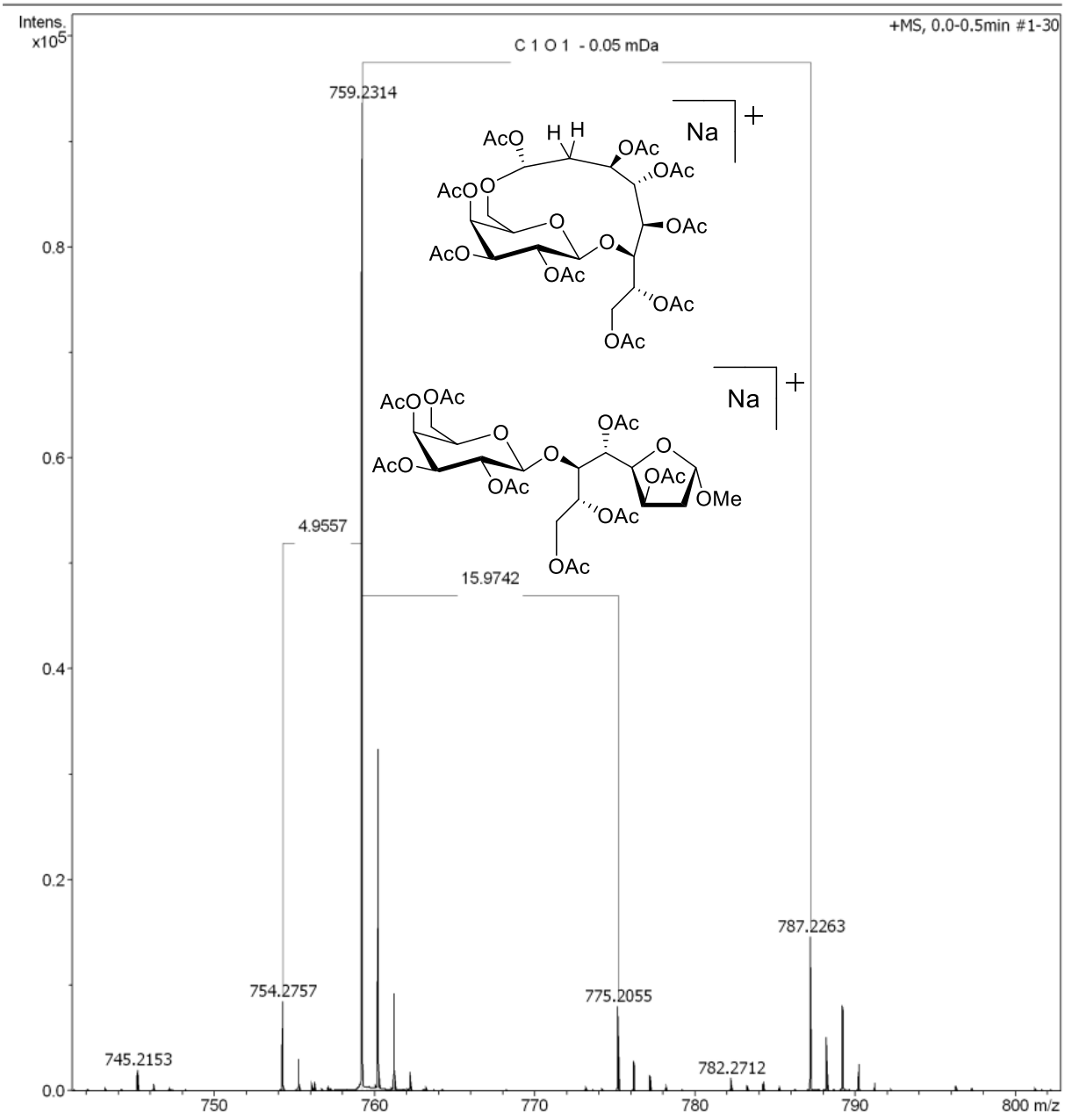

2’,3’,4’,6’-Tetra-*O*-acetyl-β-D-galactopyranosyl-(1’→6)-1,3,4,7,8-penta-*O*-acetyl-2-deoxy-β-D-*glycero*-D-*ido*-octopyranose (**21**)

HRMS (ESI+) m/z: $[M + Na]^+$ calcd. for $C_{32}H_{44}O_{21}Na^+$, 787.2268; found, 787.2269.

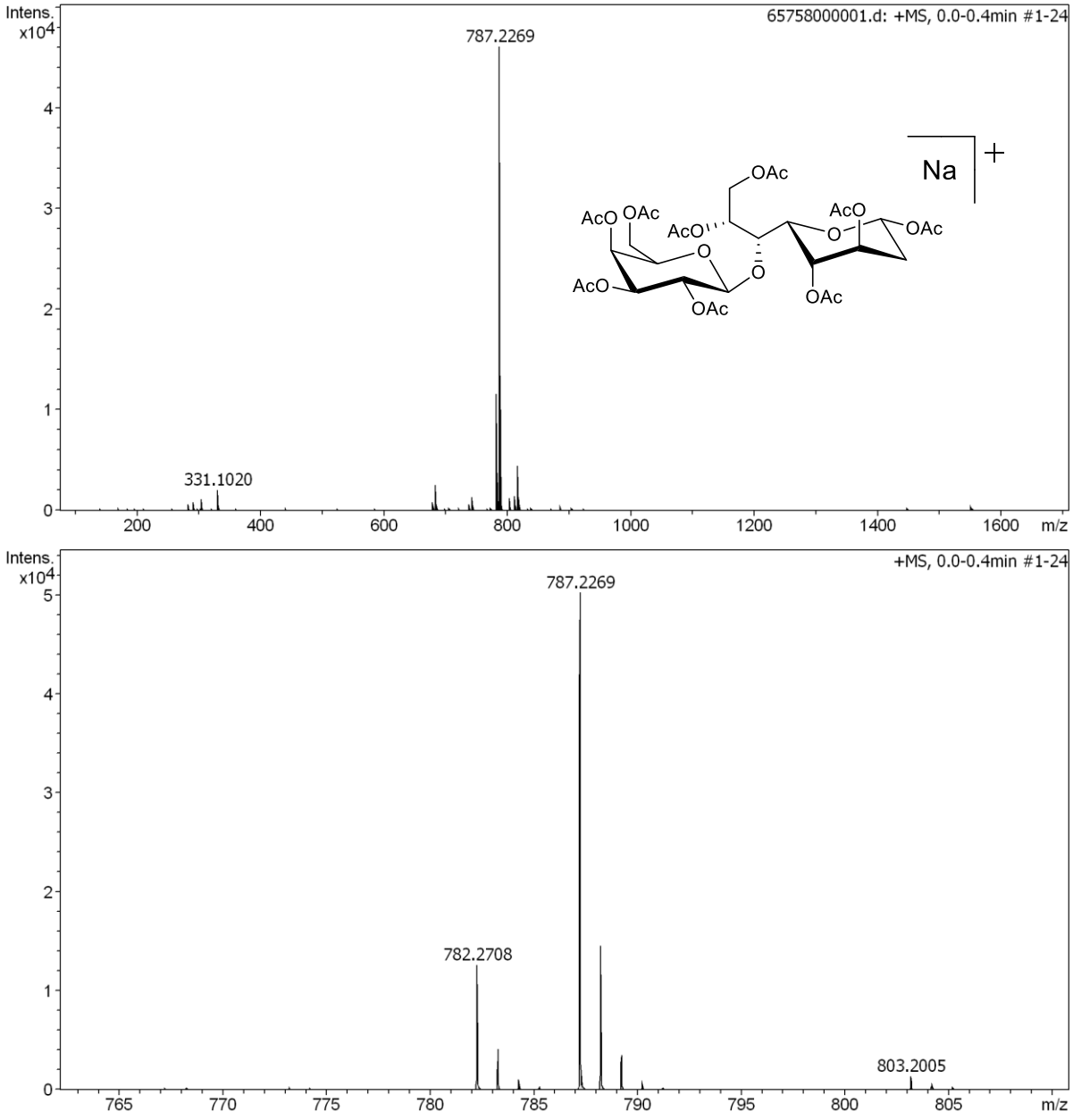

2’,3’,4’,6’-Tetra-*O*-acetyl-β-D-glucopyranosyl-(1’→6)-1,3,4,7,8-penta-*O*-acetyl-2-deoxy-β-D-*glycero*-D-*ido*-octopyranose (**24**)

HRMS (ESI+) m/z: $[M + Na]^+$ calcd. for $C_{32}H_{44}O_{21}Na^+$, 787.2268; found, 787.2266.

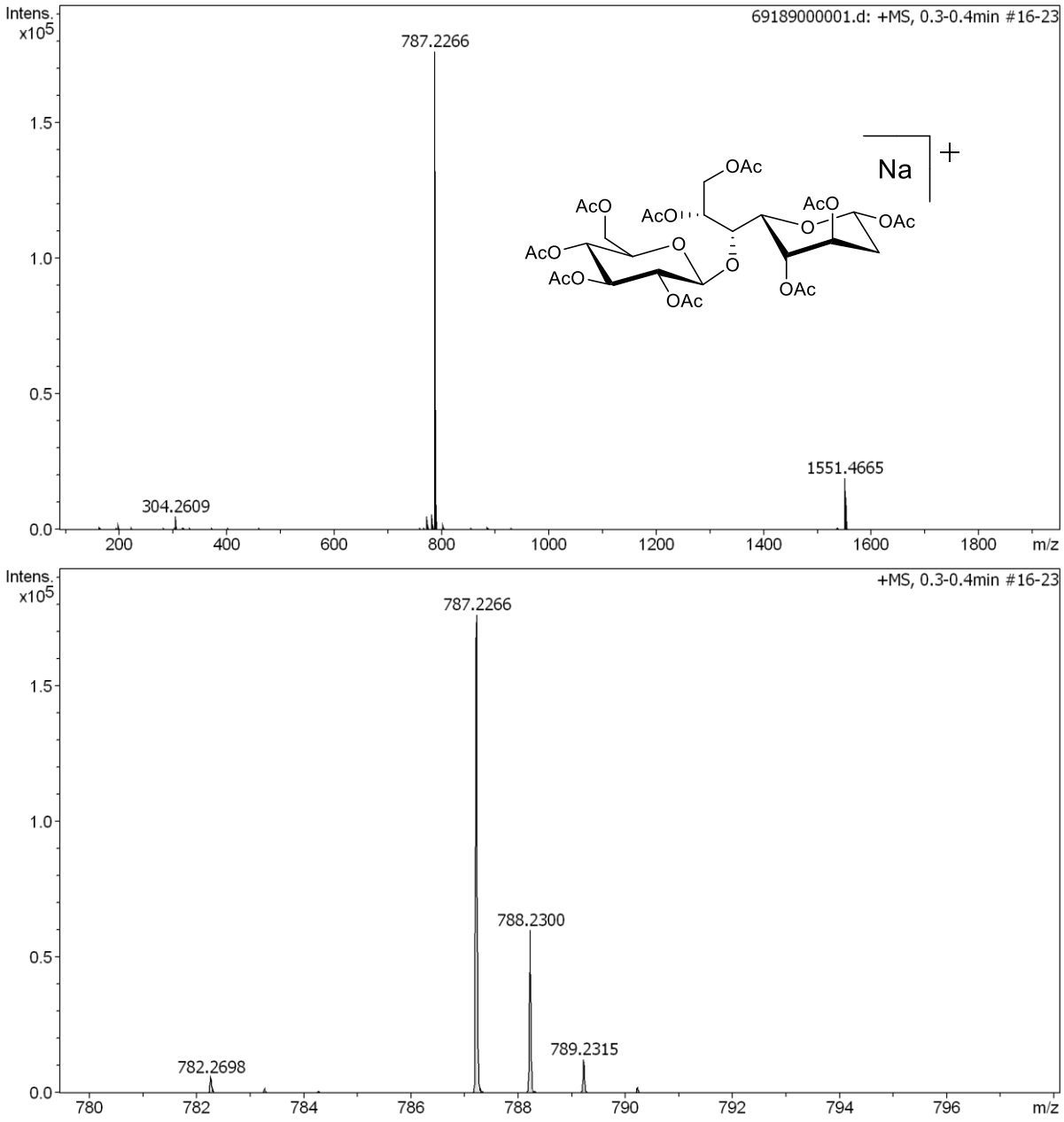

2’,3’,4’,6’-Tetra-*O*-acetyl-α-D-glucopyranosyl-(1’→6)-1,3,4,7,8-penta-*O*-acetyl-2-deoxy-β-D-*glycero*-D-*ido*-octopyranose (**25**)

HRMS (ESI+) m/z: $[M + Na]^+$ calcd. for $C_{32}H_{44}O_{21}Na^+$, 787.2268; found, 787.2268.

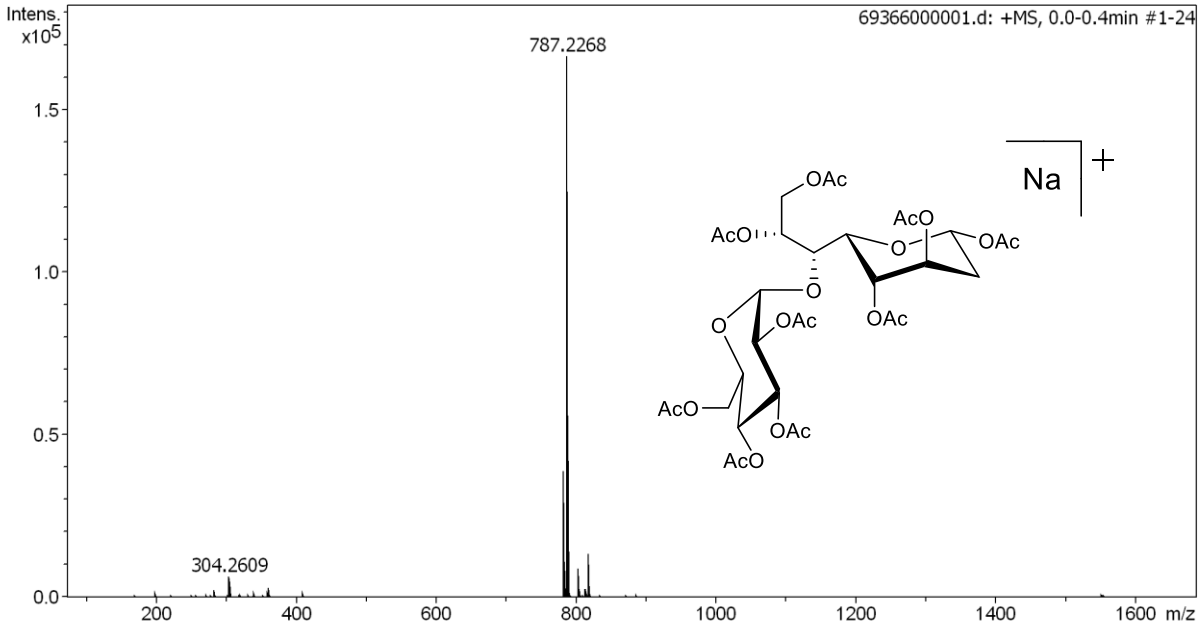

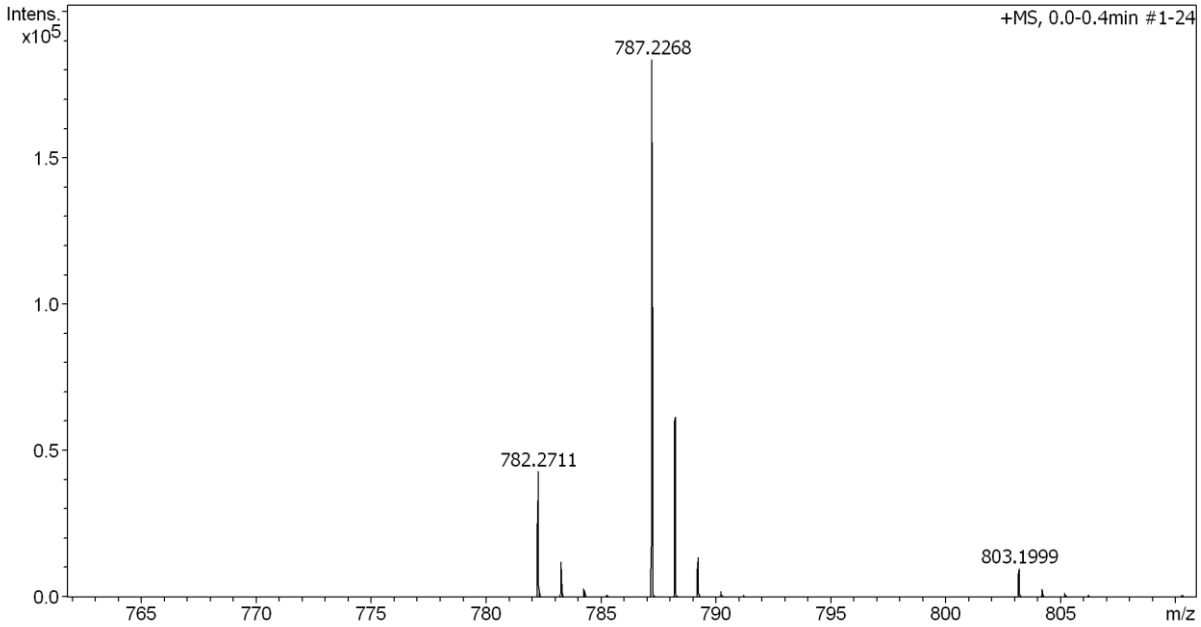

X-ray Analysis

The X-ray intensity data were measured on Bruker D8 Venture diffractometer equipped with multilayer monochromator, Mo K/α INCOATEC micro focus sealed tube and Oxford cooling system. The structure was solved by *Direct Methods*. Non-hydrogen atoms were refined with *anisotropic displacement parameters*. Hydrogen atoms were inserted at calculated positions and refined with riding model. The following software was used: *Bruker SAINT software package*[i] using a narrow-frame algorithm for frame integration, *SADABS*[ii] for absorption correction, *OLEX2*[iii] for structure solution, refinement, molecular diagrams and graphical user-interface, *Shelxle*[iv] for refinement and graphical user-interface *SHELXS-2015*[v] for structure solution, *SHELXL-2015*[vi] for refinement, *Platon*[vii] for symmetry check. Experimental data and CCDC-Codes Experimental data (Available online: http://www.ccdc.cam.ac.uk/conts/retrieving.html) can be found in Table 1. Crystal data, data collection parameters, and structure refinement details are given in Tables 2 and 3. Asymmetric Unit visualized in Figure 1.

Table 1 Experimental parameter and CCDC-Code.

Sample	Machine	Source	Temp.	Detector Distance	Time/ Frame	#Frames	Frame width	CCDC
	Bruker		[K]	[mm]	[s]		[°]	
[15]	D8	Mo	100	25	5	4110	0.500	2010237

2',3',4',6'-Tetra-O-acetyl-β-D-glucopyranosyl-(1'→3)-1,2,4,5,6-penta-O-acetyl-7,8,9-trideoxy-D-*glycero*-L-*gulo*-8,9-nonenitol

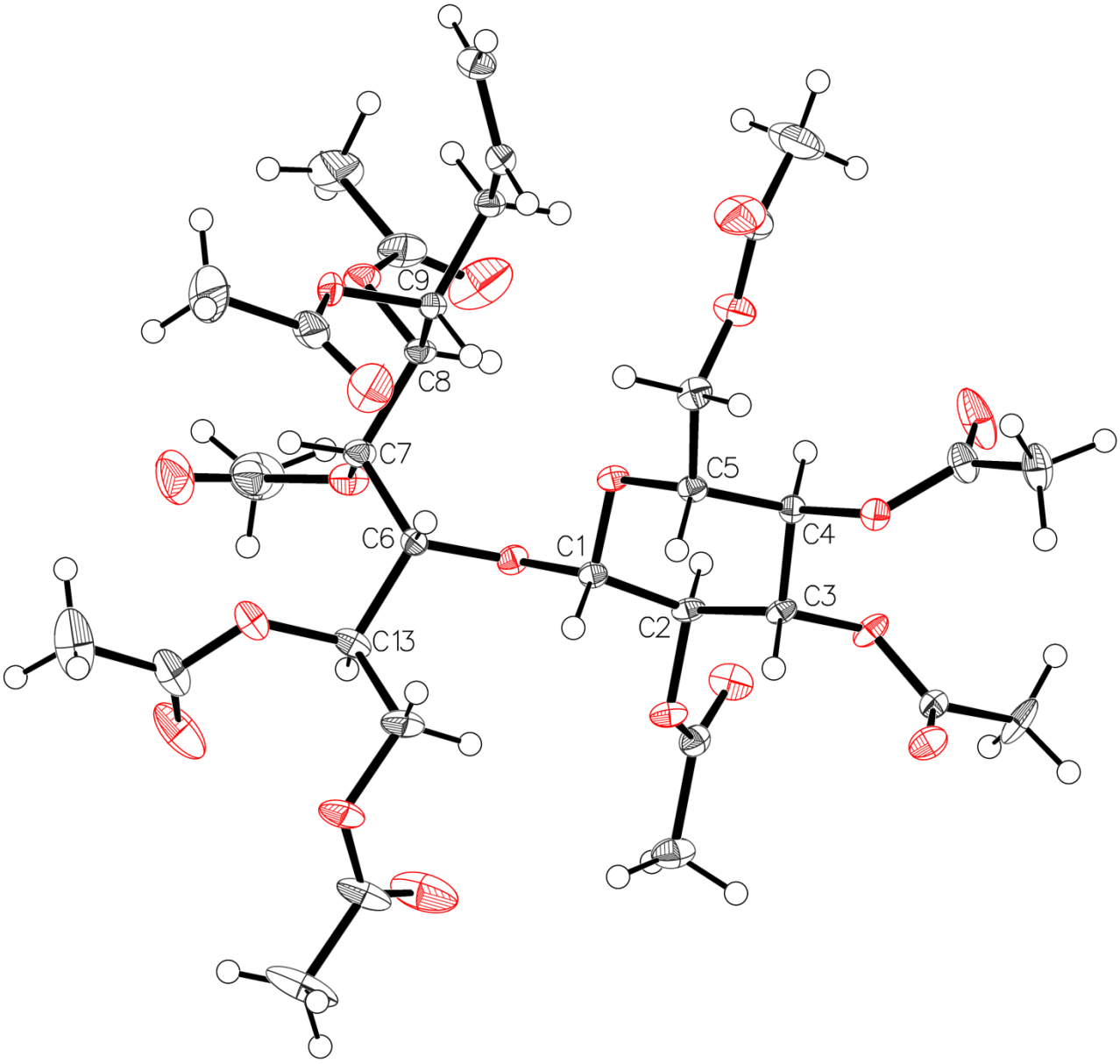

Figure 1 Crystal Structure of **[15]** drawn with 50% displacement ellipsoid. The chiral space group $P2_12_12_1$ and the according results of Flack (-0.1(5)) and Hooft (-0.81(17)) parameter proof the chirality in C1(*S*), C2(*R*), C3(*S*), C4(*R*), C5(*R*), C6(*R*), C7(*S*), C8(*S*), C9(*R*) and C13(*R*). Disordered second part (B) omitted for clarity. Main Residue Disorder 13%. The bond precision for C-C single bonds is 0.0050Å.

Table 2 Sample and crystal data. **[15]**

Radiation [Å]	MoKα (λ = 0.71073)	Z	4	Measurement method	\f and \w scans
Crystal habit	clear colourless block	a [Å]	9.4753(3)		
Crystal size [mm^3]	0.55 × 0.5 × 0.4	b [Å]	19.2827(7)	Abs. correction type	multiscan
Empirical formula	C33H46O20	c [Å]	20.9032(7)	Abs. correction Tmin	0.6628
Formula weight [g/mol]	762.70	α [°]	90	Abs. correction Tmax	0.7470
Temperature [K]	100.0	β [°]	90	Density (calculated) [g/cm^3]	1.326
Crystal system	Orthorhombic	γ [°]	90	Absorption coefficient [mm^{-1}]	0.111
Space group	$P2_12_12_1$	Volume [Å^3]	3819.2(2)	F (000) [e$^-$]	1616.0

Table 3 Data collection and structure refinement. **[15]**

2Θ range for data collection [°]	4.432 to 71.262	Index ranges		Goodness-of-fit on F^2	1.015
Reflections collected	342684	h	-15 ≤ h ≤ 15	Diff. peak and hole [e$^-$Å^{-3}]	0.54/-0.39
Data / restraints / parameters	17622/49/536	k	-31 ≤ k ≤ 31		
Refinement method	Direct Methods	l	-34 ≤ l ≤ 34	Function minimized	$\Sigma w (F_o^2 - F_c^2)^2$
		all data	R1 = 0.0930, wR2 = 0.2203	Weighting scheme	where
		I>2σ(I)	R1 = 0.0821, wR2 = 0.2148	$w=1/[\sigma^2(Fo^2) + (0.0474P)^2 + 0.3425P]$	$P=(F_o^2+2F_c^2)/3$

[i] Bruker SAINT v8.38B Copyright © 2005-2019 Bruker AXS.

[ii] Sheldrick, G. M. (1996). *SADABS.* University of Göttingen, Germany.

[iii] Dolomanov, O.V., Bourhis, L.J., Gildea, R.J, Howard, J.A.K. & Puschmann, H. , OLEX2, (2009), J. Appl. Cryst. 42, 339-341.

[iv] C. B. Huebschle, G. M. Sheldrick and B. Dittrich, ShelXle: a Qt graphical user interface for SHELXL, J. Appl. Cryst., 44, (2011) 1281-1284.

[v] Sheldrick, G. M. (2015). *SHELXS v 2016/4* University of Göttingen, Germany.

[vi] Sheldrick, G. M. (2015). *SHELXL v 2016/4* University of Göttingen, Germany.

[vii] A. L. Spek, Acta Cryst. 2009, D65, 148-155.

3 Summary and conclusion

Elongated carbohydrates are present in many metabolic pathways of various organisms and play an important role in cell-cell recognition events because they are present on the cell-walls of many organisms. Therefore, they are interesting synthetic targets as they represent metabolic tracers and are especially important in the interactions of the human body with malignant cells as well as pathogens such as bacteria and viruses. Consequently, such compounds are an important research goal in Glycoscience, to enhance our understanding of these interactions and further explore the possibility of medical interventions such as drugs or vaccines.

The aim of this PhD thesis was the synthesis of new complex carbohydrates derived from the elongation of disaccharides such as melibiose, maltose, cellobiose as well as lactose. Thus, the indium-mediated allylation was performed and optimized on these substrates. Different metals, temperatures and solvent systems were tested and different experimental setups such as sonication and stirring protocols were evaluated. The allylation resulted in an epimeric product mixture with diastereomeric ratios from 78:22 up to 90:11 and conversions from 85% up to 98%. The expected *syn* configuration of the main product could be proven by X-Ray crystallography. The resulting highly polar compounds were per-*O*-acetylated for the purification and separation of the epimeric mixture. The pure allylated disaccharides were then deprotected under Zemplén conditions, conventional work-up, neutralization with acidic ion exchange resin followed by filtration and removal of the solvent under reduced pressure, led to precipitation of the unprotected compounds. These structures were not soluble under normal ozonolysis conditions, therefore, in an optimized protocol the resulting reaction mixture of the Zemplén deacetylation was directly diluted with dichloromethane and subsequently used for the ozonolysis step. Initial 'longer reaction times' of the ozonolysis reactions led to *O*-methylation of the anomeric position due to increasing acidic reaction conditions over time. This *O*-methylation could be suppressed with shorter ozonolysis protocols. On the side, during the optimization process of the elongation of lactose an interesting novel 12 membered bridged disaccharide has been identified. The optimized ozonolysis protocol led to the desired product mixture of α/β-pyranoid as well as α/β-furanoid

isomers. This mixture was then per-*O*-acetylated and the main product, which adopted β-pyranose conformation, was isolated and purified for structural elucidation using nuclear magnetic resonance spectroscopy with the help of spin simulations (Daisy, TopSpin software, Bruker BioSpin). The yields of this three step sequence - deprotection, ozonolysis, acetylation - ranged from 50% up to 72% and the main products could be isolated with yields up to 51%. With this we could demonstrate the IMA reaction to be a powerful synthetic tool for the efficient and diastereoselective elongation of disaccharides allowing for further options for the possible modifications of complex glycosides.

Further contributions during the PhD thesis:

M. Gintner, Y. Yoneda, C. Schmoelzer, C. Denner, H. Kaehlig, W. Schmid;
A versatile de novo synthesis of legionaminic acid and 4-epi-legionaminic acid starting from D-serine.
Carbohydrate Research **2019**, 474, 34-42.

M. Gintner, C. Denner, C. Schmoelzer, M. Fischer, P. Fruehauf,H. Kaehlig, W. Schmid;
Synthesis of 3-deoxy-2-uloses via the indium-mediated allylation reaction.
Monatshefte fuer Chemie **2019**, 150, 849-860.

List of conference participations during the PhD thesis:

Christian Denner, Manuel Gintner, Hanspeter Kählig, Walther Schmid;
Indium-Mediated Allylation of Disaccharides;
24th Austrian Carbohydrate Workshop, February 13-14, 2020, Vienna, Austria; **oral presentation**.

Christian Denner, Walther Schmid;
Diastereoselective Synthesis of Elongated Carbohydrate Analogues via the Indium Mediated Allylation of Disaccharides;
EUROCARB 2019, June 30 – July 04, 2019, Leiden, Netherlands; **poster presentation**.

Christian Denner;
Indium-Mediated Allylation of Disaccharides;
ORC SYMPOSIUM, June 05, 2019, Vienna, Austria; **oral presentation**.

Christian Denner;
Diastereoselective Elongation of Disaccharides Taking Advantage of the Indium-mediated Allylation Reaction;
23rd Austrian Carbohydrate Workshop, February 14-15, 2019, Graz, Austria; **oral presentation**.

Christian Denner, Walther Schmid;
Indium-Mediated Allylation of Disaccharides;
29th International Carbohydrate Symposium, July 15-19, 2018, Lisbon, Portugal; **poster presentation**.

Christian Denner, Walther Schmid;
Indium-mediated allylation of disaccharides;
ORC SYMPOSIUM, June 05, 2018, Vienna, Austria; **poster presentation**.